

PROBING CHEMICAL DYNAMICS NEAR ELECTRODE SURFACES WITH
ULTRAMICROELECTRODES

Thesis by
Russell John Pylkki

In Partial Fulfillment of the Requirements
for the Degree of
Doctor of Philosophy

California Institute of Technology
Pasadena, California

1993

(Submitted October 14, 1992)

© 1993

Russell John Pylkki

All rights reserved

To Kathy

Acknowledgment

As my stay at Caltech has come to an end, I would like to thank those who have assisted me during the past six years. I would like to thank both Fred Anson and Nate Lewis for the opportunity to work in their groups. I learned much from those that I worked with in the STM lab: Reggie Penner, Rik Blumenthal and Teri Longin. Throughout my stay at Caltech, I have had the pleasure of meeting a number of people with whom I could discuss science and now call my friends: Janet Nelson, Paul Bernhard, Paolo Ugo, Tom Jozefiak, Gail Ryba, Dave Conrad, John Bart and Matt Bonner.

My introduction to the field of tunneling microscopy came through a collaboration at the Jet Propulsion Laboratory. Thanks go to Perry Bankston for the use of facilities. I am grateful to Bill Kaiser and Doug Bell for helping me learn the basics. A special thanks goes to Jim Smart, whom I met at JPL, for his continued personal interest, support and encouragement over the years. I also appreciate the help with the electronics provided by Tom Dunn.

Passage through the past six years would have been much more perilous without the help of a number of friends outside the Caltech Community. Before coming to Caltech, I had the good fortune of working with Kurt Heikkila and Rod Williams. I appreciate their support and encouragement as well as the occasional "reality check." Randy Pell was also helpful in this respect. I am indebted to Fred Raimondi for his assistance and the use of the facilities at Planet Blue to produce my music video. Along with Fred, other friends have helped keep my life balanced through music: Mary Blanche, Joe Gutierrez and Francis Villapondo.

I owe my deepest gratitude, however, to my wife Kathy. She has gone through this process herself and remained a never-ending source of support, understanding and encouragement.

Abstract

This thesis describes work carried out to observe the dynamics of diffusion layer growth near electrode surfaces. For the first time, these processes are observed within 1 μm of an electrode. This is accomplished by positioning an ultramicroelectrode near an electrode surface with a scanning tunneling microscope. A bipotentiostat is integrated with the scanning tunneling microscope to allow potential control of the sample cell, permitting independent control of both the electrode substrate and the ultramicroelectrode tip potentials.

The response of the diffusion layer to potentiostatic and galvanostatic stimulus of the substrate is described. The responses to the stimulus in the absence of coupled chemical reactions are shown to agree well with theory. The observed effects of a coupled chemical reaction are also reported and compared to the responses generated from a simulation program. Good agreement of the experimental data to the simulated data is shown, which demonstrates the ability of the instrument to study homogeneous kinetics.

Table of Contents

	<u>Page</u>
Acknowledgment	iv
Abstract	vi
Table of Contents	vii
Chapter 1 Introduction	1
Introduction	2
Thesis Outline	4
References	6
Chapter 2 Instrumentation	8
Introduction	9
STM Modifications	9
Galvanostat	11
Tip Preparation	11
Z-Piezo Lock	12
Kaiser STM	12
Other Items	12
References	14
Figures	15
Appendix	19
Chapter 3 Diffusion Layer Dynamics: Theory and Simulations	27
Introduction	28
The Potentiostatic Step without a Coupled Chemical Reaction	28
The Potentiostatic Step with a Coupled Chemical Reaction	31
The Galvanostatic Step without a Coupled Chemical Reaction	33
The Galvanostatic Step with a Coupled Chemical Reaction	35
Summary	38

Symbols	39
References	40
Figures	41
Appendix	77
Chapter 4 Results and Discussion	90
Introduction	91
The Galvanostatic Experiment	91
The Effect of Varying the Tip/Substrate Separation	93
The Effect of Varying the Galvanostatic Step	93
The Potentiostatic Experiment	94
Ruthenium(III) Hexaamine Complex	95
The Effect of Varying the Tip/Substrate Separation	96
The Effect of Changing Tip Potential	97
Ruthenium(III) Chloropentaamine Complex	97
Summary and Conclusion	100
References	102
Figures	103

Chapter 1

Introduction

Introduction

The development of the scanning tunneling microscope (STM) by Binnig and Rohrer (1) opened the door to a new realm in the study of surfaces. Additional excitement was generated when it was shown that this surface technique was not limited to an ultra-high vacuum environment. The ability to tunnel in an ambient air environment meant that the tunneling was not seriously affected by the surface contaminants that inherently exist on exposed surfaces. Soon researchers began studies *in-situ*, with the imaging of surfaces in a variety of liquids (2,3). These initial studies were conducted without potential control of the cell. Potential control of the cell has been approached in several ways. One approach is to use a standard three-electrode potentiostat and to hold the tip at a constant bias with respect to the substrate (working electrode) (4,5). A slightly different approach holds the tip at a constant potential versus the reference electrode (6,7). A third approach is to control the cell with a bipotentiostat (8,9). This enables the user to choose between the first two experimental approaches as needs dictate.

Initially, the conditions for *in-situ* tunneling had to be chosen carefully. Tips were fully exposed to the solution and currents at the tip needed to be kept low with respect to the tunneling current (1-10 nA) for the feedback control electronics to operate properly. This restriction was overcome with advances in tip coating techniques. Materials used to insulate the tips include wax (10) and varnish (11). Heben et al. (12), refined the tip coating process using glass and polymer to create tips with subnanoamp faradaic currents even in the presence of high concentrations of electroactive species. With the reduction of tip surface area exposed to the solution, it was possible to work in a wider range of conditions and environments.

Studies employing the STM and the related atomic force microscope (13) advanced to the electrochemical modification of surfaces, including deposition of metals on surfaces (2), underpotential deposition (14), the potential dependence of surface migration (15), and the potential dependence of surface structure (6), to name a few. It was also shown that the tunneling tip could be used to modify the substrate by reducing metal in a surface polymer film (16) and, more recently, to deposit different metal "dots" on a surface to form a "nano" galvanic cell (17).

With the use of the STM in an electrochemical cell, it was realized that at close distance the faradaic process of the tip and substrate would interact. This led to the development of the scanning electrochemical microscope (SECM) (18). The interaction of the SECM tip (an ultramicroelectrode (UME)) with the substrate relies on the diffusion of electroactive species between tip and the substrate. This was first demonstrated by Engstrom *et al.* (19). They showed that the presence of an electrode array undergoing a potential step could be detected electrochemically by a UME placed in its diffusion layer. Bard and coworkers focused on the tip as the generator and collector to develop the SECM. This technique used the overlap of the diffusion layer of the tip with the substrate to yield a current response that varies with tip/substrate separation. A different response is observed for insulating and conductive substrates. When the diffusion layer of the UME overlaps with the conducting substrate, an enhancement of current is seen due to diffusional feedback. Species generated at the tip which diffuse to the substrate are converted back to their original state. This conversion increases the concentration of reactant in the UME's diffusion layer, i.e., the regenerated reactant diffuses back to the tip, where it reacts again, enhancing the tip current. This is called "positive" feedback. Alternatively, when probing an insulating substrate, "negative" feedback is observed. In this case, the insulating substrate blocks diffusion of reactant to the tip, decreasing the

current. In both cases of negative and positive feedback, the effect is a function of the tip sample separation. As such, surface topography can be mapped.

The SECM uses diffusing electroactive species to probe the electrochemical nature of the substrate (19a) as well as the separation between the tip and substrate. The fate of unstable species diffusing in the tip/substrate gap can also be examined (19a, 20). The use of a disk UME for the probe tip in an SECM limits the approach of the tip to the substrate. This is because it is difficult to keep the disk and its shroud of glass coplanar to the substrate. This also creates an uncertainty in the determination of the tip/substrate separation (18b).

With the STM, electrode separation has no boundary. The tip can freely be positioned at any distance from the substrate. When working with conducting substrates, the separation of the tip is known because the tip can be brought to tunneling distance of the substrate. This thesis describes work carried out which breaks through the limitation of the SECM techniques described above by using an STM to position an ultramicroelectrode in close proximity to a substrate.

Thesis Outline

The body of the thesis is organized into three chapters. Chapter two describes the instrumentation. Integration of the STM and its electronics with a bipotentiostat is described in detail. Chapter three reviews the dynamics of the diffusion layer in close proximity to the surface of an electrode in response to both a potentiostatic and a galvanostatic step. The effect of a coupled chemical reaction of the diffusion layer is investigated via simulation. Chapter four presents the results obtained when using a UME to probe diffusion layer growth in response to a galvanostatic and potentiostatic

step of the substrate electrode. In addition, the effect of a coupled chemical reaction on the diffusion layer is also shown.

References

1. Binnig, G.; Rohrer, H.; Gerber, C.; Weiber, E. *Phys Rev. Lett.*, **1982**, *49*, 57.
2. Sonnenfeld, R.; Hansma, P. K. *Science*, **1986**, *323*, 211.
3. Liu, H.-Y.; Fan, F.-R. F.; Lin, C. W.; Bard, A. J. *J. Am Chem. Soc.*, **1986**, *108*, 3838.
4. Green, M. P.; Hanson, K.; Scherson, D. A.; Xing, X.; Richter, M.; Ross, P. N.; Carr, R.; Lindau, I. *J. Phys. Chem.*, **1989**, *93*, 2181.
5. Otsuka, I.; Iwasaki, T. *J. Microsc.*, **1988**, *1542*, 289.
6. Trevor, D. J.; Chidsey, C. E. D.; Loiacono, D. W. *Phys. Rev. Lett.*, **1989**, *62*, 929.
7. Weichers, J.; Twomey, T.; Kolb, D. M.; Behm, R. J.; *J. Electroanal. Chem.*, **1988**, *248*, 451.
8. Itaya, K.; Tomito, E.; *Sur. Sci.*, **1988**, *201*, L507.
9. Christoph, R.; Siegenthaler, H.; Rohrer, H.; Wiese, H. *Electrochem. Acta*, **1989**, *34*, 1011.
10. Twomey, T.; Wiechers, J.; Kolb, D. M.; Behm, R. J. *J. Microsc.*, **1988**, *152*, 537.
11. Gewirth, A. A.; Cranston, P. H.; Bard, A. J. *J. Electroanal. Chem.*, **1989**, *261*, 477.
12. Heben, M. J.; Dovek, M. M.; Lewis, N. S.; Penner, R. M.; Quate, C. F. *J. Microsc.*, **1988**, *152*, 651.
13. Binnig, G.; Quate, C. F.; Gerber, C. *Phys. Rev. Lett.*, **1986**, *52*, 930.
14. Magnusssenn J.; Hotlos, R. J.; Kolb, D. M.; Behm, R. J. *Phys. Rev. Lett.*, **1990**, *64*, 2929.
15. 16. Wuttig, M.; Franchy, R.; Ibach, H. *Sur. Sci.*, **1989**, *244*, L979.
16. Huessser, O. E.; Cranston, D. H.; Bard, A. J. *J. Vac. Sci. Tech. B*, **1988**, *6*, 1873.
17. Li, W.; Virtanen, J. A.; Penner, R. M. *J. Phys. Chem.* **1992**, *96*, 6529.
18. (a) Bard, A. J.; Fan, F.-R. F.; Kwak, J.; Lev, O. *Anal Chem.* **1989**, *61*, 132. (b) Kwak, J.; Bard, A. J. *Anal. Chem.*, **1989**, *61*, 1221.

19. (a) Engstrom, R. C.; Weber, M.; Wunder, P. J.; Burgess, R.; Winqvist, S.; *Anal. Chem.*, **1986**, *58*, 844. (b) Engstrom, R. C.; Meaney, T.; Tople, R.; Wightman, R. M. *Anal. Chem.*, **1987**, *59*, 2005. (c) Engstrom, R. C.; Wightman, R. M.; Kristensen, E. W. *Anal. Chem.*, **1988**, *60*, 652.
20. (a) Unwin, P. R.; Bard, A. J. *J. Phys. Chem.*, **1991**, *95*, 784. (b) Zhou, F.; Unwin, P. R.; Bard, A. J. *J. Phys. Chem.* (submitted).

Chapter 2

Instrumentation

Introduction

In order to carry out the electrochemical experiments, it was necessary to modify the STM to allow potential control of the sample cell. This chapter begins by describing this modification. Following is a discussion of additional changes to the system that include the integration of a bipotentiostat with the tunneling electronics, the design of an electronic circuit to galvanostatically control the substrate, and a switch to "freeze" the z-piezo position as needed during the experiments. The Appendix to the chapter shows updated schematics and details of changes that were made to the various electronic circuits.

STM Modifications

The scanning tunneling microscope used in this experiment was modified from the device described by Heben (1) (Fig. 2.1). A bipotentiostat (Model RDE-4, Pine Instruments Co., Grove City, PA) was added to control the potential of both the tip and the substrate during electrochemical experiments. Initially the bipotentiostat and the STM electronics were isolated from each other. When the cell was under potentiostatic control, the tip current was measured with a commercial current amplifier (Model 427, Keithley Instruments, Inc., Cleveland, OH). A series of relays was used to switch control of the tip and substrate between the STM electronics and the bipotentiostat. It was later determined that the current amplifier had a frequency response similar to the STM pre-amp. The current amplifier was thereafter used to provide the current signal to the STM feedback control circuit and the cell was kept under potentiostatic control at all times. A block diagram of the system is shown in Figure 2.2. Another feature of the current amplifier is the ease with which the gain can be changed, simplifying the use of the system with tips of various sizes.

In the unmodified STM design, the current is monitored at the substrate (1a). If the experiment is carried out with only two electrodes, currents at the tip and substrate are

equal and opposite and either can be monitored by the tunneling feedback control circuit. However, with the above modification of the design to a four electrode system, the current must be measured at the tip since it is independent of the substrate current. Relocation of the point where the tunneling current is measured introduced two interferences. The first was capacitive coupling between the voltage applied to the z-piezo and the tip current monitor. Since the lead to the STM tip holder passes through the interior of the piezo tube, which controls movement normal to the substrate, a significant amount of capacitive coupling to z-piezo movements occurred (30 pF). (Coupling to the x and y electrodes on the exterior of the piezo tube can also occur, but to a lesser extent.) One of the problems of the capacitive coupling is that it creates a non-tunneling current which interferes with the tunneling feedback control circuit. Another problem occurs when monitoring the current of the tip while approaching the tip to (or retracting the tip from) the substrate. 30 pF of capacitive coupling adds a 0.1 nA background current to these "approach curves." The amount of coupling was reduced by an order of magnitude by shielding the lead tip holder inside the piezo tube. Experiments showed that the amount of capacitive coupling could be further reduced by mounting the tip holder on the exterior of the piezo tube. The piezo tube has four exterior electrodes, two of which are grounded. If the tip holder is attached to one of these grounded segments, the capacitive coupling drops by two orders of magnitude to 0.04 pF.

The second interference introduced when measuring the current at the tip was a leakage current between the piezo electrodes and the tip holder. If the surface resistance drops to one gigaohm between one of the piezo electrodes and the tip holder, a current on the order of 0.1 nA is generated. Surface resistance can drop into this range when the STM is in a humid environment. To minimize this interference the piezo tube was sealed with an electronic grade silicone sealant (Part No. 162, General Electric, Waterford, NY). Even

with a sealed tube, however, leakage currents continued to be a problem when using the STM with DMSO solutions, increasing to the 0.1 nA level in several hours.

Galvanostat

The current amplifier used to monitor the tip current references the current to ground. It can therefore only be used with the working electrode which is kept at ground by the bipotentiostat. In this configuration only the tip, not the substrate, can be galvanostated by the bipotentiostat. However, the bipotentiostat allows the input of external signals to control the potential of each working electrode. A simple circuit was therefore built that uses this external input to force the potentiostat to behave as a galvanostat (Fig. A.1). The circuit operates by comparing the signal from the current amplifier to a set-point voltage. The resulting error signal is amplified and applied to the external input of the bipotentiostat, completing the feedback loop. A low pass filter is adjusted as necessary to stabilize the circuit and to minimize ringing when stepping to the desired current.

Tip Preparation

Tips were prepared from 0.020 inch platinum wire (commercial hard, Sigmond Cohn, Mount Vernon, NY) All tips were electrochemically etched in a cyanide/hydroxide solution as previously described (2). The initial current was 2 amps. After etching, the tips were inspected with an optical microscope (400X) and the etching voltage was adjusted as necessary to produce sharp tips. In general, once a satisfactory etching voltage was found, it was only necessary to change it when a new lot of wire was used.

The tips were coated with glass using the previously described apparatus (2). A circular loop has replaced the omega-shaped loop reported. Only the loop temperature was varied, while the translation speed was kept at 0.1 mm/s. The appropriate loop temperature

is strongly dependent on the loop's size and geometry. More consistent results were obtained when the loops were formed by wrapping them around a metal rod (1.9 mm dia.).

Z-Piezo Lock

During electrochemical experiments, it is necessary to hold the z-piezo in a fixed position and to prevent the STM feedback control electronics from moving the tip in response to the faradaic currents. This was accomplished by inserting a switch between the feedback control circuit (Fig. A.2) and the z-piezo high-voltage circuit (Fig. A.3). The capacitor (C2) at the input of the z-piezo high-voltage circuit will hold the last voltage when the switch is opened because of the low input bias current of the op-amp IC3 (*circa* 10 pA). Drainage of the capacitor charge at such a low rate would cause the z-piezo to relax at 0.1 nm/hr. The actual relaxation rate of the "locked" circuit ranged from 0.5 nm/hr to 2.6 nm/hr.

Other Items

The bipotentiostat for the potential step and the current step experiments was controlled using the external input controls and a signal generator (Model 175, PARC, Princeton, NJ). The data for the step experiments was collected with a digital storage oscilloscope (Model 2090, Nicolet Instrument Co., Madison, WI).

Kaiser STM

A comment should be made about the STM design by Kaiser and Jaklevic (3) that was initially used in these experiments. The coarse approach of the tip to the substrate is made by turning screws that pass through the body of the STM, lowering the STM to the substrate. It is nearly impossible not to move the STM laterally while turning these screws. This has two deleterious effects. Since the STM is pushed laterally from its rest position, it tends to relax back to that position once the lateral force is removed. When trying to

observe a surface on the atomic scale, this drift can be considerable and long lasting. On an atomic scale, the tip is being moved rapidly when adjusting the approach screws, which greatly increases the likelihood that the tip will contact the substrate. This will occur when either the feedback control electronics cannot retract the tip rapidly enough to avoid contact or because the z-piezo range ($0.32\ \mu\text{m}$) is exceeded. This is less of a problem in tunneling experiments in air or vacuum, since atomic resolution is still possible with a tip that has contacted the substrate. Tip "crashes" are usually catastrophic for coated tips used *in-situ* since the glass is easily broken, significantly increasing the area exposed to the solution. For these reasons and the availability of the other STM (with a larger dynamic range: $0.8\ \mu\text{m}$ vs. $0.3\ \mu\text{m}$), the Kaiser STM was abandoned. This is not to say, however, that its design is without merit. Because of the location of its tip holder in relation to the piezo electrodes, this STM's design has inherently low capacitive coupling to the current measuring circuit ($0.4\ \text{pF}$) and a low susceptibility to leakage currents. To take advantage of these design advantages and eliminate the problems outlined above would require a new base to be designed for the STM. Approach screws would pass through the base and the STM would rest upon them. This design is commonly used on the commercial STMs.

References

1. (a) Heben, M. J. Ph. D. Thesis, California Institute of Technology, 1990. (b) Dovek, M. M.; Heben, M. J.; Lamg, C. A.; Lewis, N. S.; Quate, C. F. *Rev. Sci. Instrum.*, **1988**, *59*, 2333.
2. Heben, M. J.; Dovek, M. M.; Lewis, N. S.; Penner, R. M. Quate, C. F. *J. Microsc.*, **1988**, *152*, 651.
3. Kaiser, W. J.; Jaklevik, R. C. *Rev. Sci. Instrum.*, **1988**, *59*, 537.

Figure 2.1 Diagram of the scanning tunneling microscope

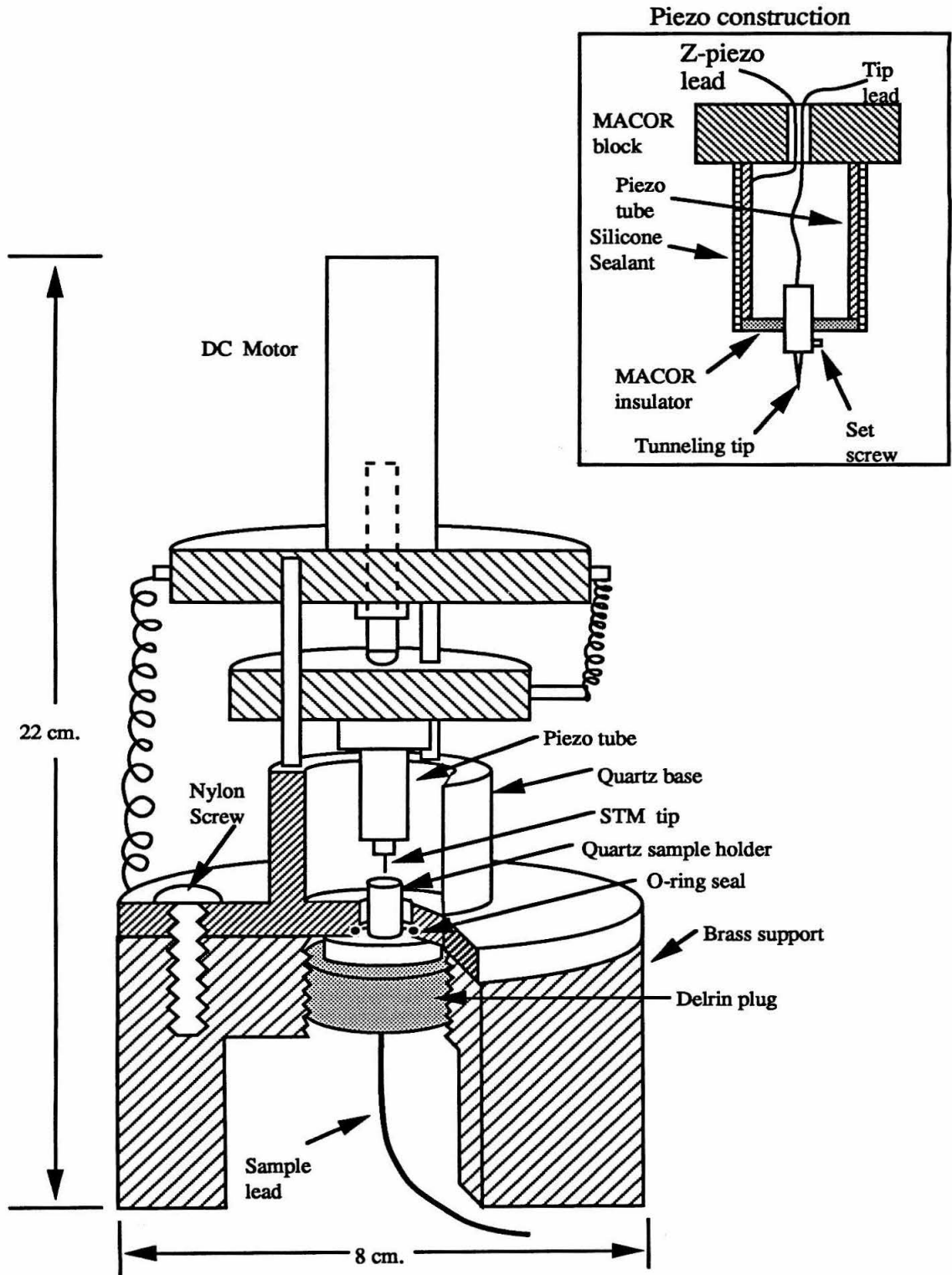


Figure 2.2 Block diagram of the electrochemical scanning tunneling microscope.

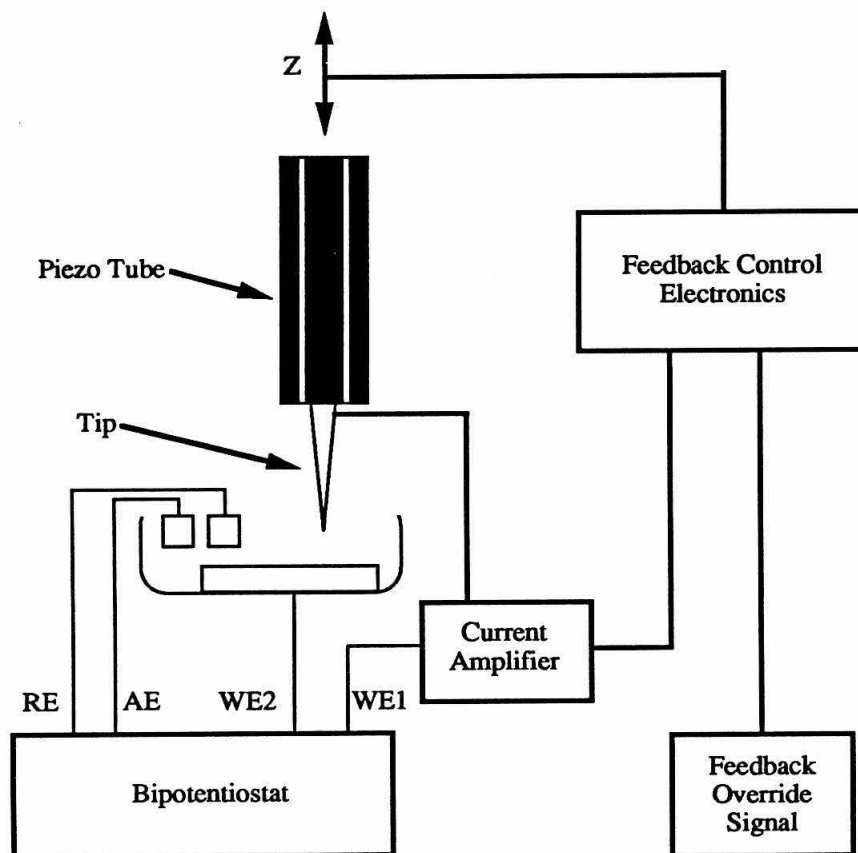


Figure A1 Schematic diagram of the galvanostatic control circuit used to control potentiostat

Galvanostatic Control Circuit

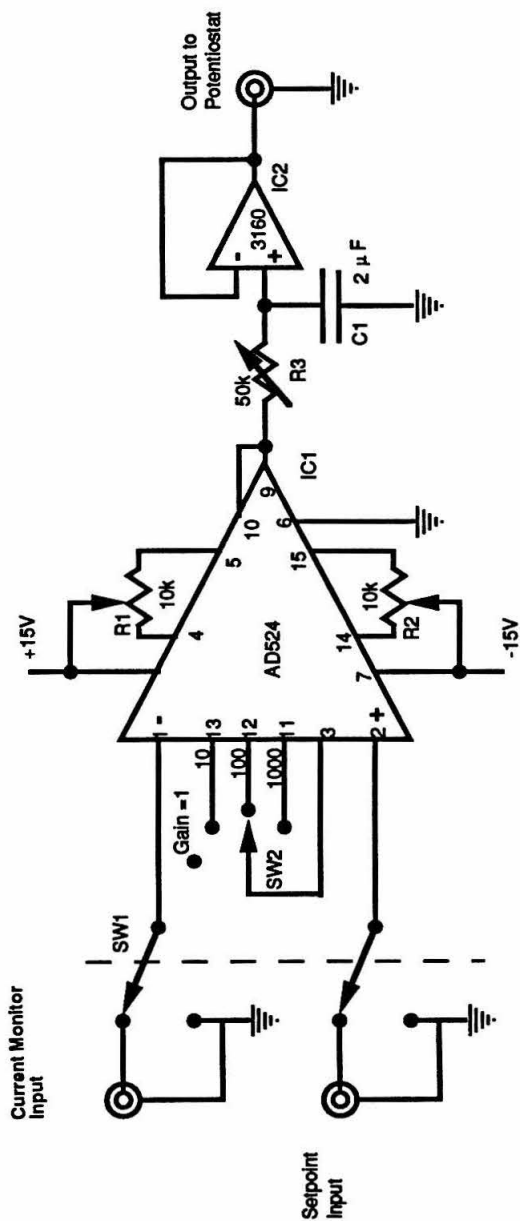


Figure A2 Updated schematic diagram of the feedback control circuit.

Feedback Control Circuit

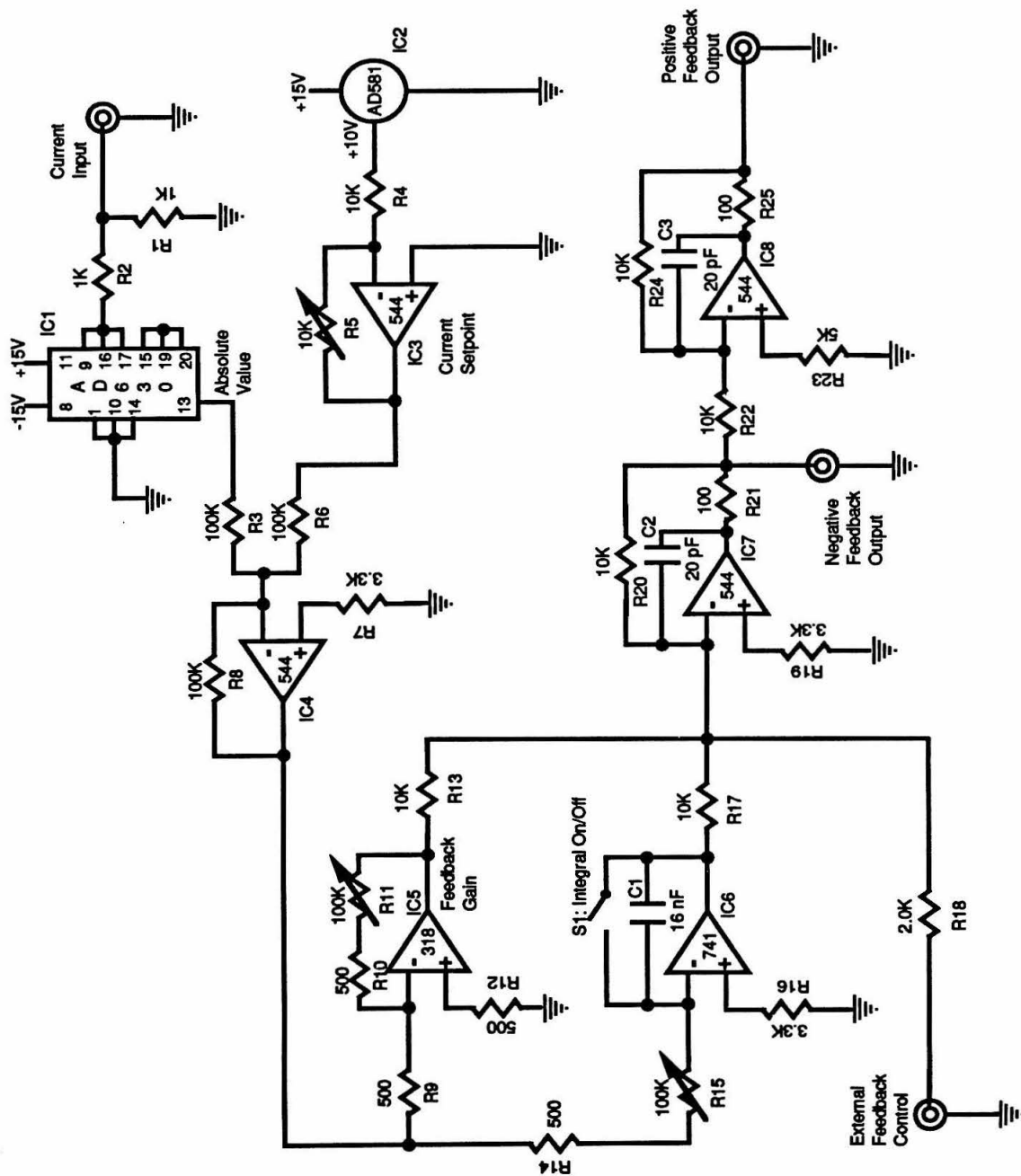


Figure A3 Updated schematic diagram of the z-piezo high-voltage circuit.

Z-Piezo High Voltage Circuit

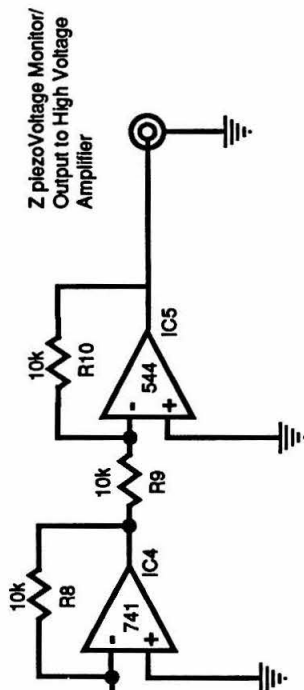
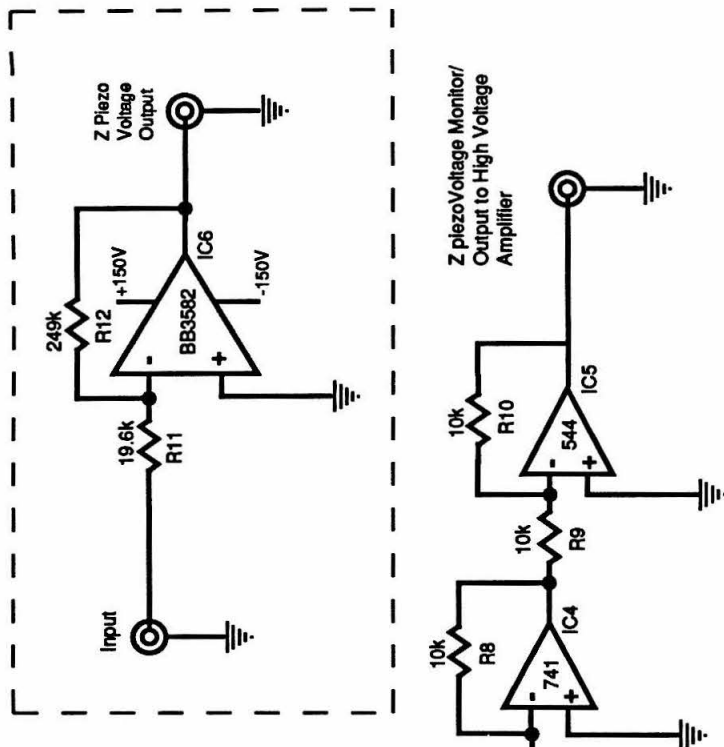
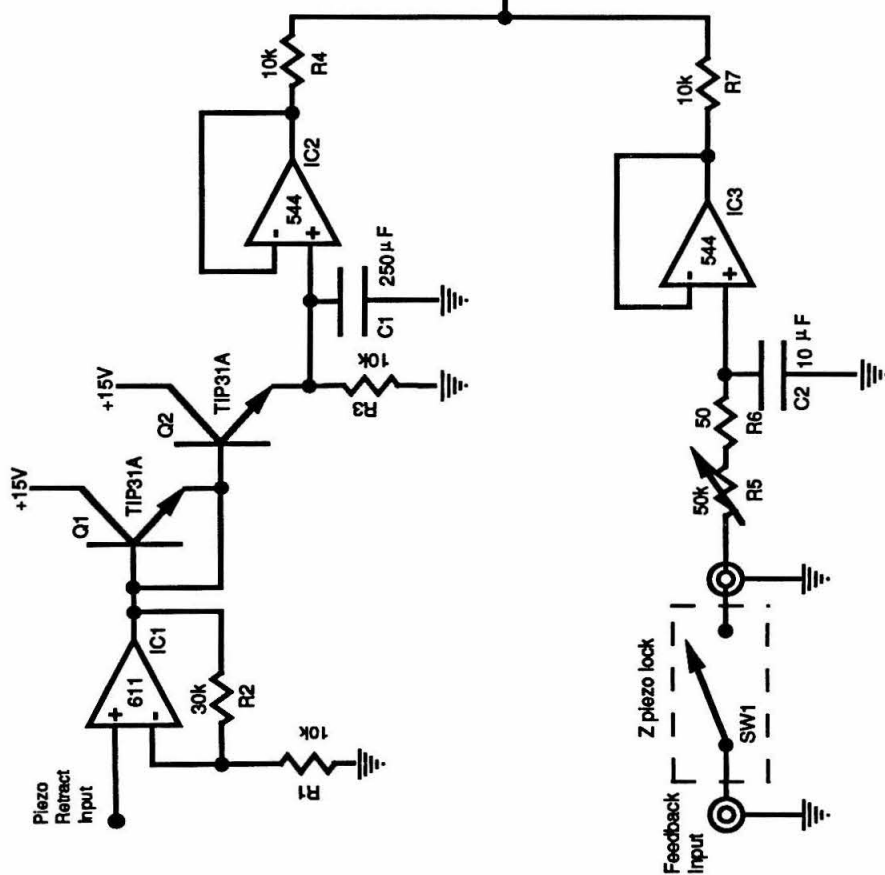


Figure A4 Updated schematic diagram of the d.c. motor pulse generator.

Chapter 3

Diffusion Layer Dynamics:

Theory and Simulations

Introduction

To evaluate the data generated during the experiments, it is necessary to have an understanding of the dynamics of the diffusion layer at an electrode in response to an electrochemical stimulus. In the case of an electron transfer without a coupled chemical reaction, the diffusion equations can be solved exactly for both a potentiostatic and galvanostatic step. These solutions are outlined and their implications on the experiment are discussed. With the inclusion of a coupled chemical reaction, exact solutions are no longer possible in most cases. However, an understanding of the diffusion layer dynamics for these cases can be developed through the use of simulations. Simulations, based on the finite difference method, of diffusion layer growth for both the potentiostatic and galvanostatic step experiments were carried out and their results are presented below. The programs used for the simulations are listed in the appendix. The definitions for the symbols used in the following equations can be found at the end of the chapter.

The Potentiostatic Step without a Coupled Chemical Reaction

Consider a planar electrode undergoing the general reaction:



In order to determine the diffusion layer profile, the linear diffusion equations given by Fick's second law of diffusion must be solved:

$$\frac{\partial C_O(x,t)}{\partial t} = D_O \frac{\partial^2 C_O(x,t)}{\partial x^2} \quad (3.2)$$

$$\frac{\partial C_R(x,t)}{\partial t} = D_R \frac{\partial^2 C_R(x,t)}{\partial x^2}. \quad (3.3)$$

The exact solution of these equations for a potentiostatic step is possible. In the case where mass transport of reactant to (and product from) the electrode is provided solely by diffusion, the potential step is large enough that the reactant concentration at the electrode surface is essentially zero and that only species O is initially present. Under these circumstances the initial conditions are

$$C_O(x,t) = C_O^* \quad \text{for } t < 0 \quad (3.4)$$

$$C_R(x,t) = 0 \quad \text{for } t < 0. \quad (3.5)$$

The semi-infinite boundary conditions are given by

$$\lim_{x \rightarrow \infty} C_O(x,t) = C_O^* \quad \text{for all } t \quad (3.6)$$

$$\lim_{x \rightarrow \infty} C_R(x,t) = 0 \quad \text{for all } t. \quad (3.7)$$

The surface boundary condition is

$$C_O(0,t) = 0 \quad \text{for } t > 0. \quad (3.8)$$

The flux balance at the electrode surface is given by

$$D_O \left[\frac{\partial^2 C_O(x,t)}{\partial x^2} \right]_{x=0} = -D_R \left[\frac{\partial^2 C_R(x,t)}{\partial x^2} \right]_{x=0}. \quad (3.9)$$

Taking the Laplace transformation to Equation 3.2 and applying the boundary conditions (Eqs. 3.6 and 3.8) yields, upon inverse transformation, the concentration profile of species O:

$$C_O(x,t) = C_O^* \left\{ 1 - \operatorname{erfc} \left[\frac{x}{2\sqrt{D_O t}} \right] \right\}. \quad (3.10)$$

Similarly, the concentration profile of species R is

$$C_R(x,t) = C_O^* \sqrt{\frac{D_R}{D_O}} \operatorname{erfc} \left[\frac{x}{2\sqrt{D_R t}} \right]. \quad (3.11)$$

It is instructive to examine the implications for diffusion layer growth of species R near the electrode surface. The diffusion layer profile of species R at several times after the imposition of a potential step is illustrated in Figure 3.1. (Note that concentration profiles of the reactant can be obtained by inverting the y-axis.) At the onset of the potential step, the surface concentration of the product is fixed at $C_O^*(D_R / D_O)^{1/2}$. The growth of the diffusion layer is rapid. After one second, the product concentration drops by only 12% at a plane 5 μm from the surface. It diminishes to half of the surface concentration at 22 μm and 10% at 50 μm .

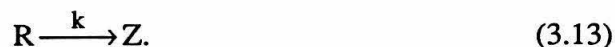
The diffusion layer dynamics within the range of the STM (*ca.* 1 μm) are of primary interest. Within 1 μm of the electrode surface, the diffusion layer becomes well established during the first millisecond after the potential step (Fig. 3.2). After 10 ms the concentration of R drops to 75% of the fixed surface concentration at a plane 1 μm away. After 100 ms, the species R is spread uniformly within 1 μm of the surface, varying by only 8%. For the general case, probing this region at times greater than 10 ms after the potential step would yield little information. Since the transition to product species is

nearly complete, concentration becomes insensitive to distance from the electrode. It is exactly this rapid growth of the diffusion layer that allows the experimental technique to detect short-lived species (*vide infra*).

Because the STM tip used to probe the diffusion layer is held at a constant distance from the electrode undergoing the potentiostatic step, it is important to understand the change over time of product and reactant concentrations at a given distance from the electrode. Figure 3.3 shows the profile of species R versus time at several distances from the electrode. As can be seen, within 1 μm of the surface the majority of the change in concentration occurs during the first 10 ms following the potential step. The rapid transition to a region where concentration is insensitive to position (within *circa* 1 μm of the surface) is clearly shown. Figure 3.4 shows an overall scope of the diffusion layer growth versus time in the form of a semi-log plot. Displayed in this manner, it can be seen that there is a specific window in time when the solution concentrations go through the transition from predominantly species O to predominantly species R.

The Potentiostatic Step with a Coupled Chemical Reaction

The EC_i case (an electron transfer followed by an irreversible chemical reaction), is described by the two reactions



If coupled chemical reaction is first-order, it will decrease the concentration of R as given by

$$\frac{\partial C_R(x,t)}{\partial t} = -kC_R(x,t). \quad (3.14)$$

The diffusion equation for species R (Eq. 3.3) must therefore be modified to account for the effect that chemical reaction has on the product concentration:

$$\frac{\partial C_R(x,t)}{\partial t} = D_R \frac{\partial^2 C(x,t)}{\partial x^2} - kC_R(x,t). \quad (3.15)$$

The addition of such a coupled chemical reaction as illustrated in Equation 3.13 will have no effect on the reactant diffusion equation or the associated boundary conditions. Therefore, the concentration of the reactant is given by the same equation derived for the general case (Eq. 3.10). The introduction of a coupled chemical reaction prevents the derivation of an exact solution of the diffusion equation for the product (Eq. 3.15). However, diffusion layer profiles may be determined in this case with the use of modeling.

A computer program using the finite difference method (1) was developed to simulate diffusion layer growth resulting from a potentiostatic step. To model the linear diffusion at a planar electrode, a series of volume elements ("boxes") are created normal to the electrode surface. The concentration is uniform in each box. During each cycle of the simulation, diffusion occurs between adjacent boxes. In addition, during each iteration, the effect of the chemical kinetics are also imposed. If the volume element and time increments are not too large with respect to the concentration fluxes induced by diffusion and kinetics, the solution of the model will match reality.

Simulations of a series of reaction rates are shown in Figure 3.5. A time increment of 10 μ s and the diffusion coefficient of 5×10^{-6} cm²/s are used. Based on these parameters, each box in the finite difference model is 0.105 μ m wide. A concentration

maximum followed by decay in the concentration of species R is a feature shared by all of the profiles (except those at the surface). This is a consequence of the time delay due to diffusion of the species, together with the decreasing rate at which R is being generated at the surface ($i \propto 1/\sqrt{t}$). The highest concentration of R will always be found at the surface since this is where R is the "freshest." As can be seen in Figure 3.5, the decrease in concentration of R is strongly dependent on k.

The Galvanostatic Step without a Coupled Chemical Reaction

The concentration profiles resulting from a galvanostatic step at an electrode can also be determined analytically for the general case. The solution is shown for a planar electrode, for which mass transport is provided by diffusion alone and only species O is initially present. The solution for the reactant concentration is derived by taking the Laplace transformation of its diffusion equation (Eq. 3.2) and applying the semi-infinite boundary condition (Eq. 3.6), along with the condition of constant flux at the surface:

$$D_O \frac{\partial C_O(0,t)}{\partial x} = -D_R \frac{\partial C_R(0,t)}{\partial x} = \frac{i}{nFA}. \quad (3.16)$$

Inverse transformation yields the solution for the reactant concentration:

$$C_O(x,t) = C_O^* - \frac{i}{nFAD_O} \left\{ 2\sqrt{\frac{D_O t}{\pi}} \exp\left(\frac{-x^2}{4D_O t}\right) - x \operatorname{erfc}\left[\frac{x}{2\sqrt{D_O t}}\right] \right\}. \quad (3.17)$$

Unlike the solution for the potentiostatic step, which is valid at all times greater than zero, the solution for the galvanostatic step has an upper time limit $t = \tau$. τ is the characteristic transition time, after which the condition of constant flux at the surface (Eq. 3.16) can no longer be maintained, i.e., the reactant concentration at the surface reaches zero and the current due to the reduction of O at the electrode surface becomes limited by

diffusion. The value of τ can be determined by evaluating Equation 3.17 at the electrode surface, setting the surface concentration equal to zero and solving for t . This yields the Sand equation:

$$\frac{i\tau^{1/2}}{C_O^*} = \frac{nFAD_O^{1/2}\pi^{1/2}}{2}. \quad (3.18)$$

The Sand equation can be used to transform Equation 3.17 into a more general form:

$$C_O(x,t) = C_O^* \left(1 - \sqrt{\frac{t}{\tau}} \left\{ \exp\left(\frac{-x^2}{4D_O t}\right) - \frac{\sqrt{\pi}x}{2\sqrt{D_O t}} \operatorname{erfc}\left[\frac{x}{2\sqrt{D_O t}}\right] \right\} \right) \quad \text{for } t \leq \tau. \quad (3.19)$$

Similarly, the product diffusion equation (Eq. 3.3) can be solved:

$$C_R(x,t) = C_O^* \sqrt{\frac{tD_O}{\tau D_R}} \left\{ \exp\left(\frac{-x^2}{4D_R t}\right) - \frac{\sqrt{\pi}x}{2\sqrt{D_R t}} \operatorname{erfc}\left[\frac{x}{2\sqrt{D_R t}}\right] \right\} \quad \text{for } t \leq \tau. \quad (3.20)$$

Diffusion layer profiles of R at various times are illustrated in Figure 3.6. As with the solutions for the potential step, a plot of O can be obtained by inverting the y-axis. The concentration of species R at the surface increases (with $1/\sqrt{t}$), reaching unity at τ . Within 1 μm of the electrode surface, the diffusion layer profiles are fairly uniform (Fig 3.7). In addition, their slopes are the same, a result of the rapid diffusion within this region coupled with the constant flux at the surface. The concentration of R versus time at various distances from the electrode are illustrated in Figure 3.8. As in the potentiostatic case, concentration profiles within 1 μm of the electrode surface are grouped closely.

The Galvanostatic Step with a Coupled Chemical Reaction

Diffusion layer dynamics in response to a galvanostatic step requires the solution to the diffusion equations (Eqs. 3.2 and 3.15) as outlined above. As with the potentiostatic case, the chemical reaction does not affect the diffusion equation or the boundary conditions for the reactant (Eqs. 3.6 and 3.16), therefore the solution is the same as that derived for the general case (Eq. 3.19). For the product, an exact solution (2) is only possible for the concentration at the surface:

$$C_R(0,t) = \frac{C_O^*}{2} \sqrt{\frac{\pi D_O}{k\tau D_R}} \operatorname{erf}[\sqrt{kt}] \quad \text{for } t \leq \tau. \quad (3.21)$$

Note that the time dependence appears only in the argument of the error function. The nature of the error function is such that it becomes constant when its argument is sufficiently large:

$$\operatorname{erf}(x) \approx 1 \quad \text{for } x \geq 1.64. \quad (3.22)$$

Therefore, the surface concentration can reach a steady-state:

$$C_R(0,t) = \frac{C_O^*}{2} \sqrt{\frac{\pi D_O}{k\tau D_R}} \quad \text{for } kt \geq 2.7 \text{ and } t \leq \tau. \quad (3.23)$$

A constant surface concentration has implications for the diffusion layer of the product. The diffusion equation of species R (Eq. 3.20) can be solved exactly if this surface boundary condition of a steady-state concentration (3.23) accompanies the galvanostatic step at $t = 0$. This was shown by Carslaw and Jeager (3), who solved a mathematically identical problem for the conduction of heat along a semi-infinite, non-insulated rod. The solution to this heat conduction problem has the same solution because

the conduction of heat along a rod behaves the same mathematically as diffusion. In addition, the radiation of heat into a medium (at constant and zero temperature) behaves the same mathematically as a coupled first-order chemical reaction. The solution, substituting diffusion and first-order reaction kinetics for heat conduction and radiation, is

$$C_R(x,t) = C_R^{ss} \left\{ \frac{1}{2} \exp\left(-x\sqrt{\frac{k}{D_R}}\right) \operatorname{erfc}\left[\frac{x}{2\sqrt{D_R}} + \sqrt{kt}\right] + \frac{1}{2} \exp\left(x\sqrt{\frac{k}{D_R}}\right) \operatorname{erfc}\left[\frac{x}{2\sqrt{D_R}} - \sqrt{kt}\right] \right\}. \quad (3.24)$$

This relationship also approaches a steady state when kt becomes large enough to dominate the argument of the error function complement:

$$\operatorname{erfc}(x) \approx 0 \quad \text{for } x \geq 1.64 \quad (3.25)$$

$$\operatorname{erfc}(x) \approx 2 \quad \text{for } x \leq -1.64. \quad (3.26)$$

Within 1 μm of the electrode surface, kt dominates the argument of erfc (Eq. 3.24) when $kt \geq 0.2$. Using the limiting values for erfc reduces Equation 3.24 to

$$C_R(x,t) = C_R^{ss} \exp\left(-x\sqrt{\frac{k}{D_R}}\right) \quad \text{for } kt \geq 2.7. \quad (3.27)$$

The diffusion layer profile thus becomes independent of time if there is a constant surface concentration and first-order chemical kinetics. Equation 3.23 shows that a steady-state surface concentration can be established during a galvanostatic step. Therefore it is reasonable to infer that a steady-state concentration profile will form during a galvanostatic step experiment with coupled first-order chemical reaction if kt is large enough.

It should be pointed out that t , the time needed to reach a steady-state surface concentration (Eq. 3.23), is not the same as t , the time necessary to establish the steady-state diffusion layer (Eq. 3.27). The latter was derived for the case in which the surface concentration is stepped to the steady-state value at $t = 0$ s. For the galvanostatic step, this condition will not be met until $kt = 2.7$. Therefore, the diffusion layer of species R cannot yet have reached a steady-state profile at $kt = 2.7$. A steady-state should be achieved before $kt = 5.4$ because the establishment of the steady-state surface concentration and the establishment of a steady-state diffusion layer are not sequential events: the diffusion layer of R has a "head start" on its approach to a steady-state. The establishment of the steady-state diffusion layer is verified with the use of simulations (Fig 3.10) and leads to the determination that a value for $kt \geq 3.5$ is necessary for its establishment. Applying the solution for the steady-state surface concentration (Eq. 3.23) to Equation 3.27 yields

$$C_R(x,t) = \frac{C_O^*}{2} \sqrt{\frac{\pi D_O}{k\tau D_R}} \exp\left(-x\sqrt{\frac{k}{D_R}}\right) \text{ for } kt \geq 3.5 \text{ and } t \leq \tau. \quad (3.28)$$

Representative steady-state concentration profiles for $t = \tau = 1$ s are shown in figures 3.10a and b. Steady-state concentration profiles are compared with the concentration profile without a coupled chemical reaction. The magnitude of the reaction rate has a marked effect on the concentration profile. The profiles for $k = 5, 10$ and 50 s^{-1} are clearly differentiated. A perspective within $1 \mu\text{m}$ of the electrode surface is shown in Figure 3.10b. Decreasing to $t = \tau = 10$ ms (Fig. 3.11) changes the range of the reaction rates that will form a measurable steady-state concentration profile. Through the help of simulations, concentration profiles are shown versus time at several distances in Figure 3.12a-c.

Summary

Both potentiostatic step and galvanostatic step experiments can be used to generate a diffusion layer that can be probed to study the kinetics of a coupled chemical reaction.

The establishment of a steady-state diffusion layer in the galvanostatic step experiment is of practical interest since more reliable measurements may be possible than with the transient response inherent with the potentiostatic step experiment.

Symbols

<u>Symbol</u>	<u>Meaning</u>	<u>Usual Dimensions</u>
A	area	cm ²
C _J *	bulk concentration of species J	mol/cm ³
C _J	concentration of species J	mol/cm ³
C _J ^{SS}	steady-state surface concentration of species J	mol/cm ³
D _J	diffusion coefficient of species J	cm ² /s
erfc(x)	error function compliment	none
F	faraday constant	C
i	current	amps
k	rate constant (for a first-order reaction)	s ⁻¹
t	time	s
x	distance	cm
τ	transition time	s

References

1. For an overview see a) Malloy, J. T. in "Laboratory Techniques in Electroanalytical Chemistry," Kissinger, P. T. and Heineman, W. P. Ed., Marcel Dekker, Inc., N. Y., 1983 and b) "Electrochemical Methods Fundamentals and Applications," Bard, A. J. and Faulkner, L. R., John Wiley and Sons, Inc., N. Y., 1980.
2. Delahay, P.; Mattox, C. C.; Berzins, T. J. Am. Chem. Soc., 1954, , 5319.
3. Carslaw, H. S.; Jeager, J. C. "Conduction of Heat in Solids," Oxford Univ. Press, Oxford, U. K., 1959, 134.

Figure 3.1

Concentration profiles of species R generated at a planar electrode undergoing a potentiostatic step with $D_O=5 \times 10^{-6} \text{cm}^2/\text{s}$.

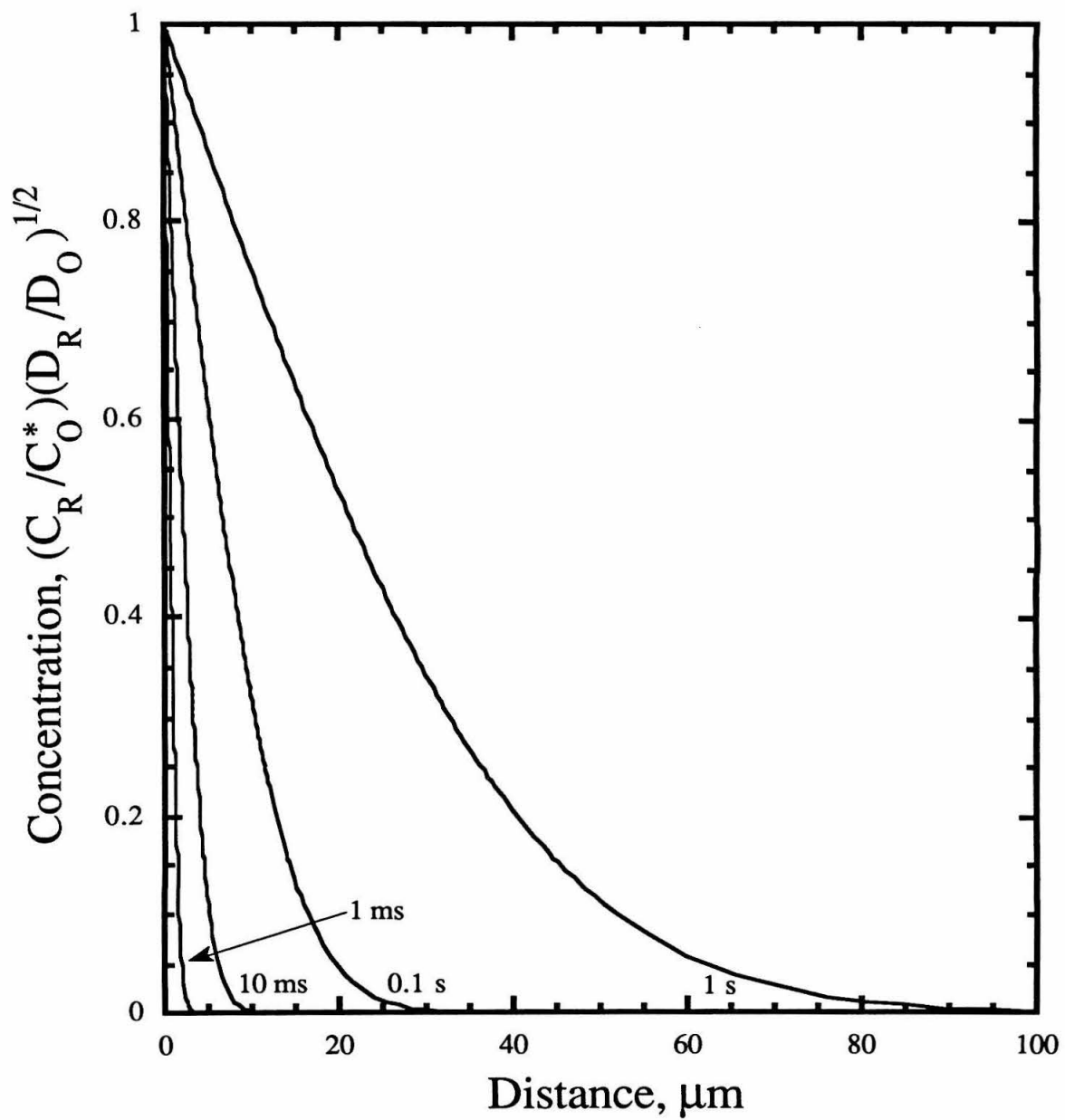


Figure 3.2

Concentration profiles of species R generated at a planar electrode undergoing a potentiostatic step with $D_O=5 \times 10^{-6} \text{cm}^2/\text{s}$.

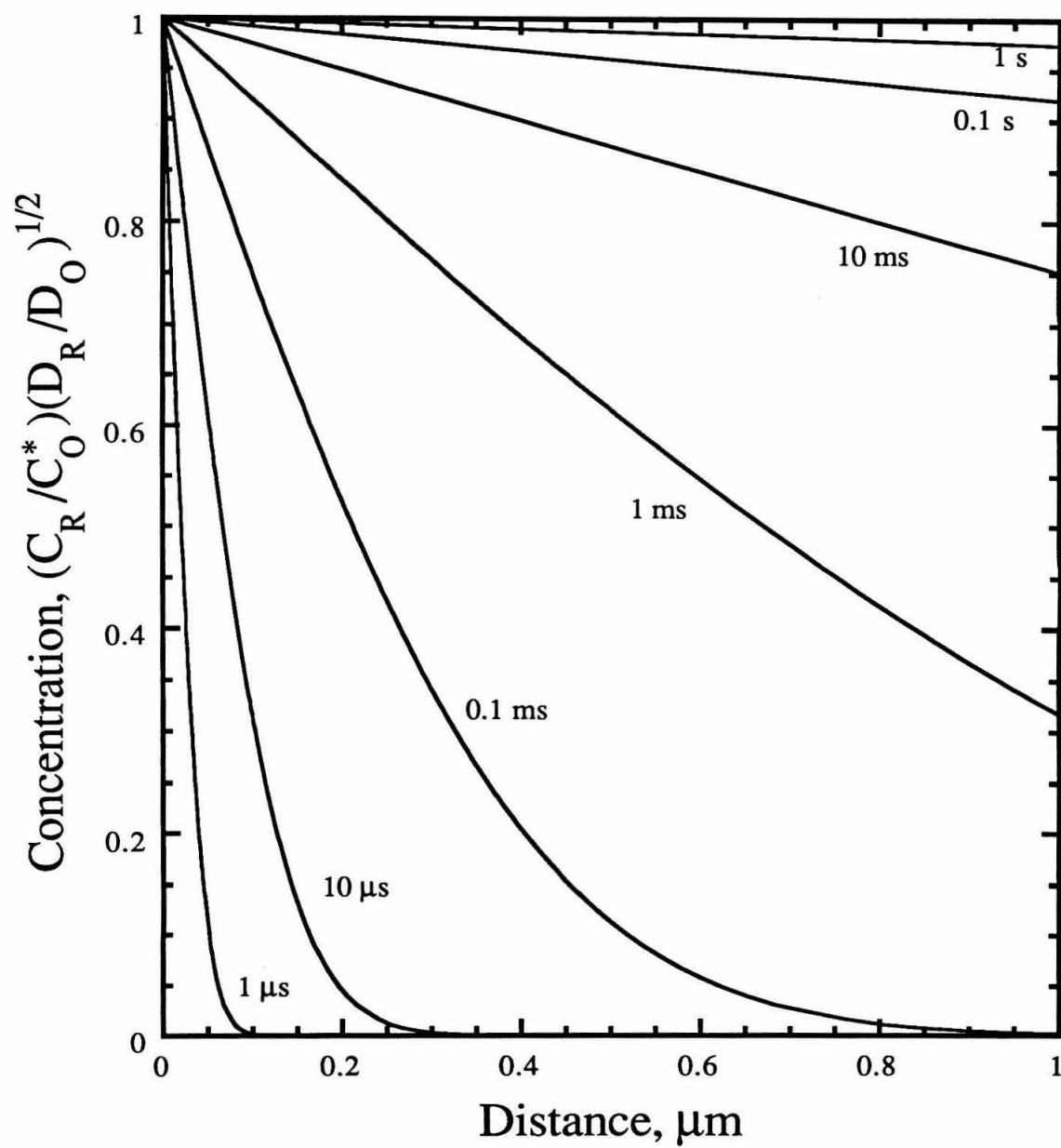


Figure 3.3

Concentration vs. time curves of species R generated at a planar electrode undergoing a potentiostatic step. Plotted at various distances with $D_O=5 \times 10^{-6} \text{cm}^2/\text{s}$.

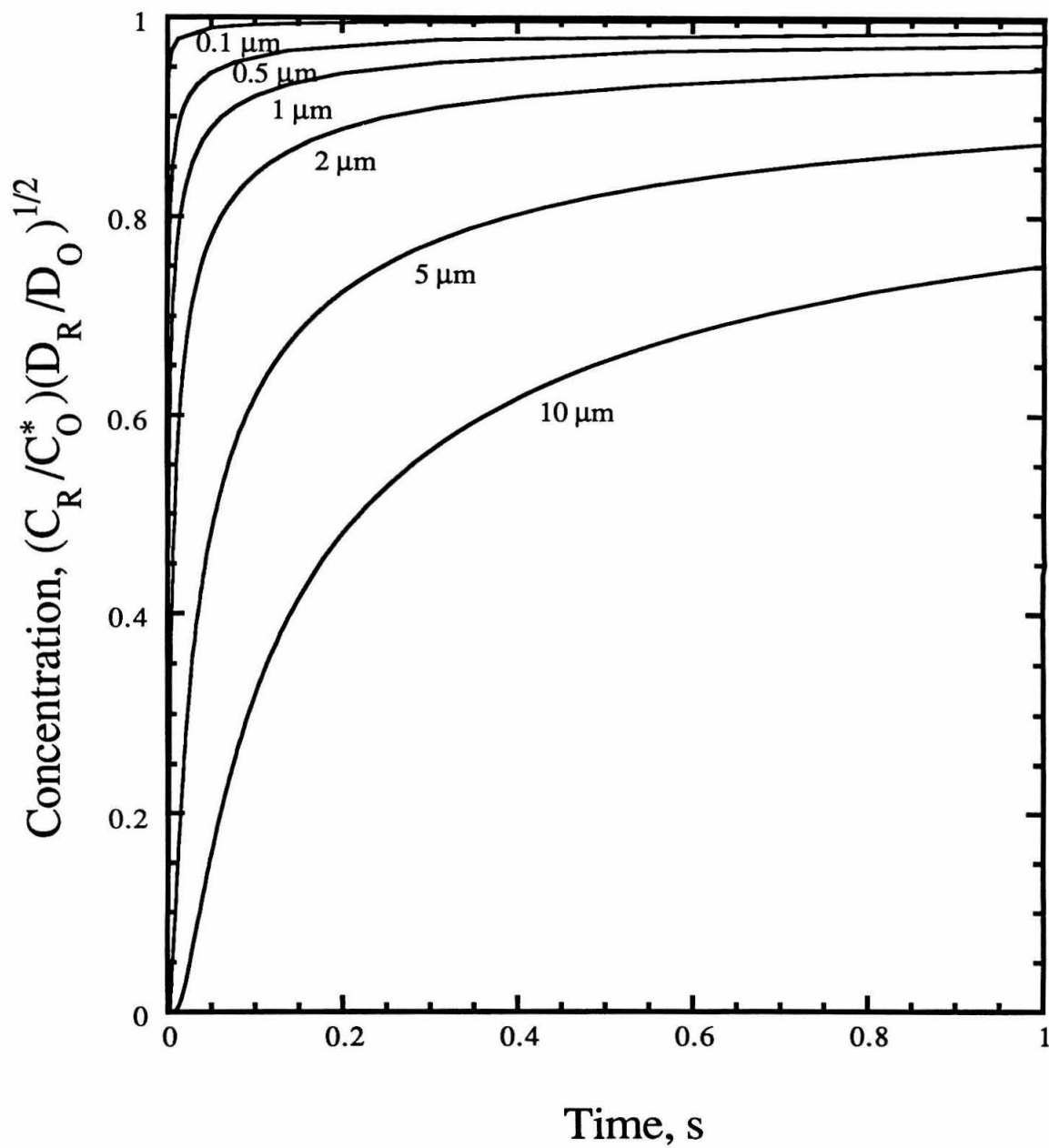


Figure 3.4

Concentration vs. time curves of species R generated at a planar electrode undergoing a potentiostatic step. Plotted at various distances with $D_O=5 \times 10^{-6} \text{cm}^2/\text{s}$.

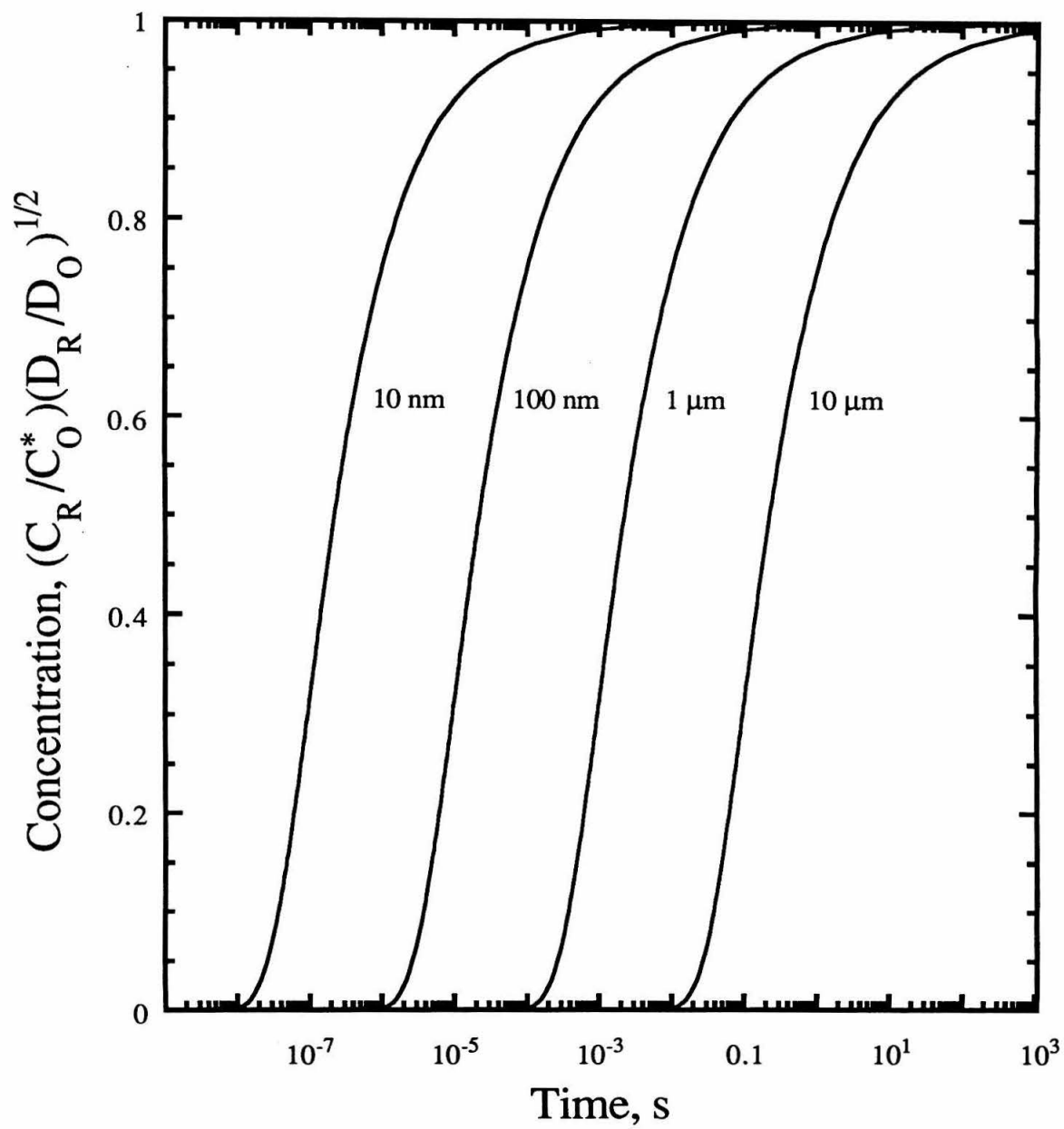


Figure 3.5a

Simulated concentration vs. time curves at $x = 0 \mu\text{m}$ of an intermediate species R generated at a planar electrode undergoing a potentiostatic step with $D_O = 5 \times 10^{-6} \text{cm}^2/\text{s}$.

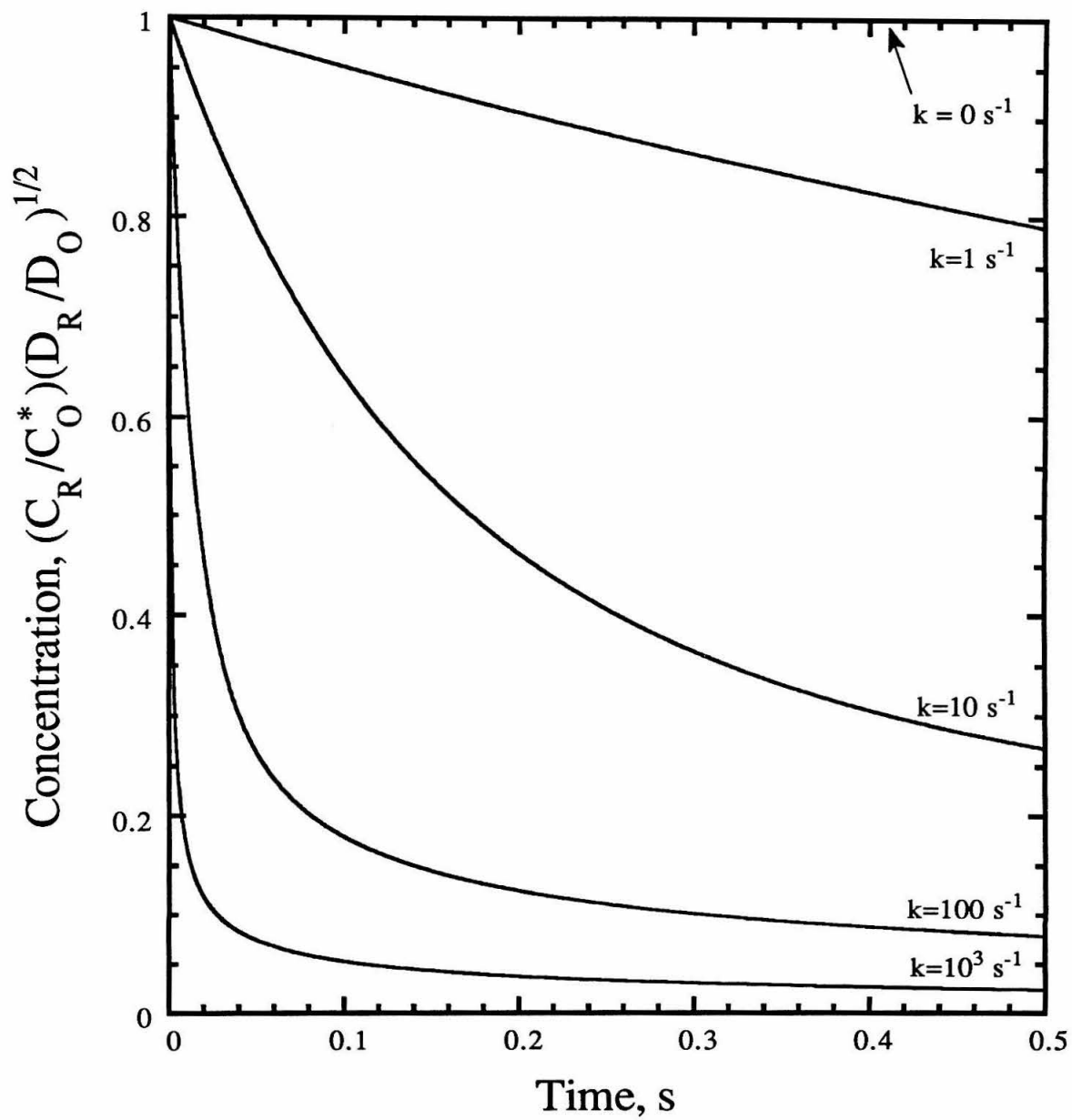


Figure 3.5b

Simulated concentration vs. time curves at $x = 0.1 \mu\text{m}$ of an intermediate species R generated at a planar electrode undergoing a potentiostatic step with $D_O = 5 \times 10^{-6} \text{cm}^2/\text{s}$.

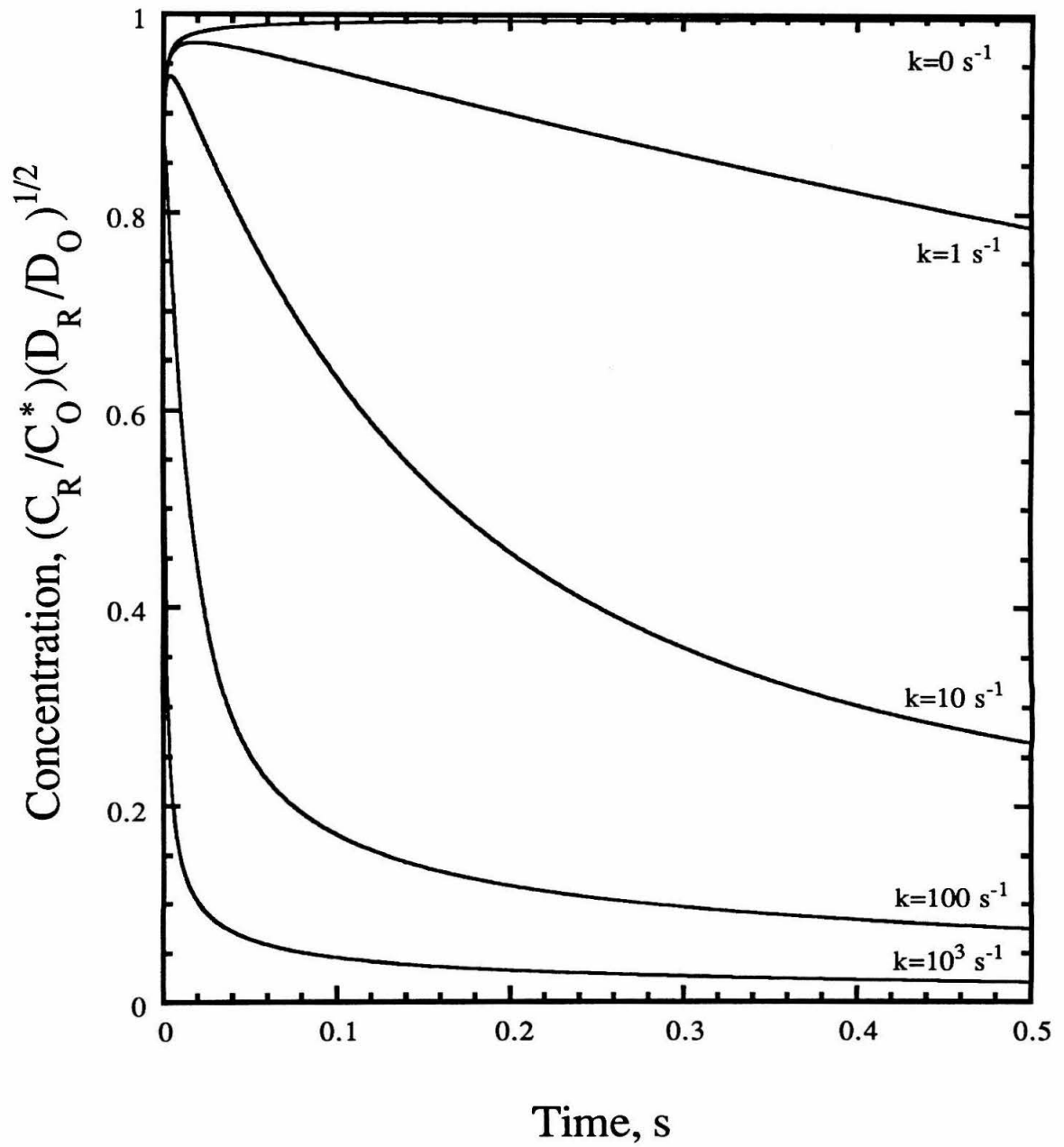


Figure 3.5c

Simulated concentration vs. time curves at $x = 1 \mu\text{m}$ of an intermediate species R generated at a planar electrode undergoing a potentiostatic step with $D_O = 5 \times 10^{-6} \text{cm}^2/\text{s}$.

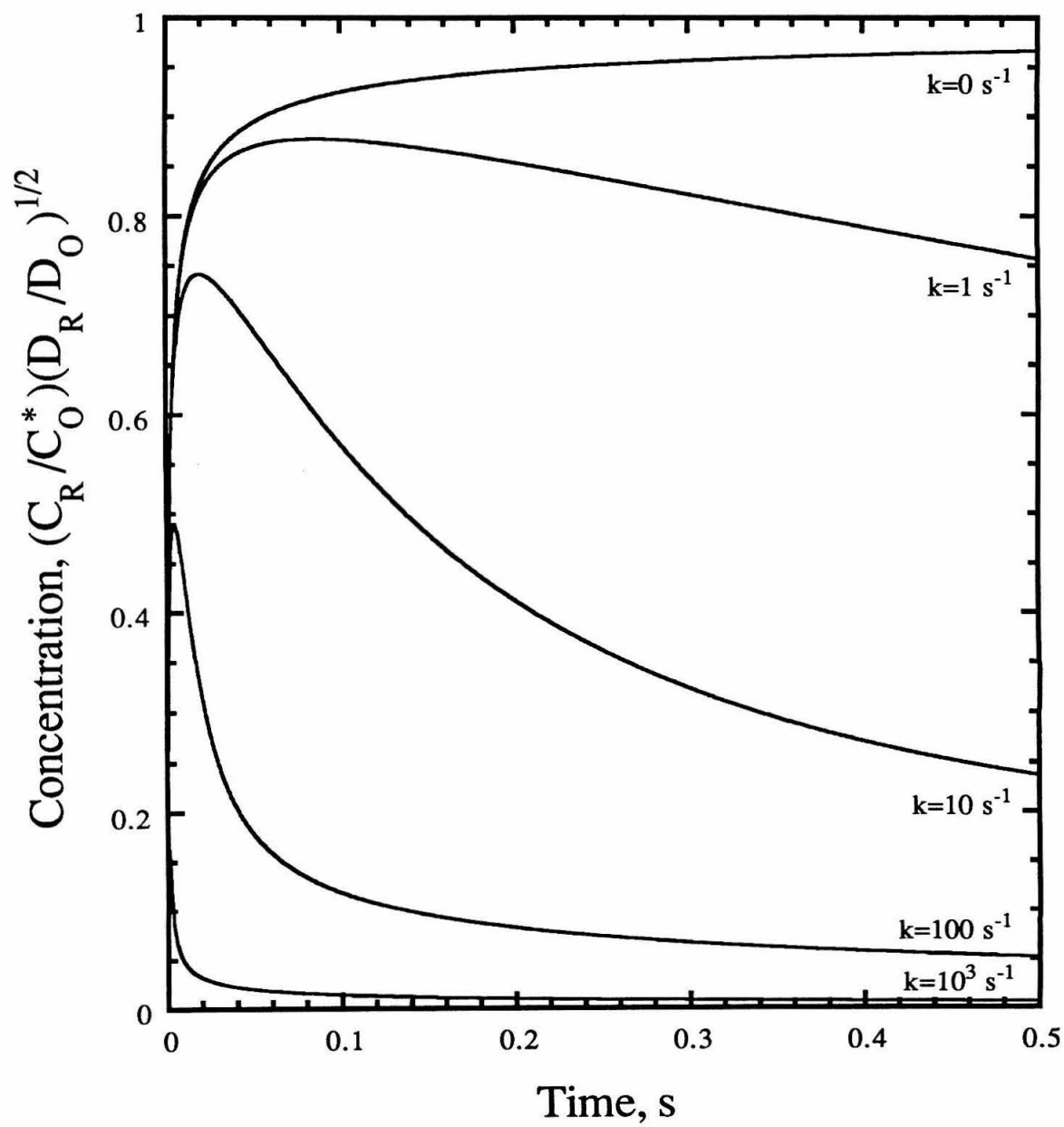


Figure 3.5d

Simulated concentration vs. time curves at $x = 5 \mu\text{m}$ of an intermediate species R generated at a planar electrode undergoing a potentiostatic step with $D_O = 5 \times 10^{-6} \text{cm}^2/\text{s}$.

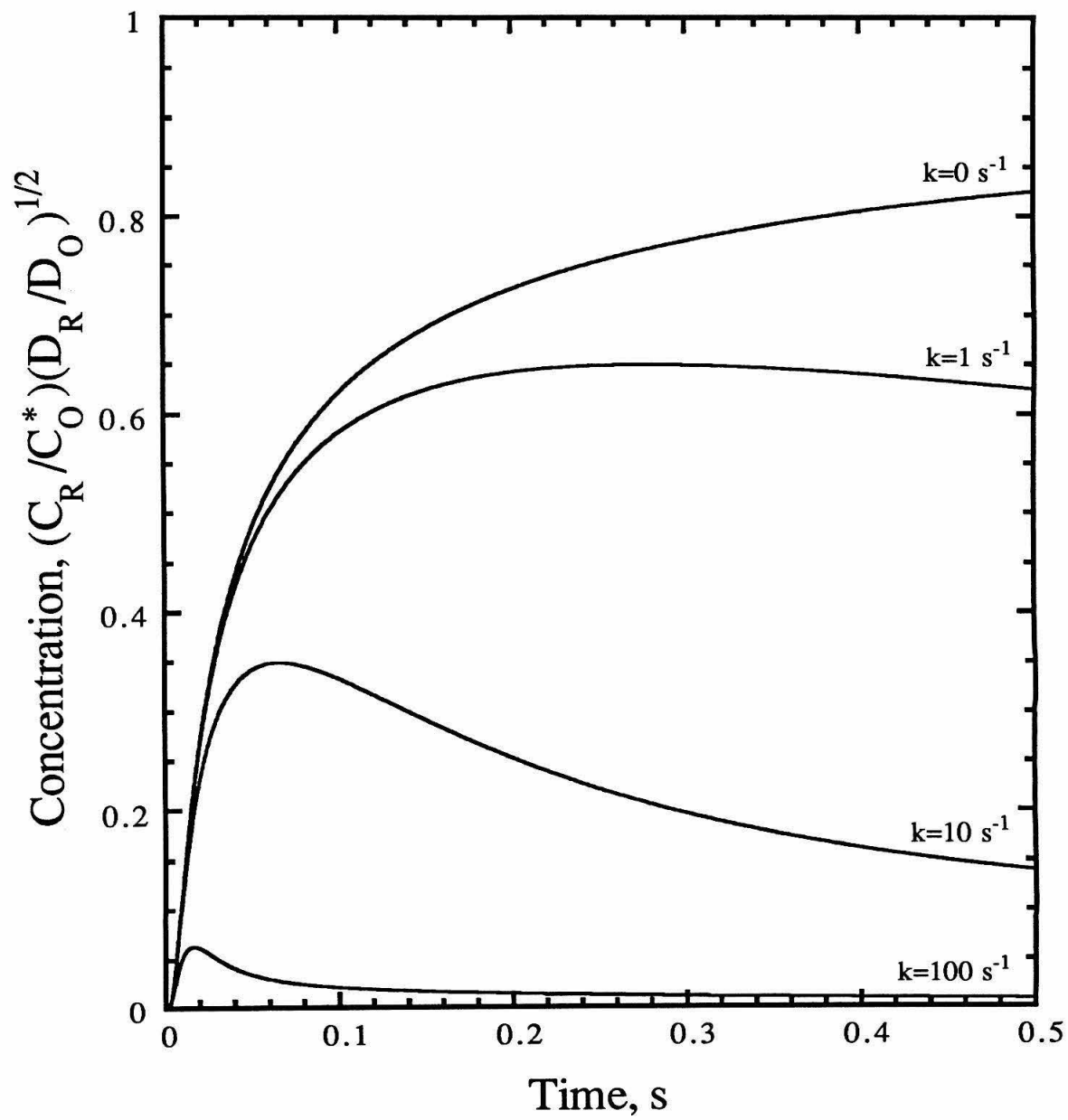
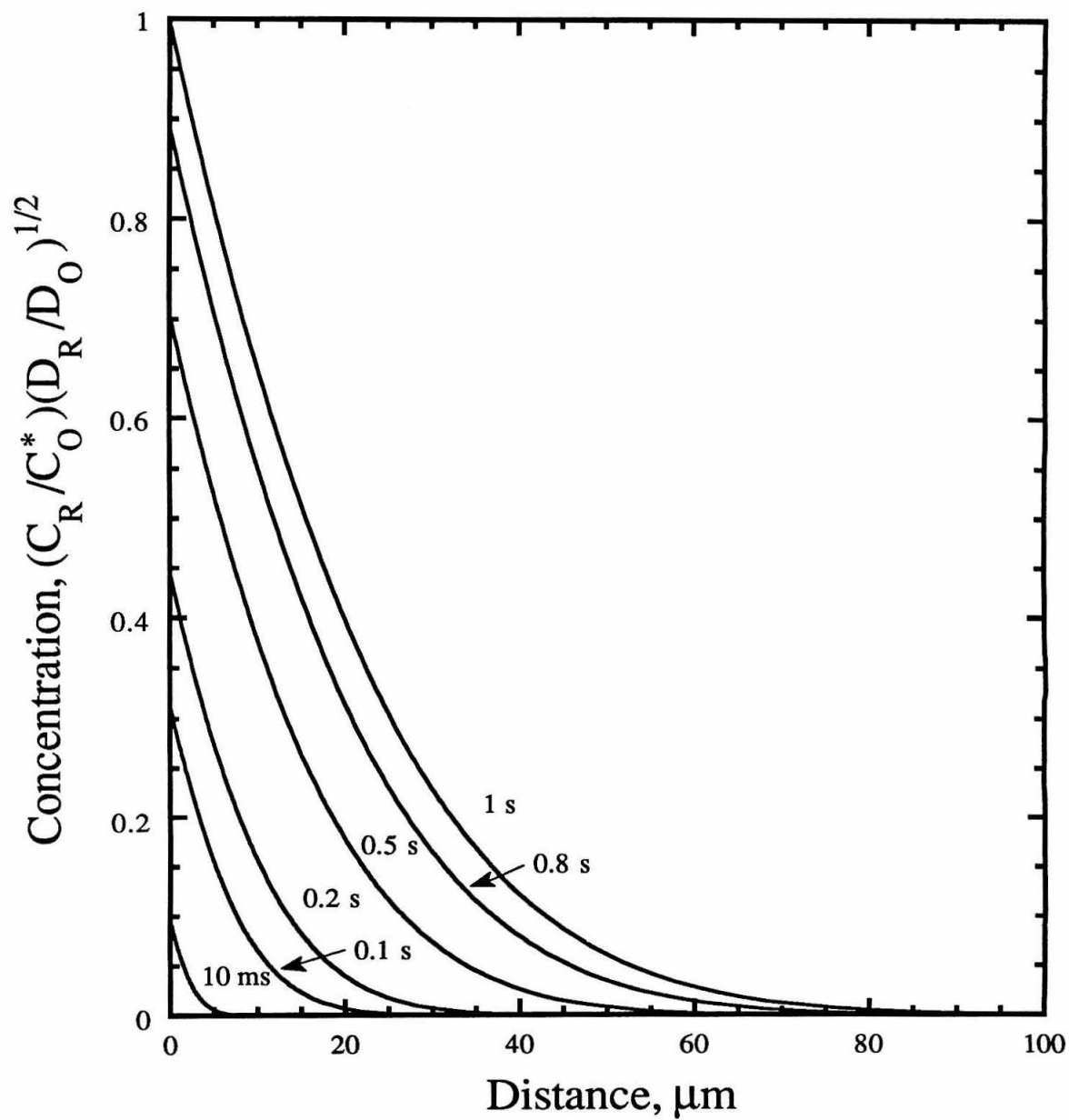


Figure 3.6

Concentration profiles of species R generated at a planar electrode undergoing a galvanostatic step. Plotted at various times with $\tau = 1$ s and $D_O = 5 \times 10^{-6} \text{cm}^2/\text{s}$.



The figure area is mostly blank, suggesting the plot content is either missing or rendered as a very faint image. The text below describes the parameters of the plot.

Figure 3.7

Concentration profiles of species R generated at a planar electrode undergoing a galvanostatic step. Plotted at various times with $\tau = 1$ s and $D_O = 5 \times 10^{-6} \text{cm}^2/\text{s}$.

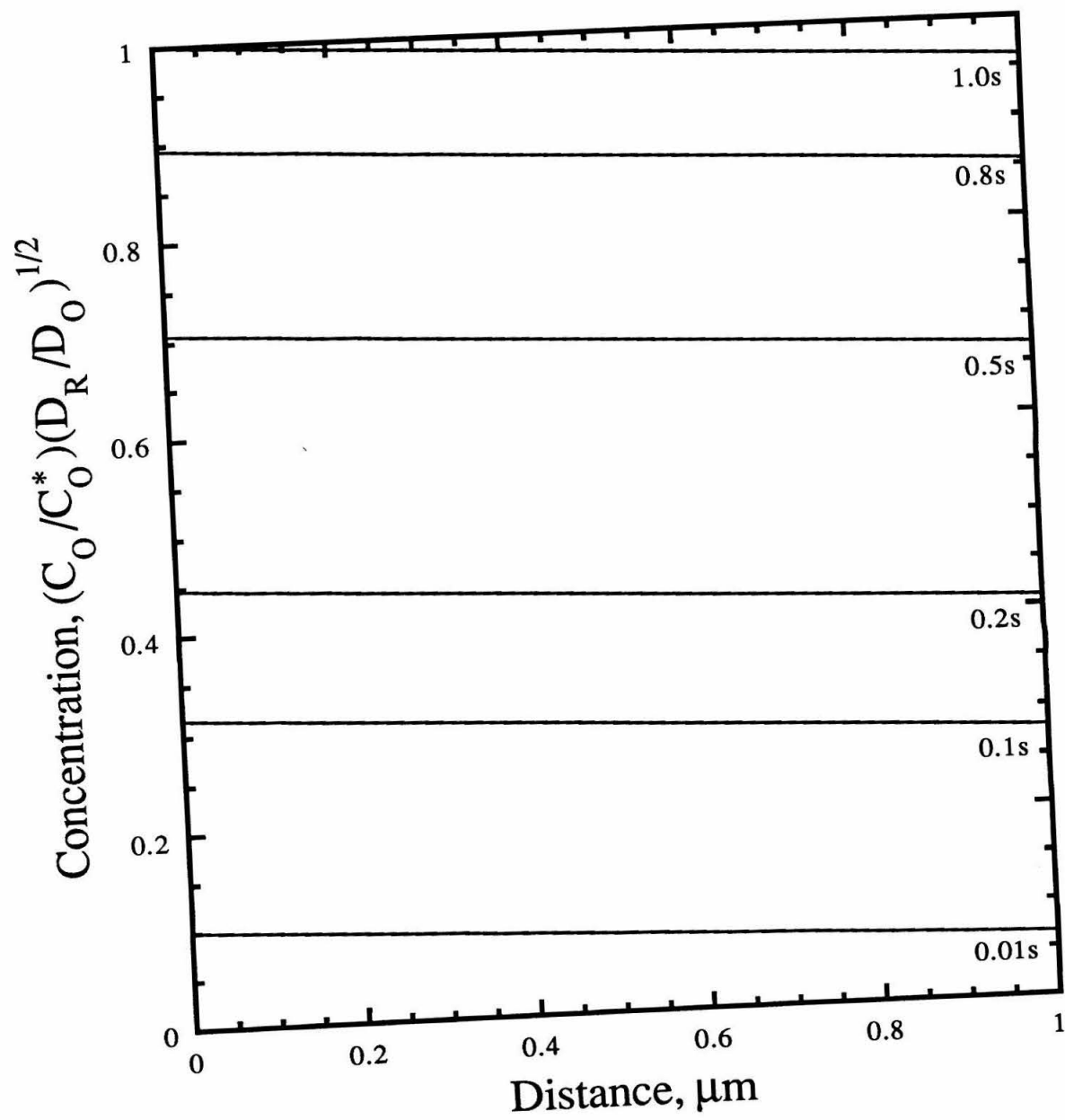


Figure 3.8

Concentration vs. time of species R generated at a planar electrode undergoing a galvanostatic step. Plotted at various distances with $\tau = 1$ s and $D_O = 5 \times 10^{-6} \text{cm}^2/\text{s}$.

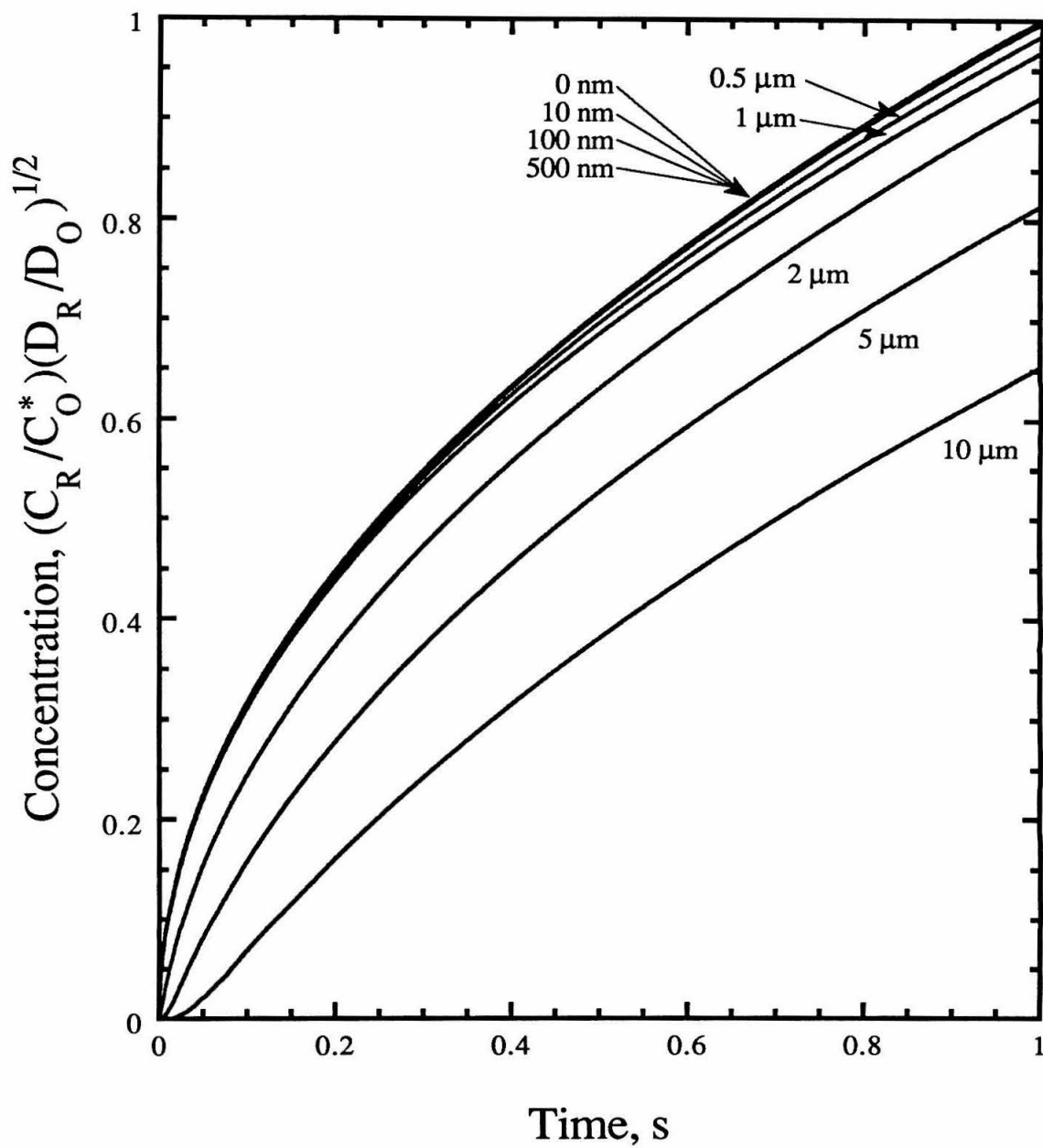


Figure 3.9

Concentration profiles showing the approach to steady-state of an intermediate species R generated at a planar electrode undergoing a galvanostatic step with $\tau = 1$ s, $D_O = 5 \times 10^{-6} \text{ cm}^2/\text{s}$, and $k = 5 \text{ s}^{-1}$.

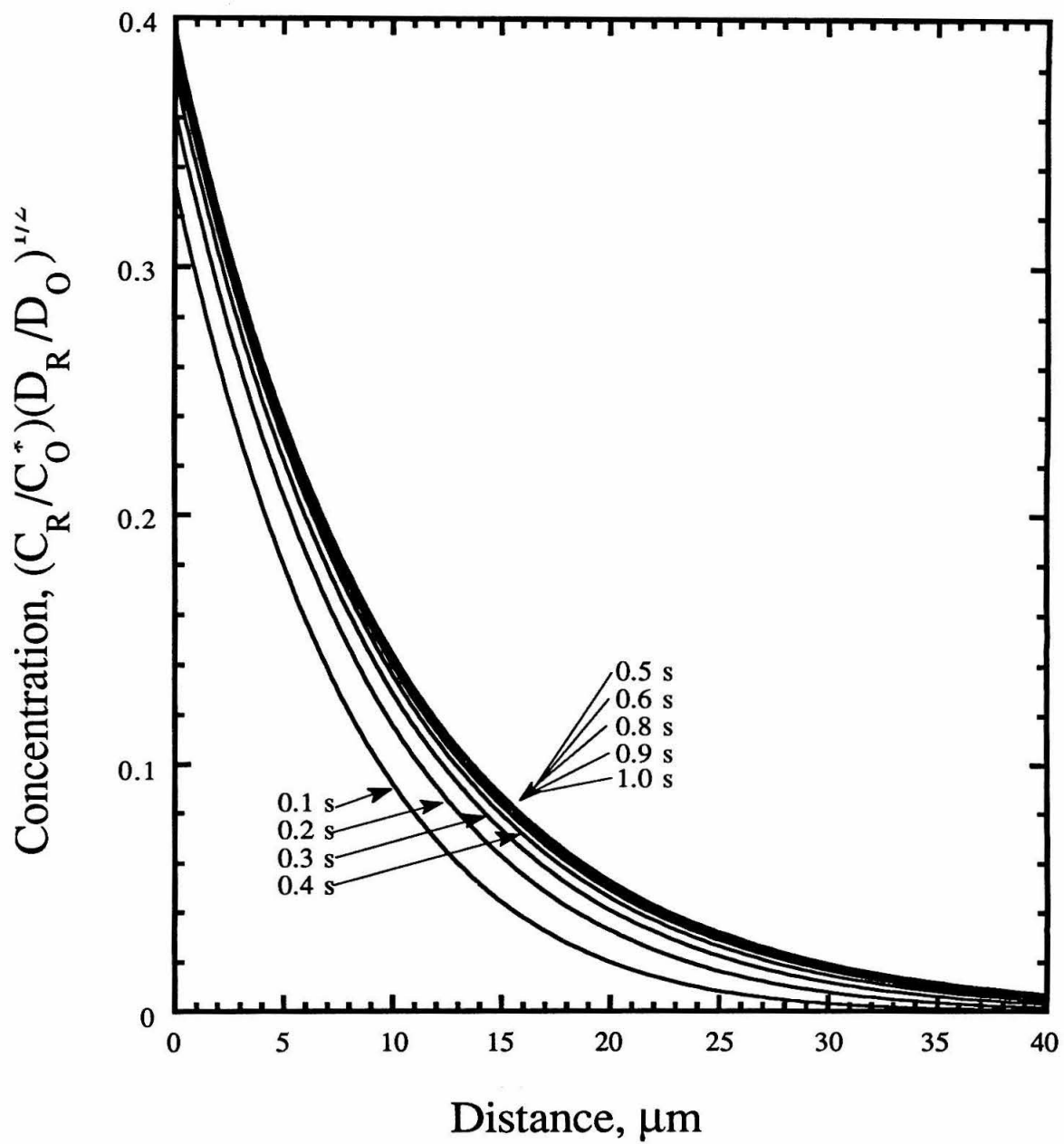


Figure 3.10a

Steady-state concentration profiles for intermediate R generated at a planar electrode undergoing a galvanostatic step at $t=\tau=1$ s and with $D_O=5\times 10^{-6}\text{cm}^2/\text{s}$, and k as indicated.

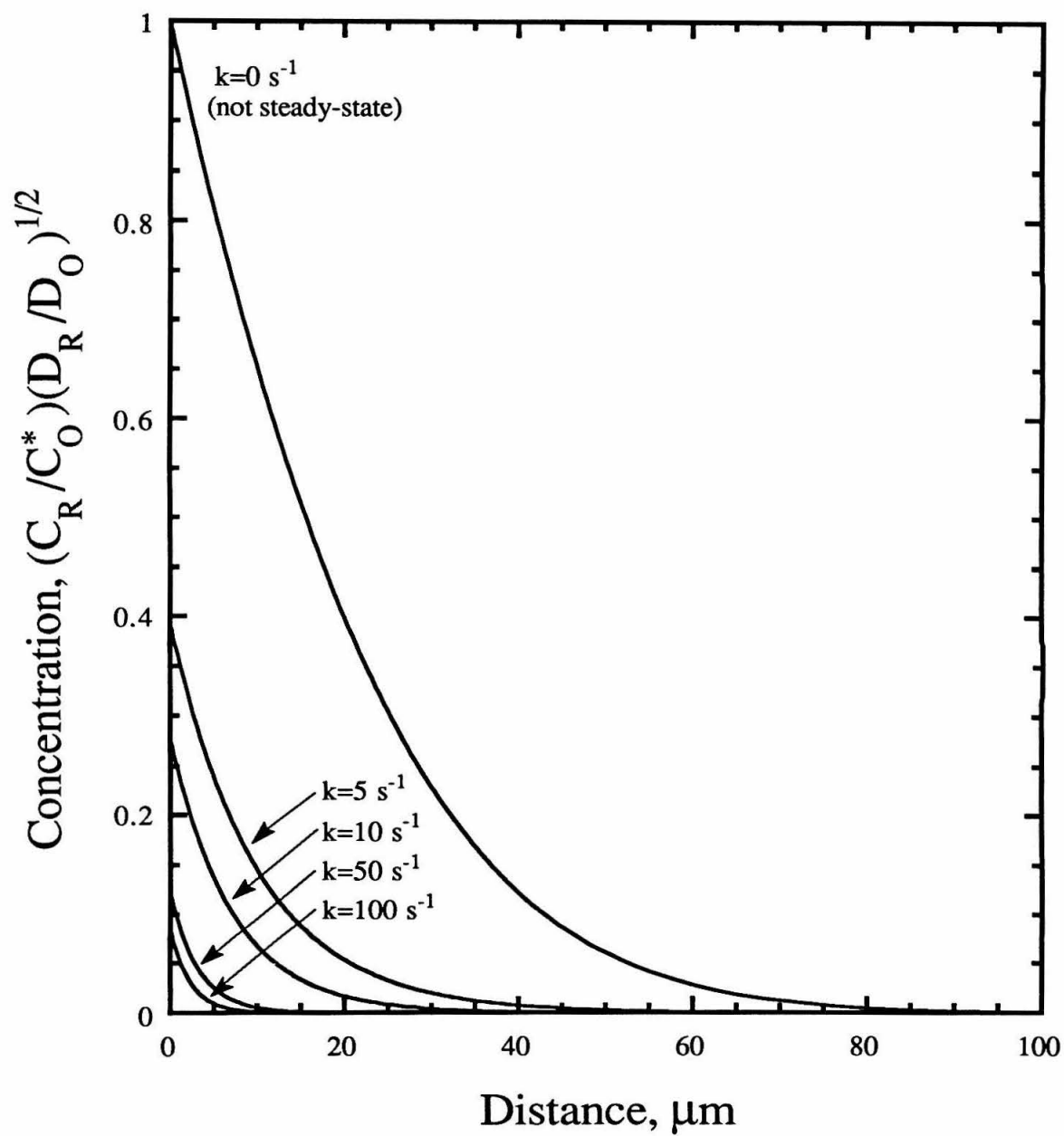


Figure 3.10b

Steady-state concentration profiles for intermediate R generated at a planar electrode undergoing a galvanostatic step at $t=\tau=1$ s and with $D_O=5 \times 10^{-6} \text{cm}^2/\text{s}$, and k as indicated.

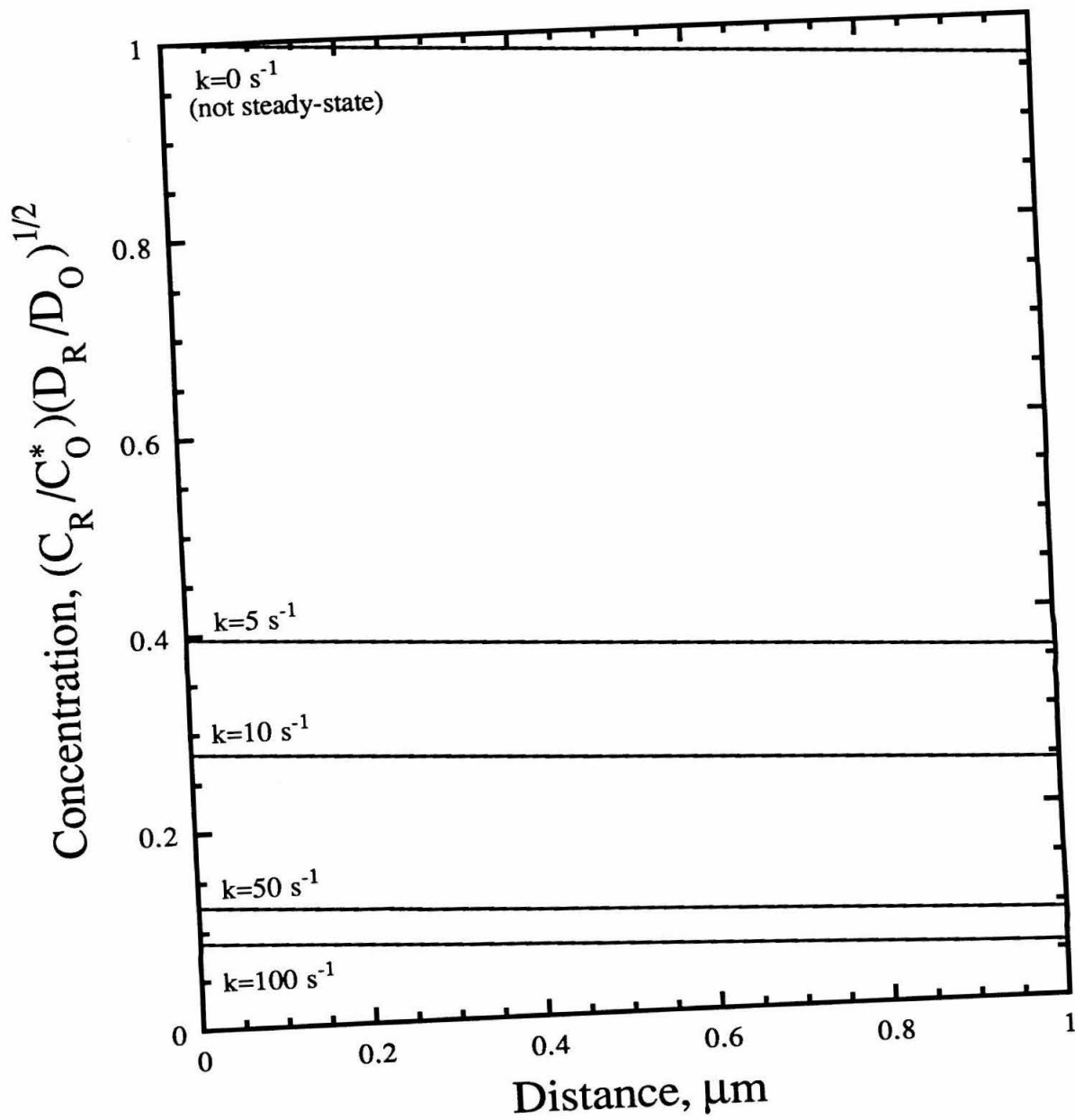


Figure 3.11

Steady-state concentration profiles for intermediate R generated at a planar electrode undergoing a galvanostatic step at $t=\tau=10$ ms and with $D_O=5\times 10^{-6}\text{cm}^2/\text{s}$, and k as indicated.

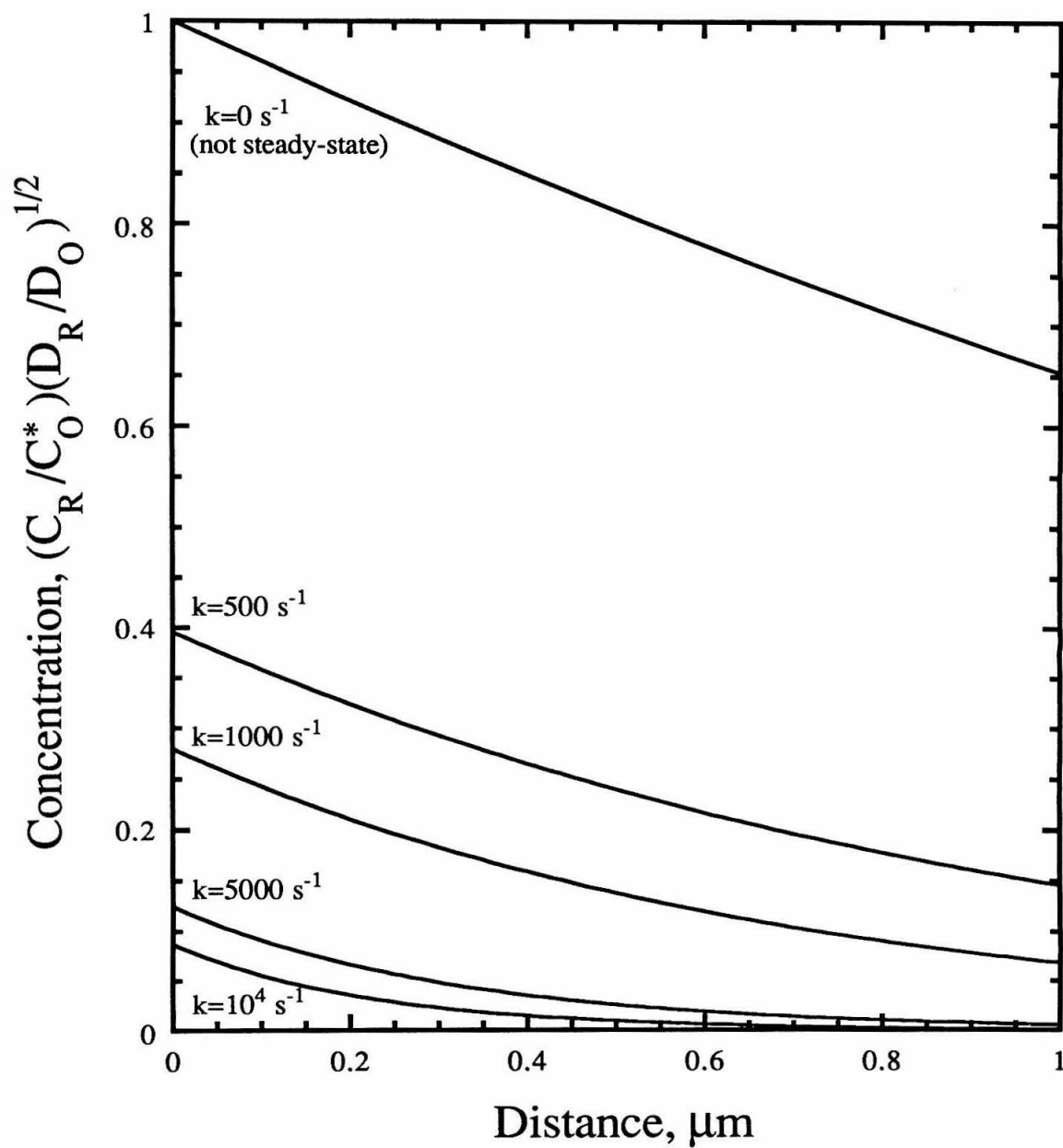


Figure 3.12a

Simulated concentration versus time curves at $x = 7$ nm of an intermediate R generated at a planar electrode undergoing a galvanostatic step with $\tau = 10$ ms, $D_O = 5 \times 10^{-6} \text{ cm}^2/\text{s}$, and k as indicated.

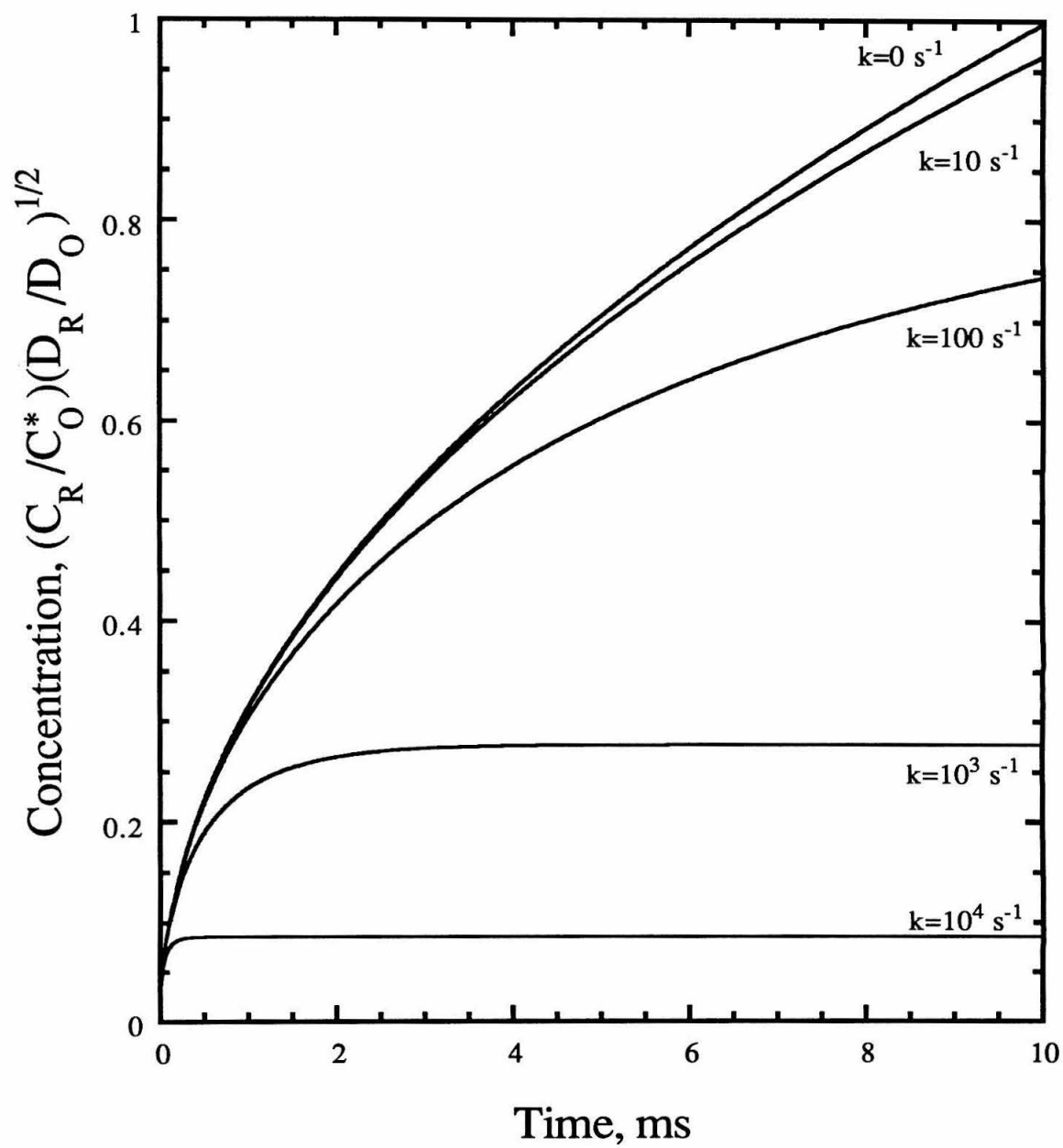


Figure 3.12b

Simulated concentration versus time curves at $x = 0.1 \mu\text{m}$ of an intermediate R generated at a planar electrode undergoing a galvanostatic step with $\tau = 10 \text{ ms}$, $D_{\text{O}} = 5 \times 10^{-6} \text{ cm}^2/\text{s}$, and k as indicated.

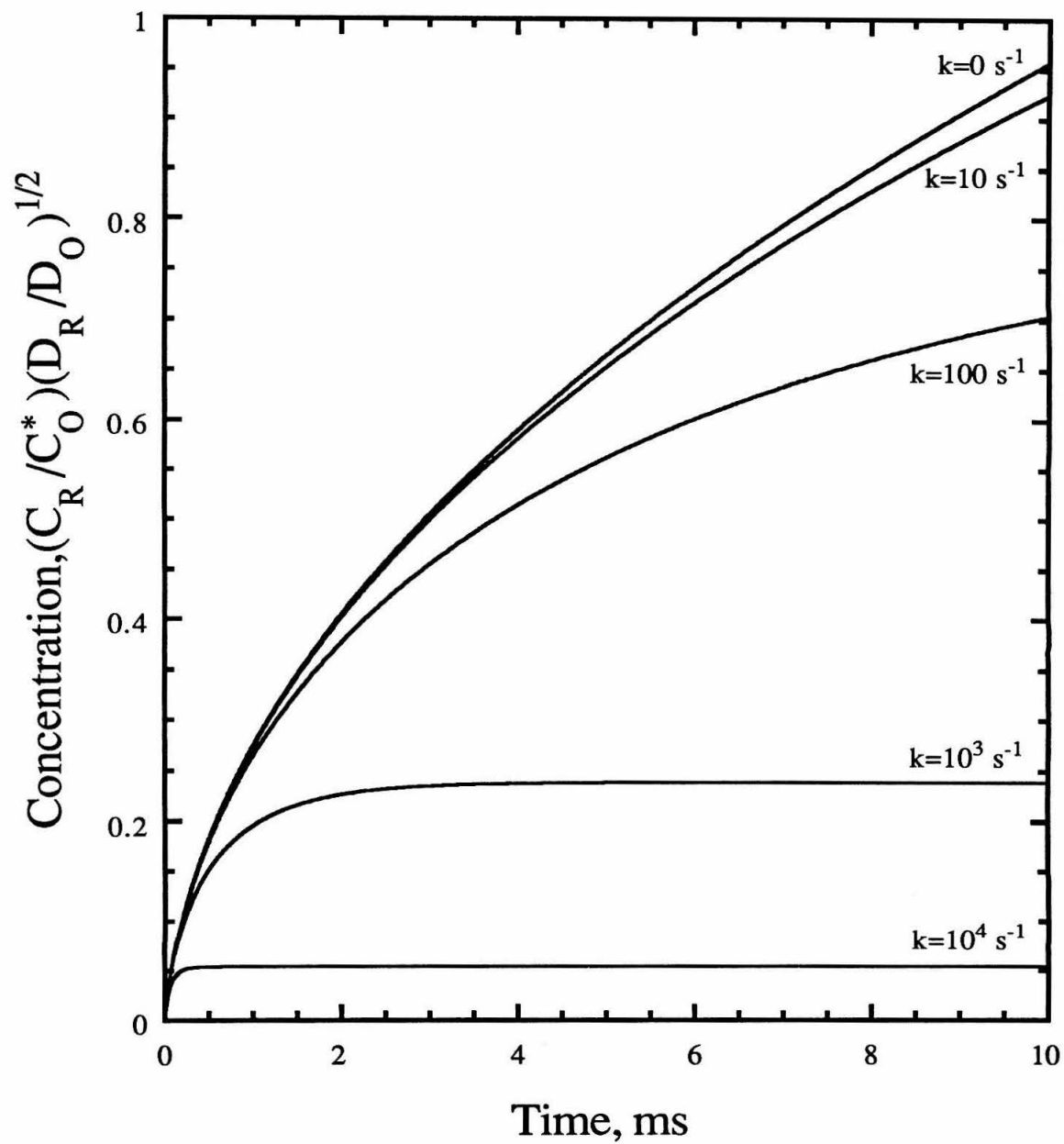
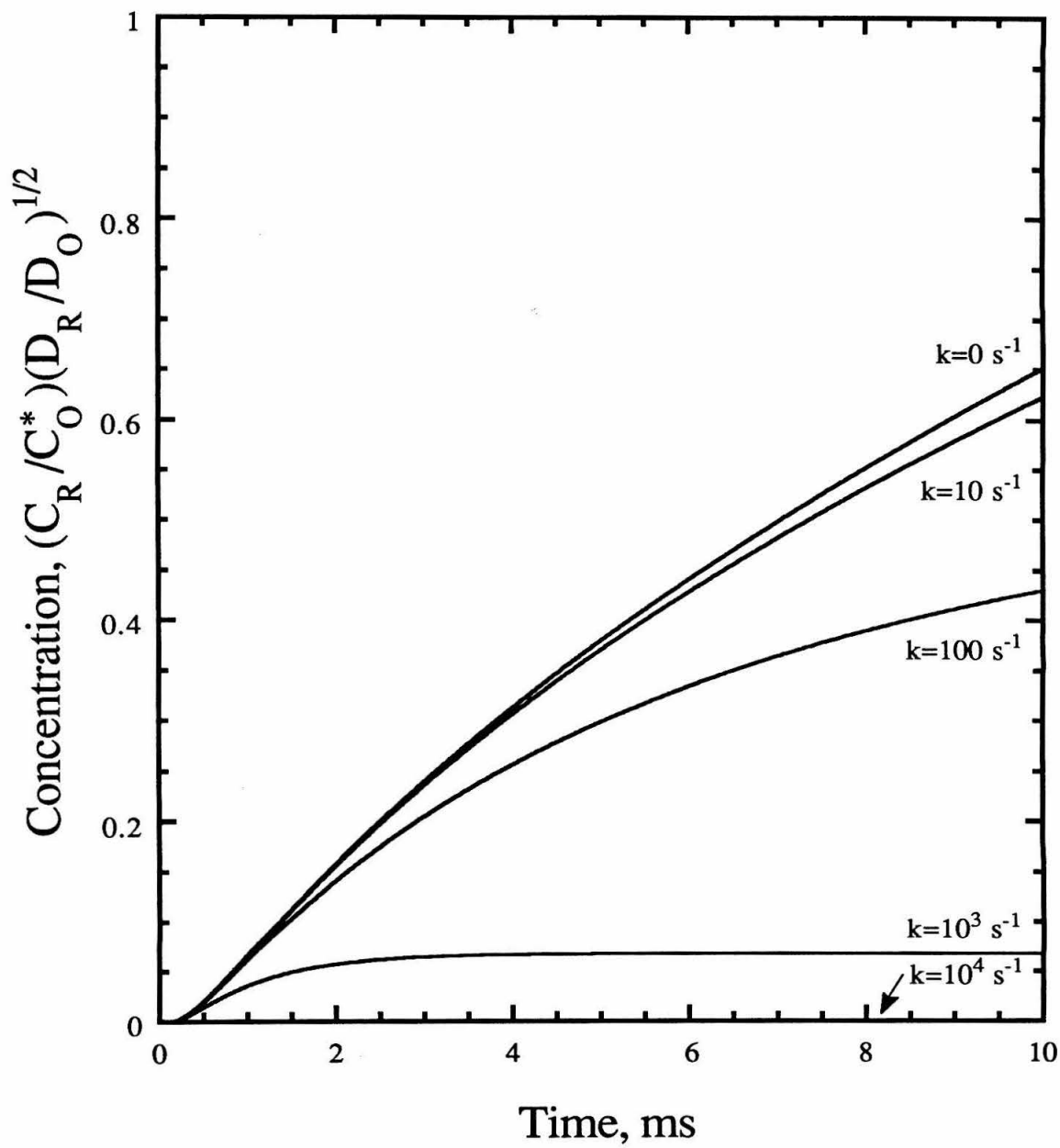


Figure 3.12c

Simulated concentration versus time curves at $x = 1 \mu\text{m}$ of an intermediate R generated at a planar electrode undergoing a galvanostatic step with $\tau = 10 \text{ ms}$, $D_O = 5 \times 10^{-6} \text{ cm}^2/\text{s}$, and k as indicated.



Appendix: Programs

The following programs POTSTEP and GALSTEP simulate the diffusion layer at a planar electrode following a potential or galvanostatic step. The diffusion layers of reactant intermediate and final product involved in a following first-order chemical reaction are modeled. The programs are written in FORTRAN and compiled with Microsoft FORTRAN Compiler Version 5.0 (Renton, WA). When run on a personal computer with a 386 processor (16 MHz) with a co-processor, circa 2 hours are necessary to run 50,000 iterations.

POTSTEP

The program will prompt the user for the following information:

Diffusion coefficient (different values possible for product, intermediate
and reactant)

Number of electrons involved

Number of iterations

Time increment per iteration

Rate constant (first-order)

file name

In order to save file space during long simulations, the user has the option of only recording some of the data (concentration versus time files only). The user will be prompted to partition the simulation into "early time" and "late time." All data is recorded during "early time" and the user selects the interval to write "late time" data to files.

The program collects the concentration profile data at ten equally spaced intervals during the simulation (plus one file after the first iteration) Data may also be stored for a given position. The user is prompted to provide the distance of interest. The closest "box" will be chosen and its position is displayed. The electrode is centered in the middle of the first box and times are recorded for the middle of the iteration.

```

PROGRAM POTSTEP
* Russ needs potentiostat, diffusion, unimolecular kinetics
* Determines the conc. vs t profiles at selected distances and conc vs x
* profiles
* Modified to conform with Maloy
* Modified to write more points at closer distances or shorter times
* calculates diffusion and kinetics on old array(Feldberg).
* Allows use of different D's for the species
* last modified 920513 by RJP
*****1
implicit real(a - y)
implicit double precision (z)
integer i,mt,imt,wrcondiv,N,boxnum(100),NBOXWR,wr_var,earlytp
integer earlyt,lt_expan
character filnam * 12, chlb1 * 1, chlb2 * 1

COMMON /concent/ c1old(999), c1new(999), C2OLD(999), c2new(999)
COMMON /concent/ c3old(999), c3new(999)
COMMON /WR/ wrcondiv,wr_var,filnam,mt,DELTAT,DELTAX,IMT,MTMAX,k
COMMON/ WR/ earlyt,lt_expan
COMMON /SURF/ DELTAC1S, DELTAC2S, DELTAC3S, N, F, D1, D2, D3
COMMON /FW2/LABEL,LABELB,NBOXWR,BOXNUM

do 1100 i=1,999
c1old(I) = 1
c1new(I) = 1
C2OLD(I) = 0
c2new(I) = 0
DC2 = 0
1100 CONTINUE
LABEL=1
LABELB=0
write(*,*)' INPUT PARAMTERS: '
write(*,*)'defaults (1) or input from keyboard (2)'
write(*,*)'D1=6.6e-6 (cm^2/s)'
write(*,*)'D2=8.0e-6 (cm^2/s)'
write(*,*)'D3=6.6e-6 (cm^2/s)'
write(*,*)'deltat = 1e-4 (s)'
write(*,*)'total number of time iterations = 50000'
write(*,*)'n=1'
read(*,*)dork
if (dork.eq.1)then
D1 = .0000066
D2 = .000008
D3 = .0000066
DELTAT = .0001
mtmax = 50000
* N = 1
else
write(*,*)'DIFFUSION COEFFICIENT D1 (cm^2/s)'
read (*,*)D1
write(*,*)'DIFFUSION COEFFICIENT D2 (cm^2/s)'
read (*,*)D2
write(*,*)'DIFFUSION COEFFICIENT D3 (cm^2/s)'
read (*,*)D3

8100 format (a20)
write (*,*)'deltat (s)'

```

```

read(*,*)deltat

write(*,*)'total number of time points'
read(*,*)mtmax
*   WRITE(*,*)'VALUE FOR N?'
*   READ(*,*)N
endif

write(*,*)'k = 5 s^-1 '
write(*,*)'defaults (1) or input from keyboard (2) '
read(*,*)dork
if (dork.eq.1)then
k = 5
else
WRITE(*,*)'RATE CONSTANT K (s^-1)'
read(*,*)k
endif
tmax = mtmax * DELTAT
DELTAx = sqrt(D2 * DELTAT / .45)
WRITE(*,*)'INPUT NAME OF STEM OF OUTPUT'
READ(*, '(A)')FILNAM

write(*,*)'enter early time (i.e. % of total time when all points are
care written)'
read(*,*)earlytp
earlyt = (earlytp * mtmax)/100
write(*,*)'Enter interval at which to store data at late times'
read(*,*)lt_expan

write(*,*)'At what x points do you want the conc. as a function of
c time? Defaults are:'
write(*,*)'Middle of 1st box:0 (this first position is taken as
c "surface" conc.)'
write(*,*)'At middle of 2nd box',1*deltax
write(*,*)'          3rd box',2*deltax
write(*,*)'          4th box',3*deltax
write(*,*)'          5th box',4*deltax
write(*,*)'          6th box',5*deltax
write(*,*)
write(*,*)'Enter 1 for defaults, 0 for your own choices'
read(*,*)writex
if(writex.eq.1)then
NBOXWR=6
boxnum(1)=1
boxnum(2)=2
boxnum(3)=3
boxnum(4)=4
boxnum(5)=5
boxnum(6)=6
else
write(*,*)'How many boxes do you want to store as function
c of time?'
read(*,*)nboxwr
do 1400 nb=1,nboxwr
write(*,*)'enter position in cm'
read(*,*)boxpos
boxnum(nb)=nint((boxpos/deltax)+1)
if(boxnum(nb).eq.0)boxnum(nb)=1
write(*,*)'closest calculated is ',(boxnum(nb)-1)*deltax
1400 continue

```

```

endif

*      F = 96485
      write(*,*)'stores 10 conc profiles '
      WRCONDIV = mtmax / 10
* TOP OF TIME ITERATIONS
do 1000 mt=1,mtmax
* CALCULATE CONC AT SURFACE DUE TO POTENTIOSTAT
C2OLD(1) = C1OLD(1) + C2OLD(1)
C1OLD(1) = 0
      xmax = 6 * sqrt(.4 * mt)
      IMT = 6 * sqrt(.4 * mt) + 1
*USING IMT CALCUALTION PER MALOY:
      IMT = 3*sqrt(2 * mt) + 1
      if (mt .eq.1)write(*,*)' mt =1 '
      call write
      CALL DIFFUSE
* do kinetics
do 200 i=1,imt
DC2 = -k * C2old(I) * DELTAT
c2new(I) = c2new(I) + DC2
c3new(I) = c3new(I) - DC2

200    CONTINUE
      do 256 i = 1,imt
      c1old(I) = c1new(I)
      C2OLD(I) = c2new(I)
      c3old(I) = c3new(I)
256    CONTINUE
1000   CONTINUE
      END
*****
C -----
SUBROUTINE DIFFUSE
implicit real(a - y)
implicit double precision (z)
integer i, mt,imt,wrcondiv,wr_var,N,earlyt,lt_expan
character filnam * 12, chlb1 * 1, chlb2 * 1

COMMON /concent/ c1old(999), c1new(999), C2OLD(999), c2new(999)
COMMON /concent/ c3old(999), c3new(999)
COMMON /WR/ wrcondiv,wr_var,filnam,mt,DELTAT,DELTAX,IMT,MTMAX,k
COMMON /WR/ earlyt,lt_expan
COMMON /SURF/ DELTAS, DELTAC2S, DELTAC3S, N, F, D1, D2, D3
*CALCULATION FOR SURFACE

      Dstar1 = D1 * DELTAT / (DELTAX * DELTAX)
      c1new(1) = C1OLD(1) + Dstar1 * (C1OLD(2) - C1OLD(1))
      if (c1new(1) .lt.0)then
      write(*,*)'c1new went less than zero Danger Danger'
      c1new(1) = 1E-18
      END IF

      Dstar2 = D2 * DELTAT / (DELTAX * DELTAX)
      c2new(1) = C2OLD(1) + Dstar2 * (C2OLD(2) - C2OLD(1))
      if (c2new(1) .lt.0)then
      write(*,*)'c2new went less than zero Danger Danger'
      c2new(1) = 1E-18
      END IF

```

```

Dstar3 = D3 * DELTAT / (DELTAX * DELTAX)
c3new(1) = C3OLD(1) + Dstar3 * (C3OLD(2) - C3OLD(1))
if (c3new(1) .lt.0)then
write(*,*)'c3new went less than zero Danger Danger'
c3new(1) = 1E-18
END IF

* for the rest of the boxes, use eqs 12 and 13.

do 200 i=2,imt
deltac1=Dstar1*((C1OLD(I+1)-C1OLD(I))-(C1OLD(I)-C1OLD(I-1)))
c1new(I) = C1OLD(I) + deltac1
if(c1new(i).lt.0)then
write(*,*)'oops c1new(i) went less than zero concentration,i =',i
c1new(I) = 1E-18
END IF

deltac2=Dstar2*((C2OLD(I+1)-C2OLD(I))-(C2OLD(I)-C2OLD(I-1)))
c2new(I) = C2OLD(I) + deltac2
if(c2new(i).lt.0)then
write(*,*)'oops c2new(i) went less than zero concentration,i =',i
c2new(I) = 1E-18
END IF

deltac3=Dstar3*((C3OLD(I+1)-C3OLD(I))-(C3OLD(I)-C3OLD(I-1)))
c3new(I) = C3OLD(I) + deltac3
if(c3new(i).lt.0)then
write(*,*)'oops c3new(i) went less than zero concentration,i =',i
c3new(I) = 1E-18
END IF

200 continue
RETURN
END

*****
SUBROUTINE WRITE
implicit real(a - y)
implicit double precision (z)
integer i, mt,imt,wrcondiv,wr_var,N,BOXNUM(100),NBOXWR,NB2,earlyt
integer lt_expan
character filnam*12,chl1*1,chl2*1,CHLB3*1,CHLB4*1

COMMON /concent/ c1old(999), c1new(999), C2OLD(999), c2new(999)
COMMON /concent/ c3old(999), c3new(999)
COMMON /WR/ wrcondiv,WR_var,filnam,mt,DELTAT,DELTAX,IMT,MTMAX,k
COMMON /WR/ earlyt,lt_expan
COMMON /SURF/ DELTAC1S, DELTAC2S, DELTAC3S, N, F, D1, D2, D3
COMMON /FW2/LABEL,LABELB,NBOXWR,BOXNUM

* write nnew(i) to file if mt/WRCONDIV is appropriate. 10/26/87
wr_var = int(1 + (mt/lt_expan))
IF (mt.eq.1) THEN
open(4,file=filnam//'.C01')
write(4,*)' Dist.(cm) Reactant Product:echem Product:kinetic'
write(4,*)filnam//'.c01','',(mt-0.5)*deltat, k, D1, D2, D3
DO 1330 I=1,IMT
WRITE(4,*) (I-1)*DELTAX,c1old(I),C2OLD(I),c3old(I)
1330 CONTINUE
CLOSE (4)

```

```

END IF

if(mod(mt,wrcondiv).eq.0)then
write(*,*)'writing file at t= ',(mt-0.5)*deltat
label = label + 1
label1 = label / 10
label2 = mod(label,10)
ch1b1 = char(label1 + 48)
ch1b2 = char(label2 + 48)
open(4,file=filnam//'.C'//ch1b1//ch1b2)
write(4,*)' Dist.(cm) Reactant Product:echem Product:kinetic'
write(4,*)mt,(mt-0.5)*deltat, k, D1, D2, D3
886 format(1x,a12,e9.4,1x,e9.4)
887 format(1x,e9.4,1x,e9.4,1x,e9.4,1x,e9.4,a1,i3)
DO 1300 I=1,IMT
wr_var = int(1 +(I/lt_expan))
IF((I.lt.earlyt).or.mod(I,wr_var).eq.0)THEN
WRITE(4,*) (I-1)*DELTAX,c1old(I),C2OLD(I),c3old(I)
END IF
1300 CONTINUE
CLOSE (4)
END IF
882 format (a)
* FOR ALL TIMES WRITE THE CHOSEN BOXES
IF(MT.EQ.1)THEN
DO 1355 NB2=1,NBOXWR
labelB = labelB + 1
labelB1 = labelB / 10
labelB2 = mod(labelB,10)
CHLB3 = char(labelB1 + 48)
ch1B4 = char(labelB2 + 48)
open(NB2+7,file=filnam//'.X'//CHLB3//ch1B4)
write(NB2+7,*)' t (s) Reactant Product:echem Product:kinetic'
write(NB2+7,*)boxnum(nb2), (boxnum(nb2)-1)*deltax, k, D1, D2, D3
1355 CONTINUE
ENDIF
*FOR ALL TIMES:
wr_var = int(1 + (MT/lt_expan))
if(wr_var.ge.100)then
wr_var = 100
end if
IF((mt.lt.earlyt).or.mod(mt,wr_var).eq.0)THEN
DO 1375 NB2=1,NBOXWR
WRITE(NB2+7,*) ((MT-0.5)*DELTAT),c1old(boxnum(nb2)),
* C2OLD(BOXNUM(NB2)), c3old(boxnum(nb2))
1375 CONTINUE
ENDIF
IF (MT.EQ.MTMAX) THEN
DO 1365 NB2=1,NBOXWR
CLOSE(NB2)
1365 CONTINUE
ENDIF
RETURN
END

```

GALSTEP

The program uses the same diffusion and file writing routines as POTSTEP. The user will be prompted to provide the transition time (τ) of the galvanostatic step. The time increment for each iteration is $\tau/\text{number of iterations}$. In this simulation, the electrode surface is located at the edge of the box.

```

PROGRAM GALSTEP
* Russ needs galvanostat, diffusion, unimolecular kinetics
* Determines the conc. vs t profiles at selected distances
* and conc vs x profiles
* Modified to conform with Maloy
* Modified to write more points at closer distances or shorter times
* calculates diffusion and kinetics on old array(Feldberg).
* Allows use of different D's for the species
* last modified 920513 by RJP
*****1
implicit real(a - y)
implicit double precision (z)
integer i,mt,imt,wrcondiv,N,boxnum(100),NBOXWR,wr_var,earlytp
integer earlyt,lt_expan
character filnam * 12, chlb1 * 1, chlb2 * 1
parameter (pi=3.141592654)

COMMON /concent/ c1old(999), c1new(999), C2OLD(999), c2new(999)
COMMON /concent/ c3old(999), c3new(999), tau, sigma
COMMON /WR/ wrcondiv,wr_var,filnam,mt,DELTAT,DELTAX,IMT,MTMAX,k
COMMON/ WR/ earlyt,lt_expan
COMMON /SURF/ DELTAC1S, DELTAC2S, DELTAC3S, N, F, D1, D2, D3
COMMON /FW2/LABEL,LABELB,NBOXWR,BOXNUM

do 1100 i=1,999
c1old(I) = 1
c1new(I) = 1
C2OLD(I) = 0
c2new(I) = 0
DC2 = 0
1100 CONTINUE
LABEL=1
LABELB=0
write(*,*)' INPUT PARAMTERS: '
write(*,*)'defaults (1) or input from keyboard (2) '
write(*,*)'D1=5.0e-6 (cm^2/s)'
write(*,*)'D2=5.0e-6 (cm^2/s)'
write(*,*)'D3=5.0e-6 (cm^2/s)'
write(*,*)'transition time (tau)= .01 (s)'
write(*,*)'total number of time iterations = 50000'
write(*,*)'n=1'
read(*,*)dork
if (dork.eq.1)then
D1 = .000005
D2 = .000005
D3 = .000005
tau = .01
mtmax = 50000
N = 1
else
write(*,*)'DIFFUSION COEFFICIENT D1 (cm^2/s)'
read (*,*)D1
write(*,*)'DIFFUSION COEFFICIENT D2 (cm^2/s)'
read (*,*)D2
write(*,*)'DIFFUSION COEFFICIENT D3 (cm^2/s)'
read (*,*)D3

8100 format (a20)

```

```

write (*,*)'tau (s)'
read(*,*)tau

write(*,*)'total number of time points'
read(*,*)mtmax

write(*,*)'value for n?'
read(*,*)n
endif

write(*,*)'k = 5 s^-1 '
write(*,*)'defaults (1) or input from keyboard (2)'
read(*,*)dork
if (dork.eq.1)then
k = 5
else
WRITE(*,*)'RATE CONSTANT K (s^-1)'
read(*,*)k
endif

deltat = tau / mtmax
tmax = mtmax * DELTAT
DELTAx = sqrt(D2 * DELTAT / .45)
* change in conc. in first box due to echem:
sigma = sqrt(.45 * pi / (4 * mtmax))

WRITE(*,*)'INPUT NAME OF STEM OF OUTPUT'
READ(*, '(A)')FILNAM

write(*,*)'enter early time (i.e. % of total time when all
c points are are written)'
read(*,*)earlytp
earlyt = (earlytp * mtmax)/100
write(*,*)'Enter interval at which to store data at late times'
read(*,*)lt_expan

write(*,*)'At what x points do you want the conc. as a function of
c time? Defaults are:'
write(*,*)'Middle of 1st box (this first position is taken as
c "surface" conc.)',0.5*deltax
write(*,*)'At middle of 2nd box',1.5*deltax
write(*,*)' 3rd box',2.5*deltax
write(*,*)' 4th box',3.5*deltax
write(*,*)' 5th box',4.5*deltax
write(*,*)' 6th box',5.5*deltax
write(*,*)
write(*,*)'Enter 1 for defaults, 0 for your own choices'
read(*,*)writex
if(writex.eq.1)then
NBOXWR=6
boxnum(1)=1
boxnum(2)=2
boxnum(3)=3
boxnum(4)=4
boxnum(5)=5
boxnum(6)=6
else
write(*,*)'How many boxes do you want to store as function
c of time?'
read(*,*)nboxwr

```

```

do 1400 nb=1,nboxwr
  write(*,*)'enter position in cm'
  read(*,*)boxpos
  boxnum(nb)=nint((boxpos/deltax)+1)
  if(boxnum(nb).eq.0)boxnum(nb)=1
  write(*,*)'closest calculated is ',(boxnum(nb)-.5)*deltax
1400  continue
endif

write(*,*)'stores 10 conc profiles '
WRCONDIV = mtmax / 10
* TOP OF TIME ITERATIONS
do 1000 mt=1,mtmax
* CALCULATE CONC AT SURFACE DUE TO GALVANOSTAT
C2OLD(1) = C2OLD(1) + sigma
C1OLD(1) = C1OLD(1) - sigma
  xmax = 6 * sqrt(.4 * mt)
*   IMT = 6 * sqrt(.4 * mt) + 1
*USING IMT CALCUALTION PER MALOY:
  IMT = 3*sqrt(2 * mt) + 1
  if (mt .eq.1)write(*,*)' mt =1 '
  call write
  CALL DIFFUSE
* do kinetics
  Do 200 i=1,imt
  DC2 = -k * C2old(I) * DELTAT
  c2new(I) = c2new(I) + DC2
  c3new(I) = c3new(I) - DC2

200  CONTINUE
  do 256 i = 1,imt
  c1old(I) = c1new(I)
  C2OLD(I) = c2new(I)
  c3old(I) = c3new(I)
256  CONTINUE
1000 CONTINUE
END
*****
C
-----
SUBROUTINE DIFFUSE
implicit real(a - y)
implicit double precision (z)
integer i, mt,imt,wrcondiv,wr_var,N,earlyt,lt_expan
character filnam * 12, chl1 * 1, chl2 * 1

COMMON /concent/ c1old(999), c1new(999), C2OLD(999), c2new(999)
COMMON /concent/ c3old(999), c3new(999), tau, sigma
COMMON /WR/ wrcondiv,wr_var,filnam,mt,DELTAT,DELTAx,IMT,MTMAX,k
COMMON /WR/ earlyt,lt_expan
COMMON /SURF/ DELTA1S, DELTAC2S, DELTAC3S, N, F, D1, D2, D3
*CALCULATION FOR SURFACE

  Dstar1 = D1 * DELTAT / (DELTAx * DELTAx)
  c1new(1) = C1OLD(1) + Dstar1 * (C1OLD(2) - C1OLD(1))
  if (c1new(1) .lt.0)then
    write(*,*)'c1new went less than zero Danger Danger'
    c1new(1) = 1E-18
  END IF

  Dstar2 = D2 * DELTAT / (DELTAx * DELTAx)

```

```

    c2new(1) = C2OLD(1) + Dstar2 * (C2OLD(2) - C2OLD(1))
    if (c2new(1) .lt.0)then
      write(*,*)'c2new went less than zero Danger Danger'
      c2new(1) = 1E-18
    END IF

    Dstar3 = D3 * DELTAT / (DELTA * DELTA)
    c3new(1) = C3OLD(1) + Dstar3 * (C3OLD(2) - C3OLD(1))
    if (c3new(1) .lt.0)then
      write(*,*)'c3new went less than zero Danger Danger'
      c3new(1) = 1E-18
    END IF

* for the rest of the boxes, use eqs 12 and 13.

    do 200 i=2,imt
      deltac1=Dstar1*((C1OLD(I+1)-C1OLD(I))-(C1OLD(I)-C1OLD(I-1)))
      c1new(I) = C1OLD(I) + deltac1
      if(c1new(i).lt.0)then
        write(*,*)'oops c1new(i) went less than zero concentration,i =',i
        c1new(I) = 1E-18
      END IF

      deltac2=Dstar2*((C2OLD(I+1)-C2OLD(I))-(C2OLD(I)-C2OLD(I-1)))
      c2new(I) = C2OLD(I) + deltac2
      if(c2new(i).lt.0)then
        write(*,*)'oops c2new(i) went less than zero concentration,i =',i
        c2new(I) = 1E-18
      END IF

      deltac3=Dstar3*((C3OLD(I+1)-C3OLD(I))-(C3OLD(I)-C3OLD(I-1)))
      c3new(I) = C3OLD(I) + deltac3
      if(c3new(i).lt.0)then
        write(*,*)'oops c3new(i) went less than zero concentration,i =',i
        c3new(I) = 1E-18
      END IF

200    continue
      RETURN
      END

*****
      SUBROUTINE WRITE
      implicit real(a - y)
      implicit double precision (z)
      integer i, mt,imt,wrcondiv,wr_var,N,BOXNUM(100),NBOXWR,NB2,earlyt
      integer lt_expan
      character filnam*12,chlb1*1,chlb2*1,CHLB3*1,CHLB4*1

      COMMON /concent/ c1old(999), c1new(999), C2OLD(999), c2new(999)
      COMMON /concent/ c3old(999), c3new(999), tau, sigma
      COMMON /WR/ wrcondiv,WR_var,filnam,mt,DELTAT,DELTA,IMT,MTMAX,k
      COMMON /WR/ earlyt,lt_expan
      COMMON /SURF/ DELTAC1S, DELTAC2S, DELTAC3S, N, F, D1, D2, D3
      COMMON /FW2/LABEL,LABELB,NBOXWR,BOXNUM

* write nnew(i) to file if mt/WRCONDIV is appropriate. 10/26/87
      wr_var = int(1 + (mt/lt_expan))
      IF (mt.eq.1) THEN
        open(4,file=filnam//'.C01')

```

```

      write(4,*)' Dist.(cm) Reactant Product:echem Product:kinetic'
      write(4,*,filnam//'.c01','',(mt-0.5)*deltat, k, D1, D2, D3
1330 DO 1330 I=1,IMT
      WRITE(4,*)(I-0.5)*DELTAX,c1old(I),C2OLD(I),c3old(I)
CONTINUE
CLOSE (4)
END IF

      if(mod(mt,wrcondiv).eq.0)then
      write(*,*)'writing file at t= ',(mt-0.5)*deltat
      label = label + 1
      label1 = label / 10
      label2 = mod(label,10)
      chlb1 = char(label1 + 48)
      chlb2 = char(label2 + 48)
      open(4,file=filnam//'.C'//chlb1//chlb2)
      write(4,*)' Dist.(cm) Reactant Product:echem Product:kinetic'
886 write(4,*,mt,(mt-0.5)*deltat, k, D1, D2, D3
887 format(1x,a12,e9.4,1x,e9.4)
      format(1x,e9.4,1x,e9.4,1x,e9.4,1x,e9.4,a1,i3)
DO 1300 I=1,IMT
      wr_var = int(1 +(I/lt_expan))
      IF((I.lt.earlyt).or.mod(I,wr_var).eq.0)THEN
      WRITE(4,*)(I-0.5)*DELTAX,c1old(I),C2OLD(I),c3old(I)
      END IF
1300 CONTINUE
      CLOSE (4)
      END IF
882 format (a)
* FOR ALL TIMES WRITE THE CHOSEN BOXES
      IF(MT.EQ.1)THEN
      DO 1355 NB2=1,NBOXWR
      labelB = labelB + 1
      labelB1 = labelB / 10
      labelB2 = mod(labelB,10)
      CHLB3 = char(labelB1 + 48)
      chlB4 = char(labelB2 + 48)
      open(NB2+7,file=filnam//'.X'//CHLB3//chlB4)
      write(NB2+7,*)' t (s) Reactant Product:echem Product:kinetic'
      write(NB2+7,*)boxnum(nb2), (boxnum(nb2)-.5)*deltax , k, D1, D2,D3
1355 CONTINUE
      ENDIF
*FOR ALL TIMES:
      wr_var = int(1 + (MT/lt_expan))
      if(wr_var.ge.100)then
      wr_var = 100
      end if
      IF((mt.lt.earlyt).or.mod(mt,wr_var).eq.0)THEN
      DO 1375 NB2=1,NBOXWR
      WRITE(NB2+7,*)((MT-0.5)*DELTAT),c1old(boxnum(nb2)),
      * C2OLD(BOXNUM(NB2)), c3old(boxnum(nb2))
1375 CONTINUE
      ENDIF
      IF (MT.EQ.MTMAX) THEN
      DO 1365 NB2=1,NBOXWR
      CLOSE(NB2)
1365 CONTINUE
      ENDIF
      RETURN
      END

```

Chapter 4

Results and Discussion

Introduction

Diffusion layer growth in response to a galvanostatic and potentiostatic step of an electrode was probed in a series of experiments. These investigations were first carried out using electroactive species for which there is no coupled chemical reaction following the electron transfers. Galvanostatic investigation employed dimethylferrocene while the ruthenium hexaamine complex was used in potentiostatic investigations. The ruthenium chloropentaamine complex was also used in potentiostatic experiments. This species has an irreversible coupled chemical reaction which follows electron transfer. The effect of this reaction on the diffusion layer of $\text{Ru}(\text{NH}_3)_5\text{Cl}^{1+}$ was observed. The ability to observe the effect a homogeneous reaction has on the fate of species in solution demonstrates that it is possible to use this technique to study chemical kinetics.

The Galvanostatic Experiment

A series of galvanostatic experiments was carried out employing a constant current step of the substrate electrode. The resulting diffusion layer growth was probed in two sets of experiments. One set of experiments used the same galvanostatic step while positioning the tip at various distances from the substrate electrode. In the second set of experiments, the tip was held in a fixed position while the length of the galvanostatic step was varied. In both sets of experiments dimethylferrocene (DMFc) is the electroactive species. A 2 mM solution was made up in dimethyl sulfoxide (DMSO) with 0.1 M tetrabutylammonium perchlorate as the supporting electrolyte. The diffusion coefficient of DMFc in DMSO was determined to be $3.4 \times 10^{-6} \text{ cm}^2/\text{s}$. A platinum(III) single crystal (2 x 2 mm) was used as the substrate. STM imaging indicated that the surface roughness of the crystal was on the order of 10 nm.

The experiments are carried out in the following manner. After the substrate is "found" by the STM and tunneling established, the tip is retracted from the substrate and held in position by isolating the piezo electronics from the tunneling feedback circuitry.

The substrate is then changed from potentiostatic to galvanostatic control and the current step is applied. (In later experiments, a reverse current step following the "forward" step was added to speed the dissipation of the diffusion layers between step experiments.) After the completion of the galvanostatic step, the substrate is returned to potentiostatic control, the feedback electronics are engaged and the tip is returned to tunneling distance. The z-piezo voltage is compared with its initial value to determine if any thermal drift normal to the substrate has occurred.

The data gathered in these experiments contain two artifacts. The first is the spikes in tip current. They appear to be an electronic artifact that accompanies the sudden change in potential applied to the substrate when the current step changes. The transients are short, returning to baseline in approximately 1 ms. They occurred in all of the experiments, although they were usually not captured during longer experiments when the transient lifetime was on the same order or shorter than the sampling cycle of the oscilloscope. Similar transients have been reported by Bard, et al. (1), with the SECM. They explain that the transient is due to capacitive and resistive coupling of the substrate to the tip and also observed that it increased with the size of the substrate electrode.

The second experimental artifact is the non-zero tip current prior to the galvanostatic step. This current is not electrochemical in nature, but is due to a leakage current between the z-piezo and the current amplifier (*vide supra*). When the tip is held in a fixed position, this leakage current is constant and the faradaic current is obtained by subtracting the leakage current from the total current. Leakage currents tend to change slowly with time. During the course of these experiments (eight hours) the leakage current increased from less than 10 pA to 300 pA.

The first set of galvanostatic experiments explores the effect on the tip's response of changing the distance between the tip and the substrate. In this set of experiments, the current step is applied to the substrate electrode for 0.1 s. A typical result is shown in Figure 4.1, where the tip current as well as the substrate current and potential are plotted. As shown, the tip current increases as the diffusion layer containing the dimethylferricinium ion (DMFc^+) is formed and the concentration of DMFc^+ in the vicinity of the tip increases. At the completion of the galvanostatic step ($t = 0.1$ s) the substrate current is returned to zero. Since DMFc^+ is no longer being generated at the substrate electrode, the tip current decreases with time as the DMFc^+ diffusion layer dissipates into the bulk of the solution. The tip current is compared with the expected concentration versus time curve in Figure 4.2. As can be seen, the current response follows the simulated curve for the DMFc^+ concentration at $2 \mu\text{m}$.

The Effect of Varying the Tip/Substrate Separation

When the tip is moved closer to the substrate, the current measured during the galvanostatic step increases (Fig. 4.3). Because the tip used in these experiments has an apparent radius of $1.4 \mu\text{m}$, which is of the same dimension as the maximum tip/substrate separation, the tip will always be in the "feedback current" mode (*vide supra*). Due to this effect, tip currents are expected to increase as the tip/substrate separation, held constant during a galvanostatic step, is decreased. To compare the data at different distances, the currents are normalized to their value at $t = 0.1$ s. The resulting current curves overlap (Fig. 4.4). The convergence of these curves is expected since the concentration versus time curves vary little with distance in this region (Fig. 4.5).

The Effect of Varying the Galvanostatic Step

In this second set of experiments, the tip is held at a constant distance from the substrate electrode while the current step is varied. In keeping with the Sand equation

(Eq. 3.18), the current imposed during the galvanostatic step is adjusted as necessary with respect to the step width to keep the product $i\sqrt{\tau}$ constant. With this restriction in place, the surface concentration of DMFc^+ will be the same for all experiments at the end of the galvanostatic step. Tip currents in response to a series of galvanostatic steps applied to the substrate are presented in Figure 4.6. The current step widths vary from 0.1 to 1.0 seconds in length, with two curves plotted for each step width. The identical tip current response to the same galvanostatic step demonstrates the reproducibility of the experiment.

Tip currents for the varied galvanostatic steps (Fig 4.6) can be compared to one another by plotting current versus $\sqrt{t/\tau}$ (Fig. 4.7). At any given point along the dimensionless time axis, all galvanostatic steps have the same surface concentration. Because the species generated during the longer step experiments will have more time to diffuse, the concentration of the product species in solution at any given dimensionless time coordinate will be greater than that of the shorter experiments. Figure 4.8 shows this effect by plotting the analytical solution for the product concentration (Eq. 3.20). However, a one-to-one correspondence between the experimental data in Figure 4.7 and the theoretical concentrations in Figure 4.8 should not be expected. This is because the tip used to collect these data is not a planar electrode. Consequently, its current is a response to the concentration in a region of space, not a plane. In contrast, the analytical solution describes the concentration at planes parallel to the substrate. This difference may also be responsible for an apparent beginning of convergence of the experimental curves at the end of the galvanostatic step.

The Potentiostatic Experiment

A series of potentiostatic experiments were carried out by applying a potential step to the substrate electrode to investigate two electroactive species: ruthenium hexaamine and ruthenium chloropentaamine. The hexaamine complex is stable with the metal center in either the 2⁺ or the 3⁺ states, while the chloropentaamine complex will undergo ligand exchange with loss of the chloride when the ruthenium center is in the 2⁺ state. Both of these complexes were prepared in aqueous solution with 0.2 M sodium trifluoroacetate as the supporting electrolyte. Solutions were degassed with nitrogen and the STM was operated in a nitrogen atmosphere in a small glove. The STM was operated in the glove box without the benefit of a Faraday cage. The experimental procedure was the same as described for the galvanostatic step experiment (*vide supra*). All potentials are reported versus a Ag/AgCl reference electrode.

Ruthenium(III) Hexaamine Complex.

The first set of potential step experiments for the hexaamine complex explores the effect on the tip's current response of changing the distance between the tip and the substrate. In this set of experiments, the substrate is stepped from 100 to -300 mV. A typical result is shown in Figure 4.9. (Tip currents are noisier in these experiments than those in the galvanostatic step since a Faraday cage was not used.) The tip current as well as the substrate current and potential are shown. The tip is potentiostated at +100 mV so there is no current prior to the potential step since Ru(NH₃)₆³⁺ is the only electroactive species in solution. The Ru(NH₃)₆²⁺ generated at the substrate electrode diffuses into solution and is detected by the tip, which oxidizes it back to the 3+ state. The tip is 0.79 μm from the substrate and as can be seen, the conversion of the electroactive species in the region is rapid with respect to the step width. This is expected when probing the diffusion layer about 1 μm from the electrode surface. Five seconds after the potential step is initiated, the substrate potential is returned to 100 mV. Previously generated

$\text{Ru}(\text{NH}_3)_6^{2+}$ is now consumed at the substrate electrode and the tip current returns to zero. The tip current after the first potential step is presented in greater detail in Figure 4.10, in which the data have been smoothed with a sliding five point average to reduce the noise in the current. The current is plotted with theoretical concentration curves in Figure 4.11. Just as for the galvanostatic step experiments, an exact fit of the data is not expected. This is because the tip samples a region in space and not a plane, and thus its response represents a weighted average of the concentration over a range of distances.

Diffusion layer growth of the reactant $\text{Ru}(\text{NH}_3)_6^{3+}$ can be monitored by adjusting the tip potential to -400 mV (Fig. 4.12). In this case, there is a non-zero tip current prior to the potential step due to reduction of the $\text{Ru}(\text{NH}_3)_6^{3+}$ at the tip. When the potential of the substrate is stepped to -300 mV, $\text{Ru}(\text{NH}_3)_6^{3+}$ is reduced at a diffusion limited rate at the substrate electrode and the region within 1 μm of the surface is depleted of most of the $\text{Ru}(\text{NH}_3)_6^{3+}$ in less than 50 ms (Fig. 3.3).

The Effect of Varying the Tip/Substrate Separation

When the tip is moved closer to the substrate, the tip current measured during a potential step increases (Fig. 4.13). The increase in tip response is due to faradaic feedback (vide supra). The reproducibility of the tip response to substrate potential steps is demonstrated in Figure 4.13. The four potential steps with the tip at 0.7 μm were collected over a 90 minute period. As the tip is moved closer to the substrate, the "rise time" of the tip current should become shorter. This effect was seen and is presented in Figure 4.14.. In order to compare tip current responses which have varying amounts of electrochemical feedback current, the tip current for each potential step in Figure 4.14 were normalized to its average value at $t = 0.5$ s. The faster tip current response when the tip is moved to 0.16 μm of the substrate is clearly shown. The effect however is not as marked as is expected (Fig 3.3). This is likely due to the size and shape of the tip. The

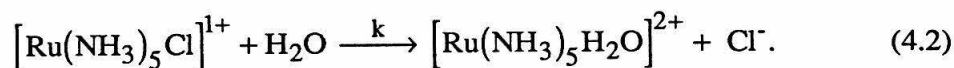
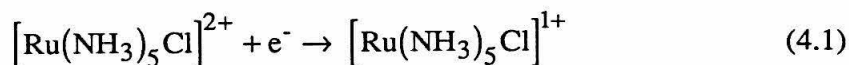
tip is modeled as a hemisphere on an infinite plane when determining its size. In the hemisphere-on-a-plane model, diffusion through the plane is not allowed and the electroactive species "behind" the plane are ignored (Fig 4.15). Kwak and Bard (2), showed that when the shroud radius of an embedded disc electrode is less than five times the disc radius, diffusion around the edge can no longer be ignored. Since the tips are not shrouded, the assumption of an isolating plane is not valid and the tip current will continue to change until the concentrations of electroactive species in the volume probed stabilize. Since it is not possible for this tip to move all of its diffusion layer significantly closer to the substrate when the tip itself is moved closer, significantly faster tip current rise times are not expected.

The Effect of Changing Tip Potential

In a second set of experiments with the ruthenium hexaamine complex, the potential of the tip was varied between the limiting values (tip potential at 100 and -300 mV) investigated above. At these intermediate potentials (Fig. 4.16), there is an orderly transition in the tip current response between the two limiting cases (Figs. 4.9 and 4.12). Note that the tip currents quickly return to their initial values when the substrate potential is stepped back to its original value.

Ruthenium(III) Chloropentaamine Complex

The $[\text{Ru}(\text{NH}_3)_5\text{Cl}]^{2+}$ complex was studied because the reduction of the metal center has a coupled chemical reaction. The chloride ion becomes labile and will undergo ligand exchange with the solvent:



The unimolecular rate constant for substitution is 4 s^{-1} (3-5). In aqueous solution, the replacement of chloride with water causes a 108 mV positive shift in the formal potential of the metal center (6).

When the tip is poised at a potential well positive of the formal potential of both reduced complexes, they are oxidized at the tip (Fig. 4.17). Since the tip is at a potential where the current due to each species is limited by diffusion, the tip current response to a substrate potential step is the same as when no coupled chemical reaction occurs. Because the oxidation potentials of the two complexes are close together, the tip cannot be poised at a potential where the oxidation of $[\text{Ru}(\text{NH}_3)_5\text{Cl}]^{1+}$ at the tip is diffusion limited and there is no current due to $[\text{Ru}(\text{NH}_3)_5\text{H}_2\text{O}]^{2+}$ oxidation.

If the tip potential is shifted negatively from a value where the oxidation of a species is diffusion limited, the current at the tip will eventually decrease when it is no longer diffusion limited. This transition will occur first for the aquopentaamine complex because it has a more positive formal potential. Tip currents in this transition zone will be larger for $[\text{Ru}(\text{NH}_3)_5\text{Cl}]^{1+}$ than for the same concentration of $[\text{Ru}(\text{NH}_3)_5\text{H}_2\text{O}]^{2+}$ and a peak in the tip current response should be seen as the coupled chemical reaction converts the chloropentaamine complex to the aquopentaamine complex. The tip was adjusted to several such intermediate potentials (Fig 4.18). The maxima and decay of the tip current is clearly shown. A potential can be found that maximizes the current response to the chloropentaamine complex versus the aquopentaamine complex. Of the tip potentials shown in Figure 4.19, the best current response is observed with the tip potential adjusted to -175 mV. This ratio is enhanced when the tip is moved closer to the substrate electrode (Fig. 4.19).

In both Figures 4.18 and 4.19, the tip currents do not return to their initial values when the substrate potential is stepped back to the original potential as they did when the ruthenium hexaamine complex was probed (Fig. 4.16). The tip has a larger cathodic current after the potential step than was recorded before it. The enhanced current is due to the reduction of $[\text{Ru}(\text{NH}_3)_5\text{H}_2\text{O}]^{3+}$ which was not present prior to the potential step. In this intermediate potential region, the tip current response at a given potential will be greater for the aquopentaamine complex than for the chloropentaamine complex due to the more positive formal potential of ruthenium aquopentaamine. The tip current after the potential step slowly decays back to its initial value as the aquopentaamine complex dissipates onto the bulk solution. In contrast, when the tip potential is well positive of the formal potential of both species (4.17) the dissipation of the aquo complex after the substrate potential is returned to its original value cannot be detected since both species are being reduced at the tip at their diffusion limited rates..

The diffusion layers for $[\text{Ru}(\text{NH}_3)_5\text{Cl}]^{1+}$ and $[\text{Ru}(\text{NH}_3)_5\text{H}_2\text{O}]^{2+}$ were modeled using the simulation described in the preceding chapter. With this information it is possible to estimate what the tip response should be under various conditions. Perspectives of the diffusion layer growth are shown in Figure 4.20 for the chloropentaamine complex and Figure 4.21 for the aquopentaamine complex. Using the tip current at -175 mV obtained from cyclic voltammograms of the tip for the $[\text{Ru}(\text{NH}_3)_5\text{Cl}]^{2+}$ and the $[\text{Ru}(\text{NH}_3)_5\text{H}_2\text{O}]^{2+}$ complexes, the simulated concentrations of these species following a potential step of a planar electrode can be used to approximate the tip response seen in Figure 4.19. The result is presented in Figure 4.22. As can be seen, there is a qualitative fit of the simulation to the experimental result. It must be remembered that the tip samples a volume in space while the simulations give the concentration at a plane normal to the surface. Therefore the tip current measured is actually a sum of the simulation curves, which would be additionally weighted by the

current enhancement due to electrochemical feedback. When the same technique is applied to simulation data using different rate constants ($k = 2 \text{ s}^{-1}$ and 10 s^{-1}), poorer fits to the data are obtained (Figs. 4.23 and 4.24).

Summary and Conclusion

The original STM has been modified to allow potential control of the sample cell. With the integration of a bipotentiostat, the potential of the tip and substrate can be controlled independently. This system was used to probe the diffusion layer growth in response to an electrochemical stimulus (current or potential) of the substrate. Diffusion layer dynamics between $0.1 \text{ }\mu\text{m}$ and $1.0 \text{ }\mu\text{m}$ of the electrode surface were investigated. Direct probing of these processes within $1 \text{ }\mu\text{m}$ of a working electrode surface was shown for the first time. The behavior of the tip current response for both the potentiostatic and galvanostatic step of the substrate electrode matches well with theory for the diffusion layer growth.

Diffusion layer dynamics in the presence of a coupled first-order chemical reaction were also probed. The transition of the unstable $[\text{Ru}(\text{NH}_3)_6\text{Cl}]^{1+}$ intermediate to the $[\text{Ru}(\text{NH}_3)_6\text{H}_2\text{O}]^{2+}$ product was easily resolved. These experimental data were compared to simulated diffusion layer curves for various reaction rates. A qualitative fit to the experimentally determined reaction rate could be seen. Poorer fits to the simulations were obtained when the simulated reaction rate changed by a factor of two. The qualitative nature of the fit of the experimental kinetic data to the simulation is likely due to the large size of the tip: the tip current represents a sum of currents corresponding to a range of tip/sample separations (which is additionally convoluted by electrochemical feedback).

More precise results should be obtained when using tips with smaller areas. Smaller tips could be approached closer to the substrate electrode before encountering electrochemical feedback effects.

References

1. Bard, A. J.; Fan, F.-R. F; Kwak, J., Lev, O. *Anal. Chem.*, **1989**, *61*, 132
2. Kwak, J.; Bard, A. J. *Anal. Chem.*, **1989**, *61*, 1221.
3. Coleman, G. N.; Gesler, J. W. Shirley, F. A.; Kuempel, J. R.; *Inorg. Chem.*, **1973**, *12*, 1036.
4. Baxendale, J. H.; Rodgers, M. A.; Ward, M. D. *J. Chem. Soc. A*, **1970**, 1246.
5. Elson, C. M.; Itzkovitch, I. J.; McKenney, J.; Page, J. A. *Can. J. Chem.*, **1975**, *53*, 2992.
6. Lim, H. S.; Barclay, D. J.; Anson, F. C. *Inorg. Chem.*, **1972**, *11*, 1460.

Figure 4.1
Tip current and substrate potential versus time in response to a galvanostatic step of the substrate. Tip retracted $0.65\ \mu\text{m}$ from the substrate. $I_{\text{sub}} = 120\ \mu\text{A}$; $E_{\text{tip}} = -200\ \text{mV}$; tip $r_{\text{app}} = 1.4\ \mu\text{m}$; $[\text{DMFc}] = 2\ \text{mM}$.

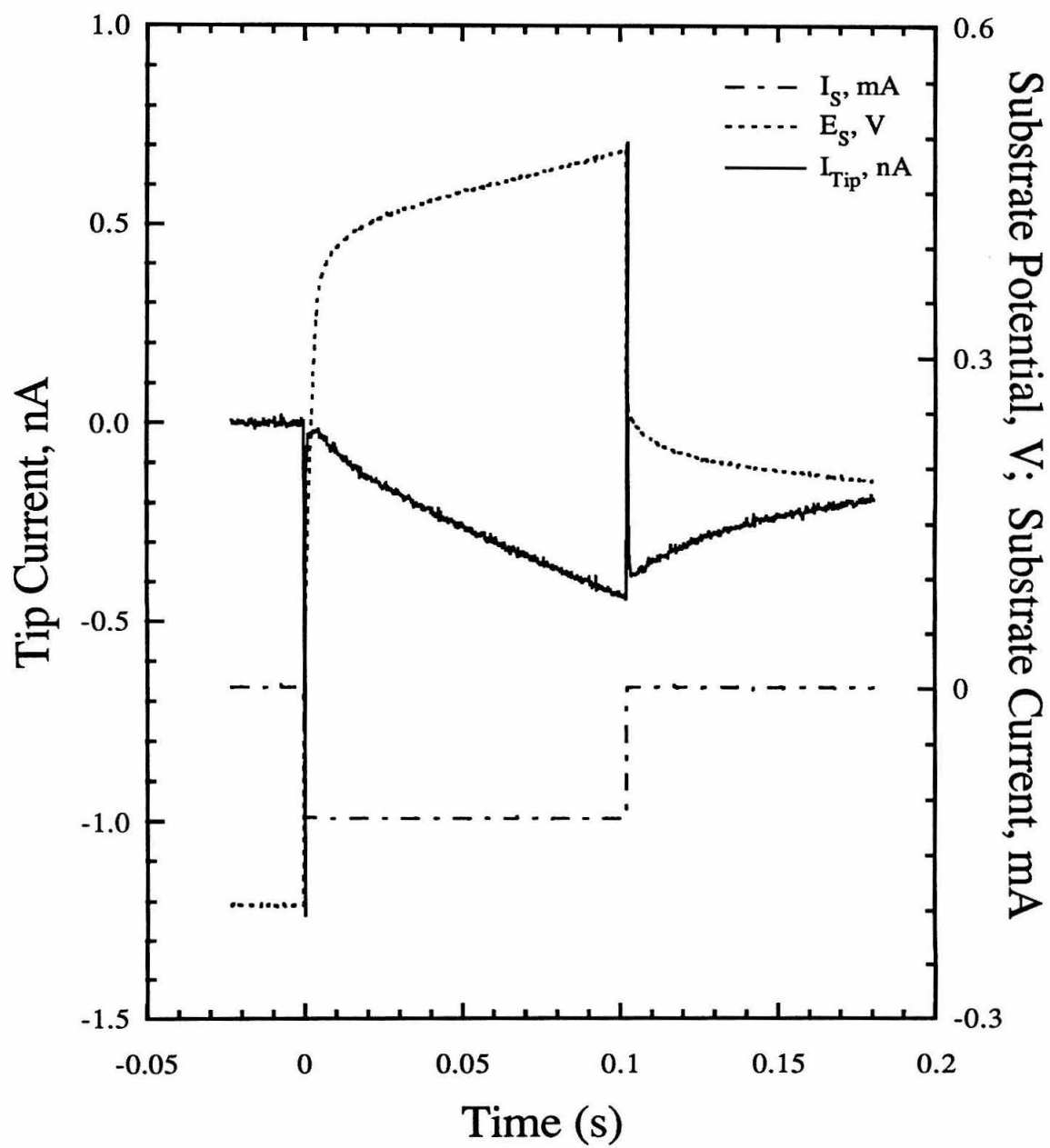


Figure 4.2

Tip current versus time in response to a galvanostatic step of the substrate. Tip current is smoothed with a 5 point sliding average and leakage current is removed. Tip retracted 0.65 μm from the substrate. $I_{\text{sub}} = 120 \mu\text{A}$; $E_{\text{tip}} = -200 \text{ mV}$; tip $r_{\text{app}} = 1.4 \mu\text{m}$; $[\text{DMFc}] = 2 \text{ mM}$.

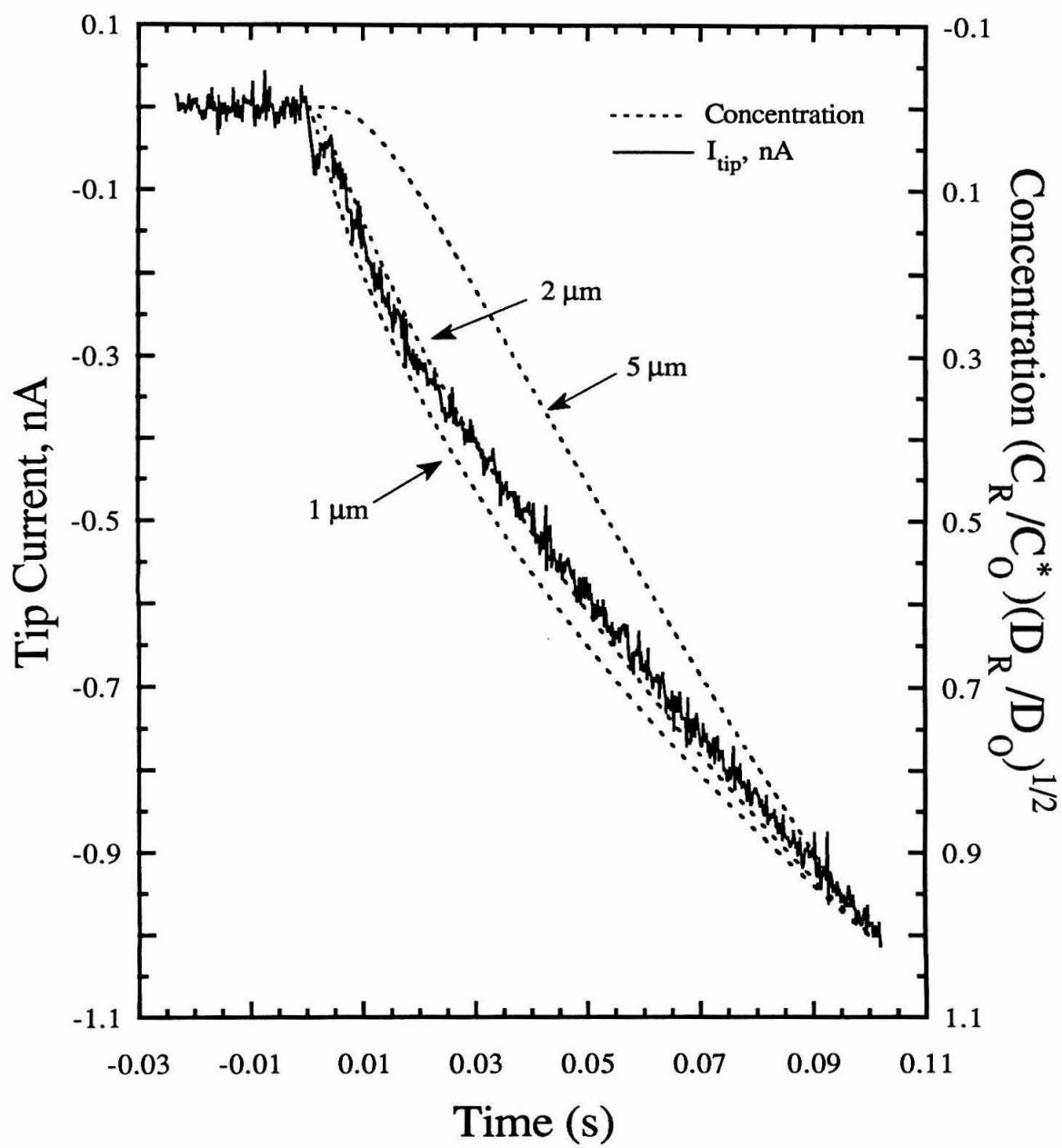


Figure 4.3

Tip current versus time in response to a galvanostatic step of the substrate. Tip is retracted various distances from the substrate. Leakage current is removed.

$I_{\text{sub}} = 120 \mu\text{A}$; $E_{\text{tip}} = -200 \text{ mV}$; tip $r_{\text{app}} = 1.4 \mu\text{m}$; $[\text{DMFc}] = 2 \text{ mM}$.

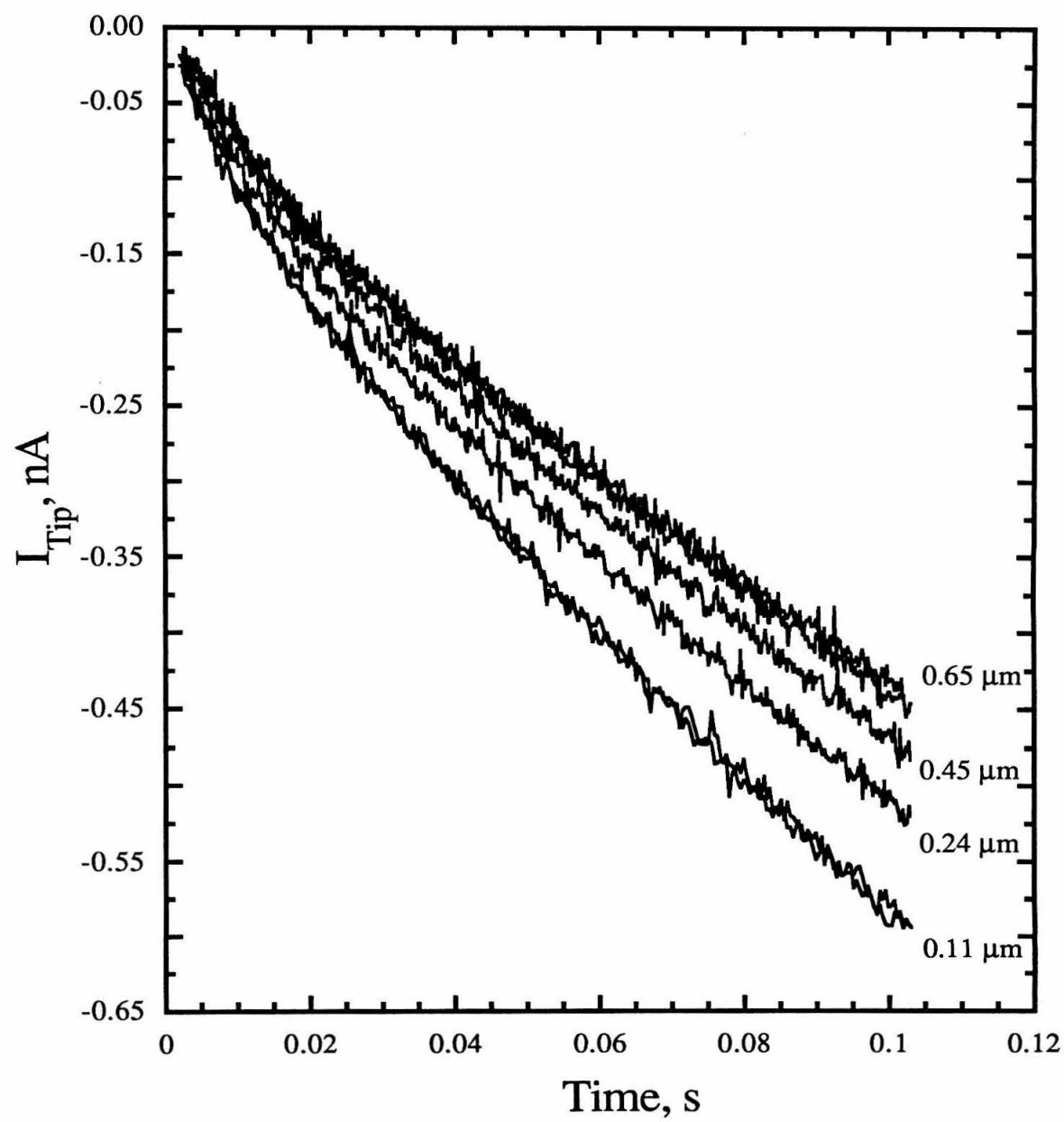


Figure 4.4

Normalized tip current versus time in response to a galvanostatic step of the substrate. Tip current is smoothed with a 5 point sliding average and leakage current is removed.

Tip is retracted various distances from the substrate: 0.11, 0.24, 0.45, and 0.65 μm .

$I_{\text{sub}} = 120 \mu\text{A}$; $E_{\text{tip}} = -200 \text{ mV}$; tip $r_{\text{app}} = 1.4 \mu\text{m}$; $[\text{DMFc}] = 2 \text{ mM}$.

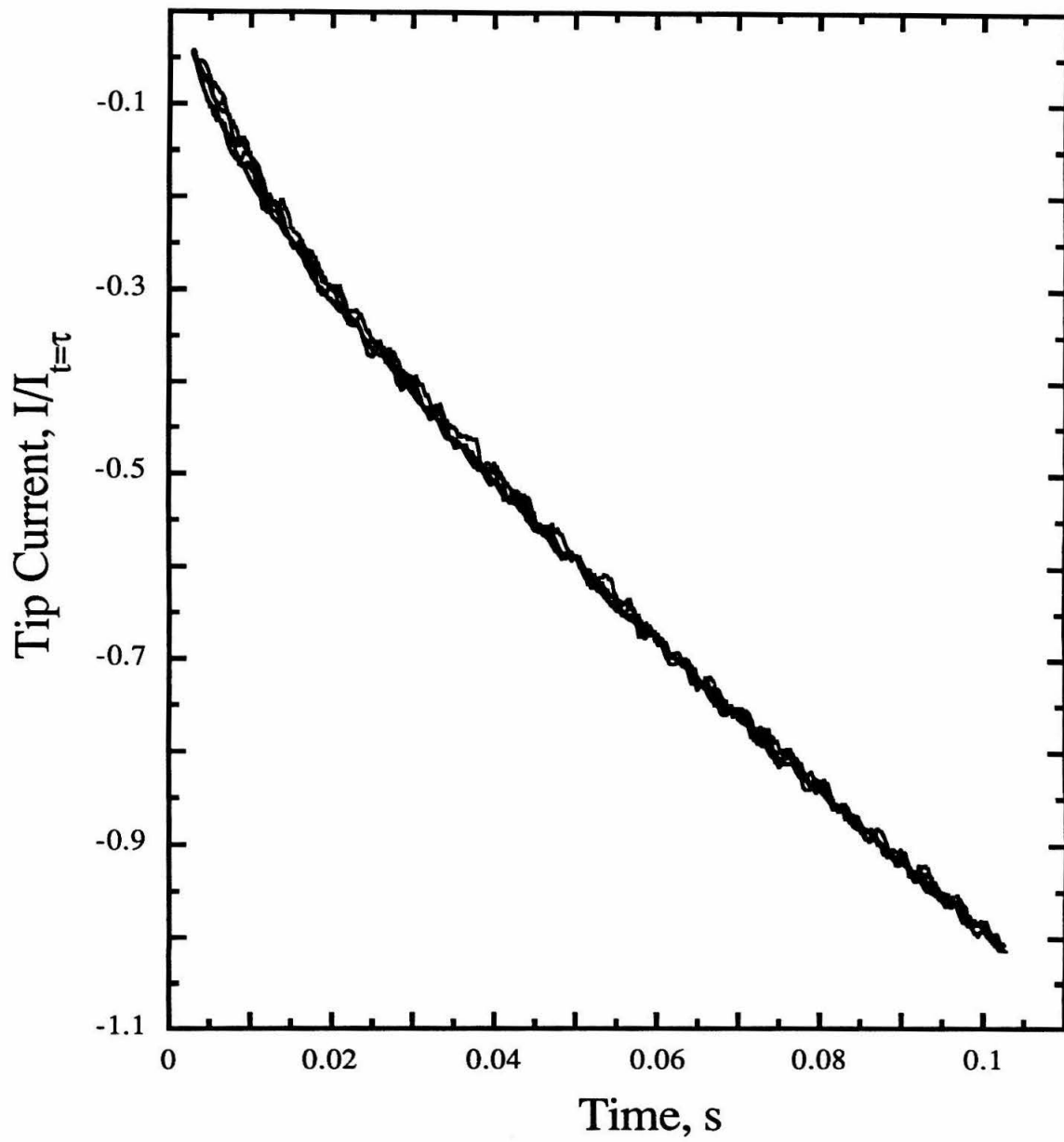


Figure 4.5
Simulated concentration versus time curves for product R generated at a planar electrode undergoing a galvanostatic step. Plotted for various distances from the substrate: 0.27, 0.55, and 1.1 μm and $D_{\text{O}} = 3.4 \times 10^{-6} \text{cm}^2/\text{s}$.

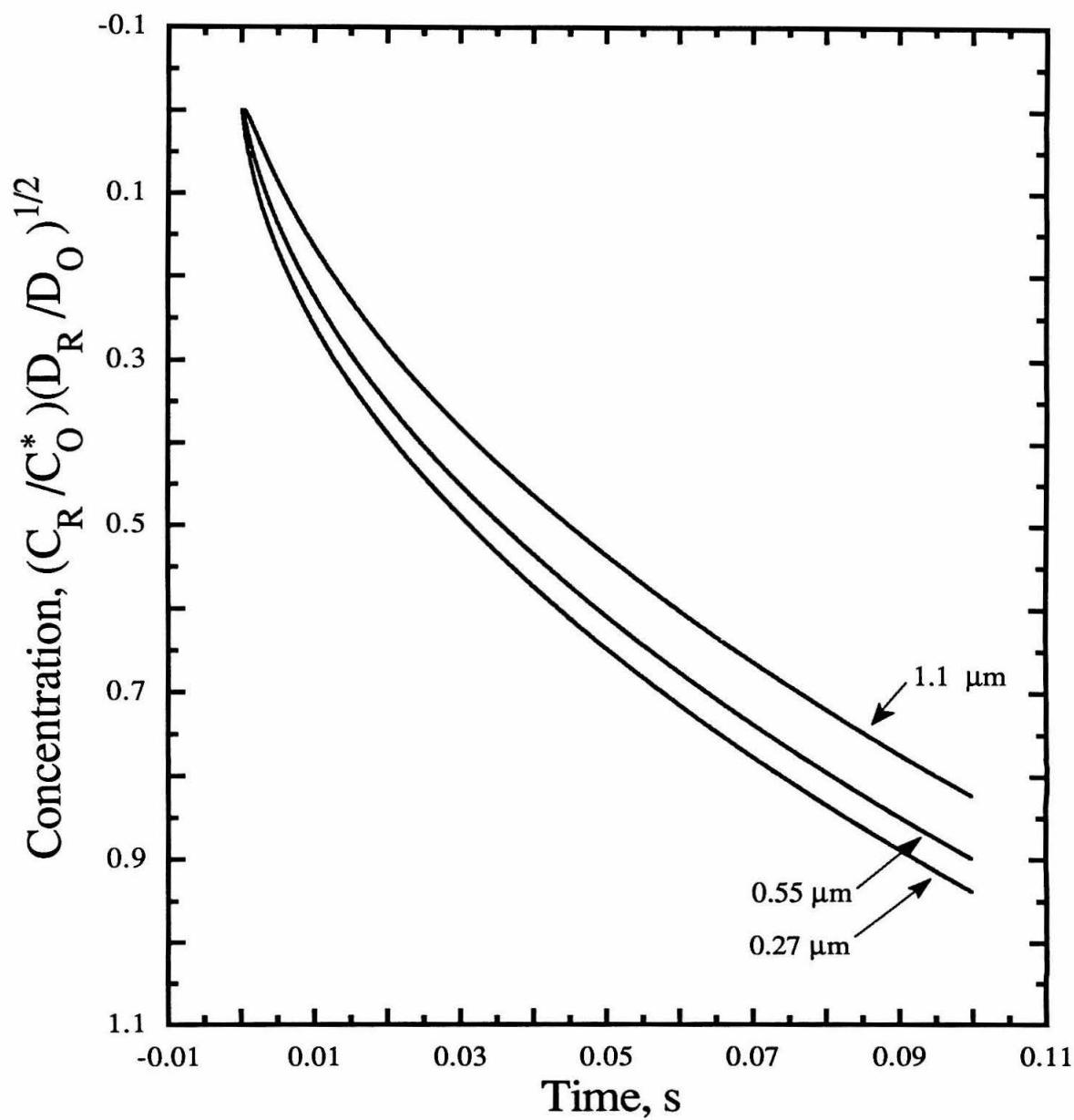


Figure 4.6

Tip current versus time in response to various galvanostatic steps of the substrate.
Leakage current is removed.

$I_{\text{sub}} = 120 \mu\text{A}$ (0.1s), $87 \mu\text{A}$ (0.2s), $55 \mu\text{A}$ (0.5s), $40 \mu\text{A}$ (1.0s); $E_{\text{tip}} = -200 \text{ mV}$; tip retracted $0.65 \mu\text{m}$ from the substrate; tip $r_{\text{app}} = 1.4 \mu\text{m}$; $[\text{DMFc}] = 2 \text{ mM}$.

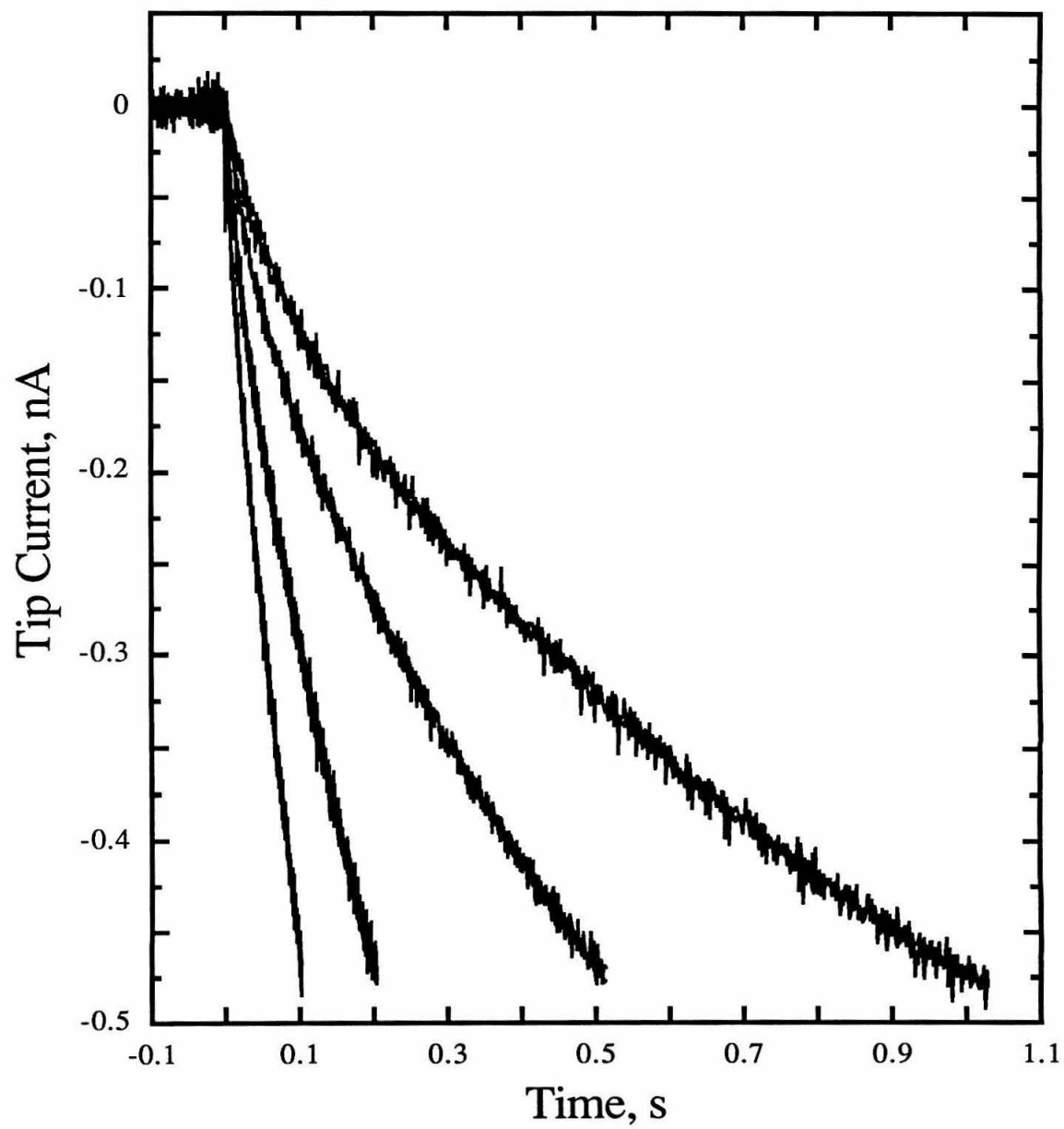


Figure 4.7

Tip current versus $(t/\tau)^{1/2}$ in response to a galvanostatic step of the substrate. Tip current is smoothed with a 5 point sliding average and leakage current is removed.

$I_{\text{sub}} = 120 \mu\text{A}$ (0.1s), $87 \mu\text{A}$ (0.2s), $55 \mu\text{A}$ (0.5s), $40 \mu\text{A}$ (1.0s); $E_{\text{tip}} = -200 \text{ mV}$;

tip $r_{\text{app}} = 1.4 \mu\text{m}$; $[\text{DMFc}] = 2 \text{ mM}$.

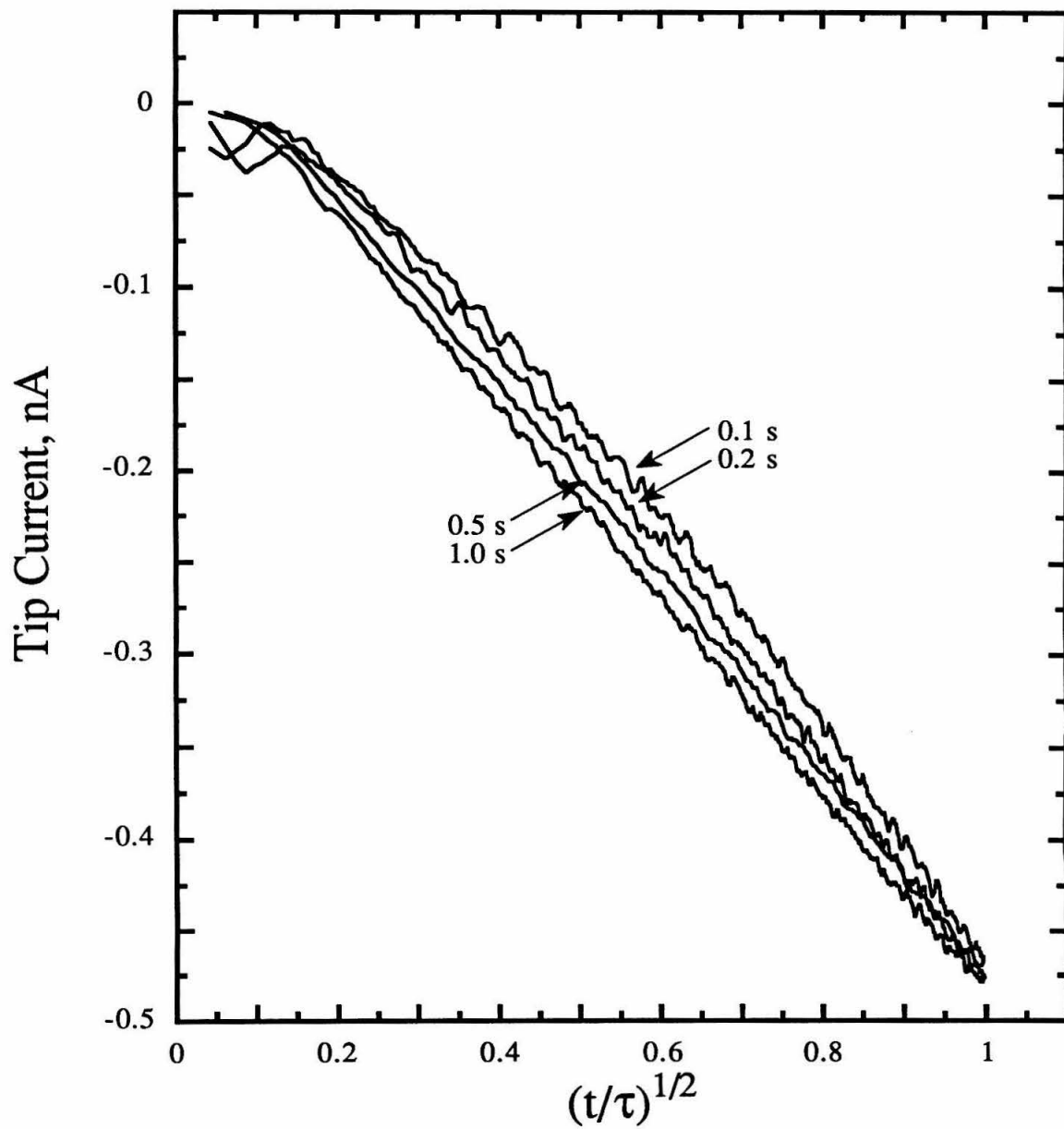


Figure 4.8

Simulated concentration curves versus $(t/\tau)^{1/2}$ of product R generated at a planar electrode undergoing various galvanostatic steps. Plotted for $x = 1 \mu\text{m}$ for various galvanostatic steps and $D_O = 5 \times 10^{-6} \text{cm}^2/\text{s}$.

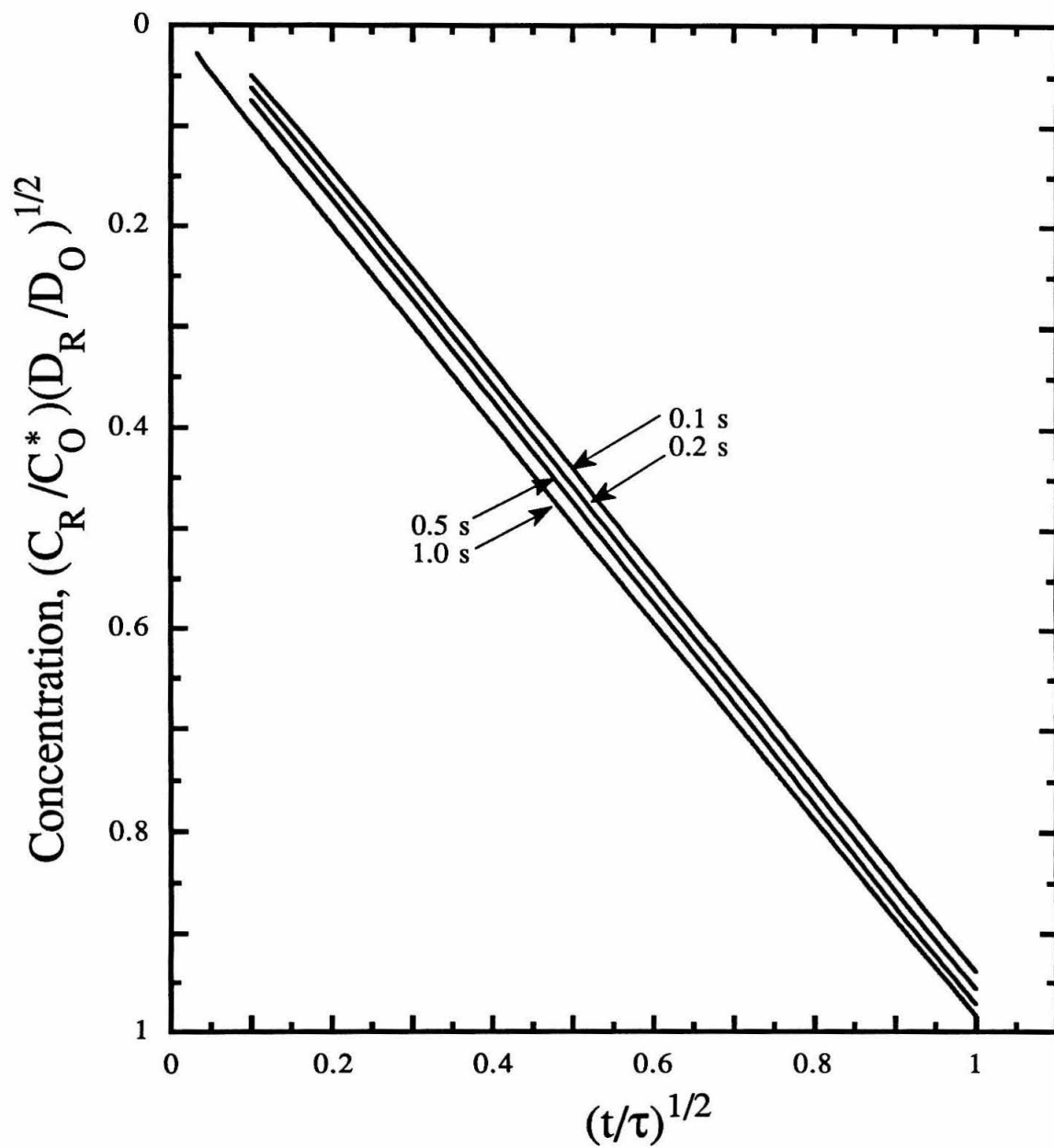


Figure 4.9

Tip current and substrate current versus time for a substrate undergoing a potential step. E_{sub} stepped from +100 mV to -400 mV. $E_{\text{tip}} = 100$ mV; tip is retracted 0.79 μm from the substrate; tip $r_{\text{app}} = 1.8$ μm ; $[\text{Ru}(\text{NH}_3)_6^{3+}] = 0.56$ mM.

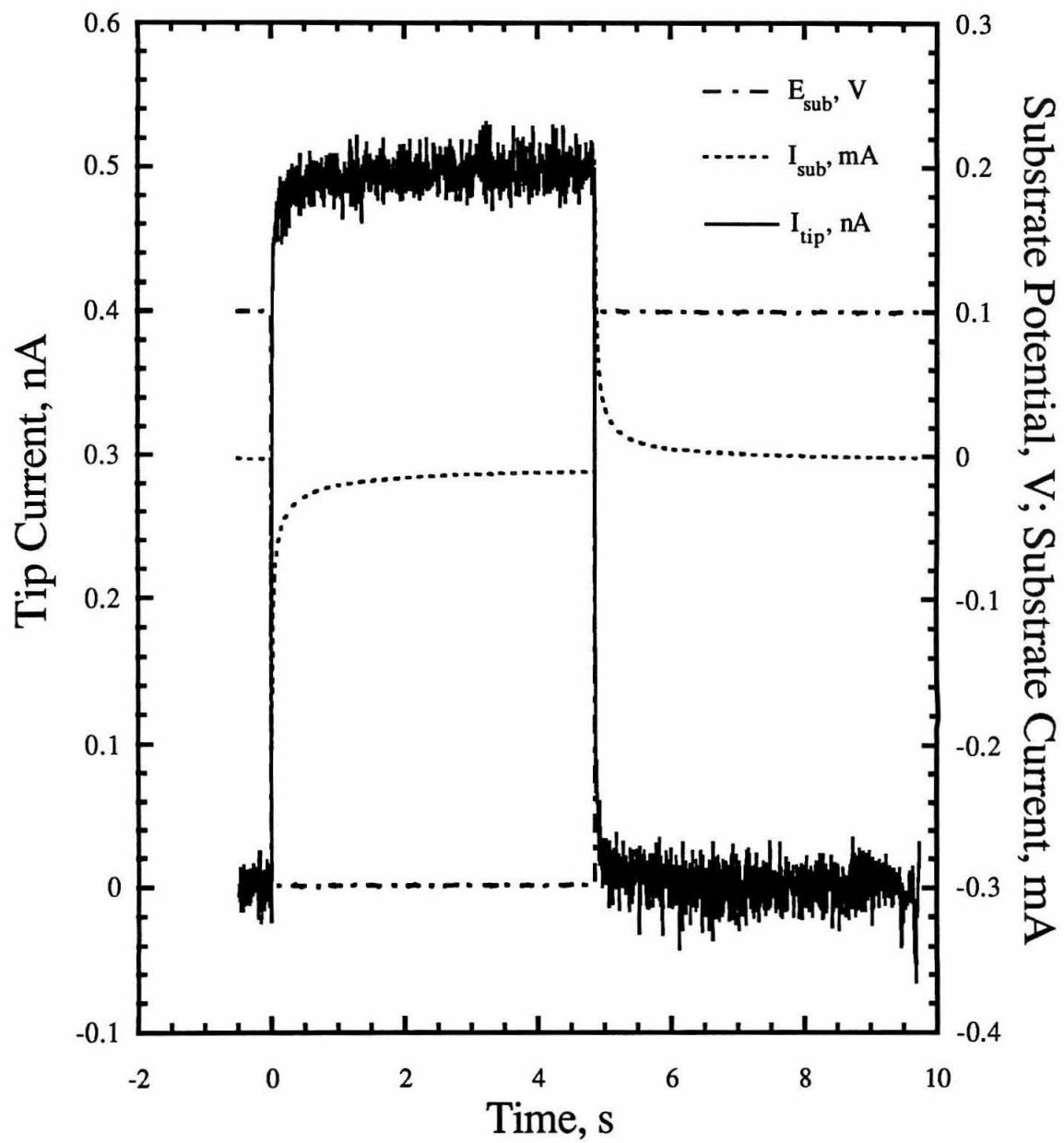


Figure 4.10

Tip current versus time for a substrate undergoing a potential step. Tip current is smoothed with a 5 point sliding average, and a 10 pA leakage current is subtracted.

E_{sub} stepped from +100 mV to -400 mV. $E_{\text{tip}} = 100$ mV; tip is retracted 0.79 μm from the substrate; tip $r_{\text{app}} = 1.8$ μm ; $[\text{Ru}(\text{NH}_3)_6^{3+}] = 0.56$ mM.

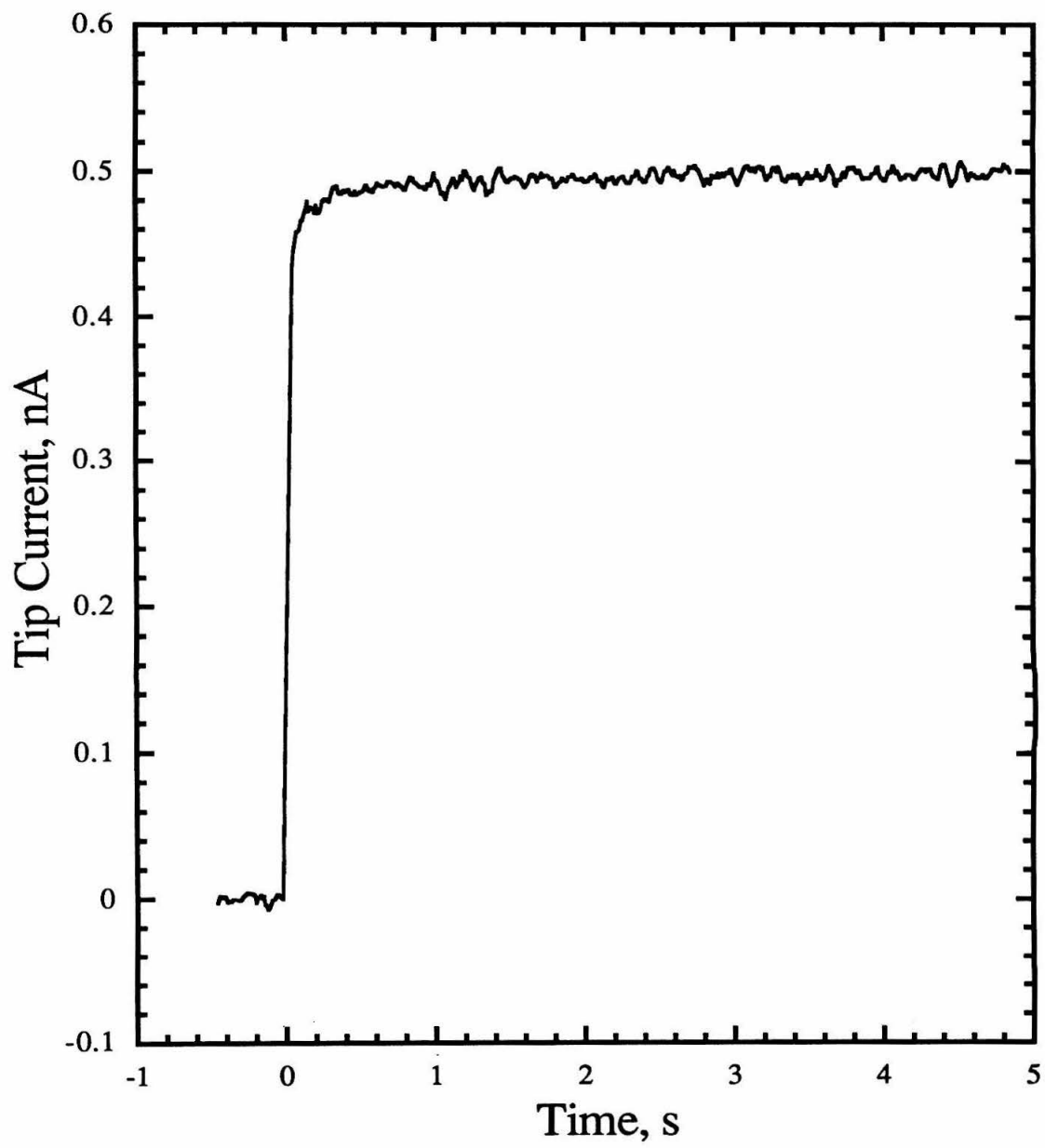


Figure 4.11

Normalized tip current versus time for a substrate undergoing a potential step compared to simulated concentration curves (dashed) at various distances. Tip current is not smoothed. A 10 pA leakage current is subtracted. E_{sub} stepped from +100 mV to -400 mV. $E_{\text{tip}} = 100$ mV; tip is retracted 0.79 μm from the substrate; tip $r_{\text{app}} = 1.8$ μm ; $[\text{Ru}(\text{NH}_3)_6^{3+}] = 0.56$ mM.

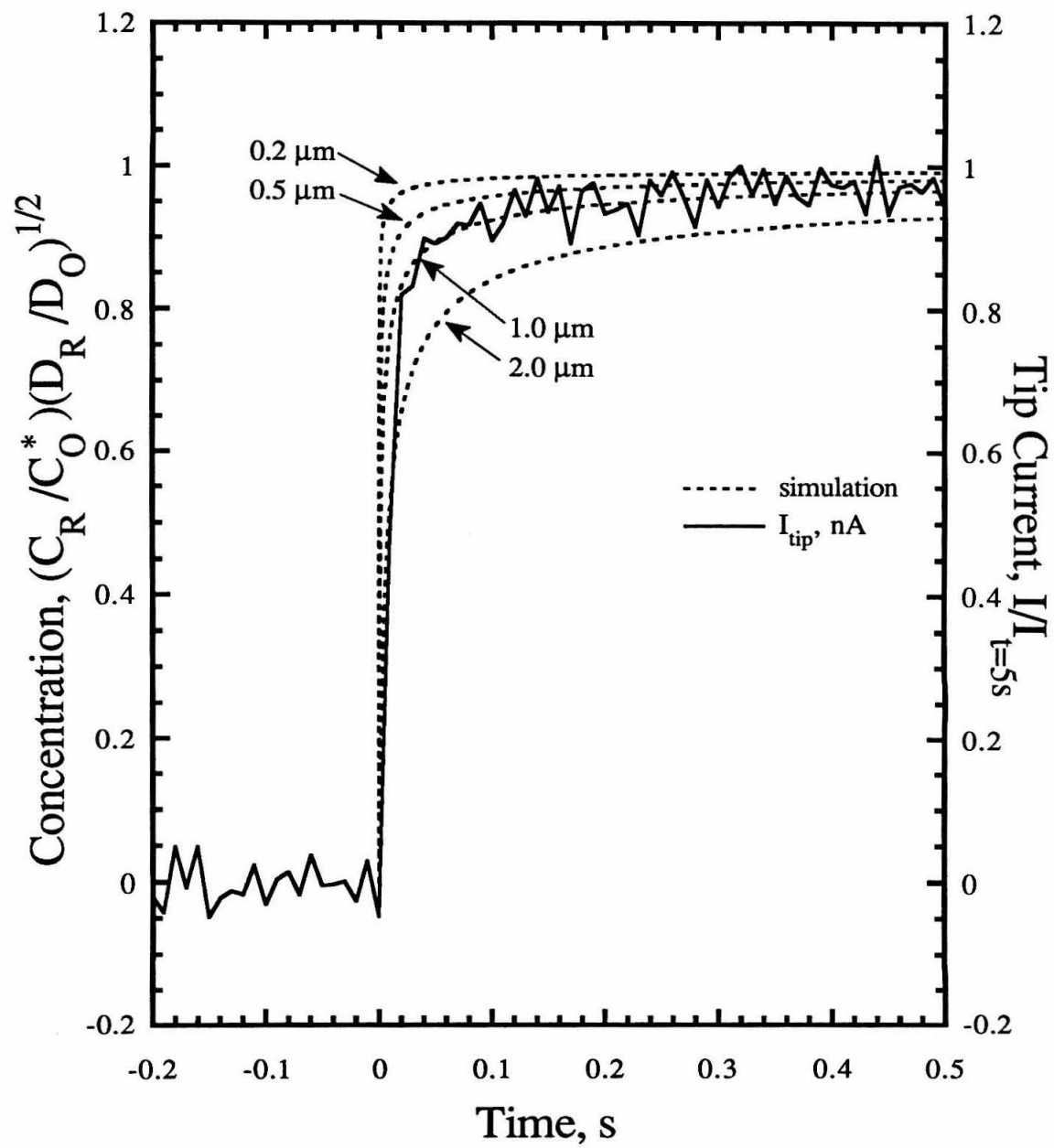


Figure 4.12

Tip current and substrate current versus time for a substrate undergoing a potential step. A 10 pA leakage current is subtracted. E_{sub} stepped from +100 mV to -400 mV.

$E_{\text{tip}} = -400$ mV; tip is retracted 0.74 μm from the substrate; tip $r_{\text{app}} = 1.8$ μm ;

$[\text{Ru}(\text{NH}_3)_6^{3+}] = 0.56$ mM.

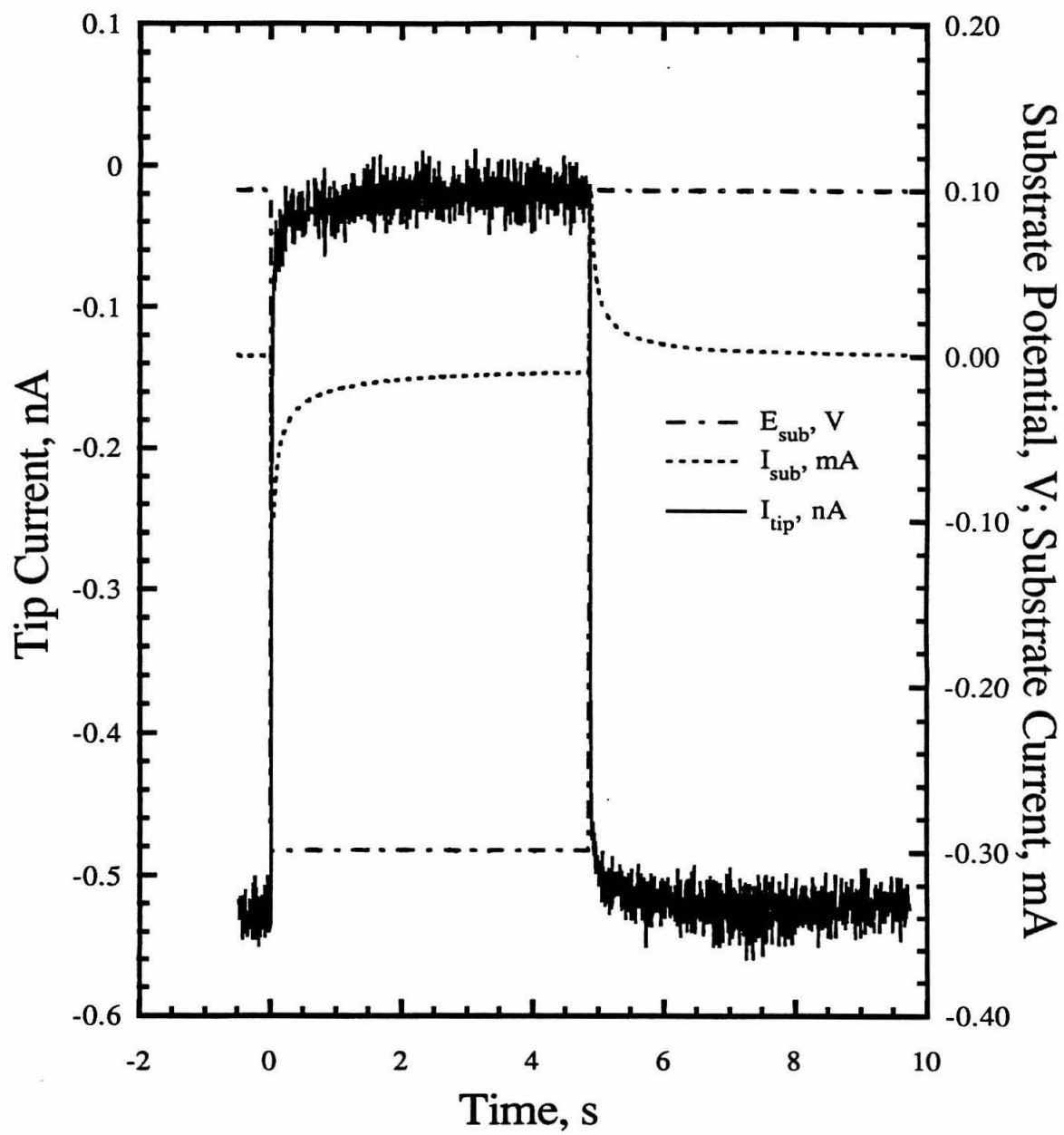


Figure 4.13

Tip current versus time for a substrate undergoing a potential step. Tip is positioned at various distances from the substrate. A 10 pA leakage current is subtracted. Three curves are plotted for $x = 0.70\text{-}0.79\ \mu\text{m}$. E_{sub} stepped from +100 mV to -400 mV.

$E_{\text{tip}} = 100\ \text{mV}$; tip $r_{\text{app}} = 1.8\ \mu\text{m}$; $[\text{Ru}(\text{NH}_3)_6^{3+}] = 0.56\ \text{mM}$.

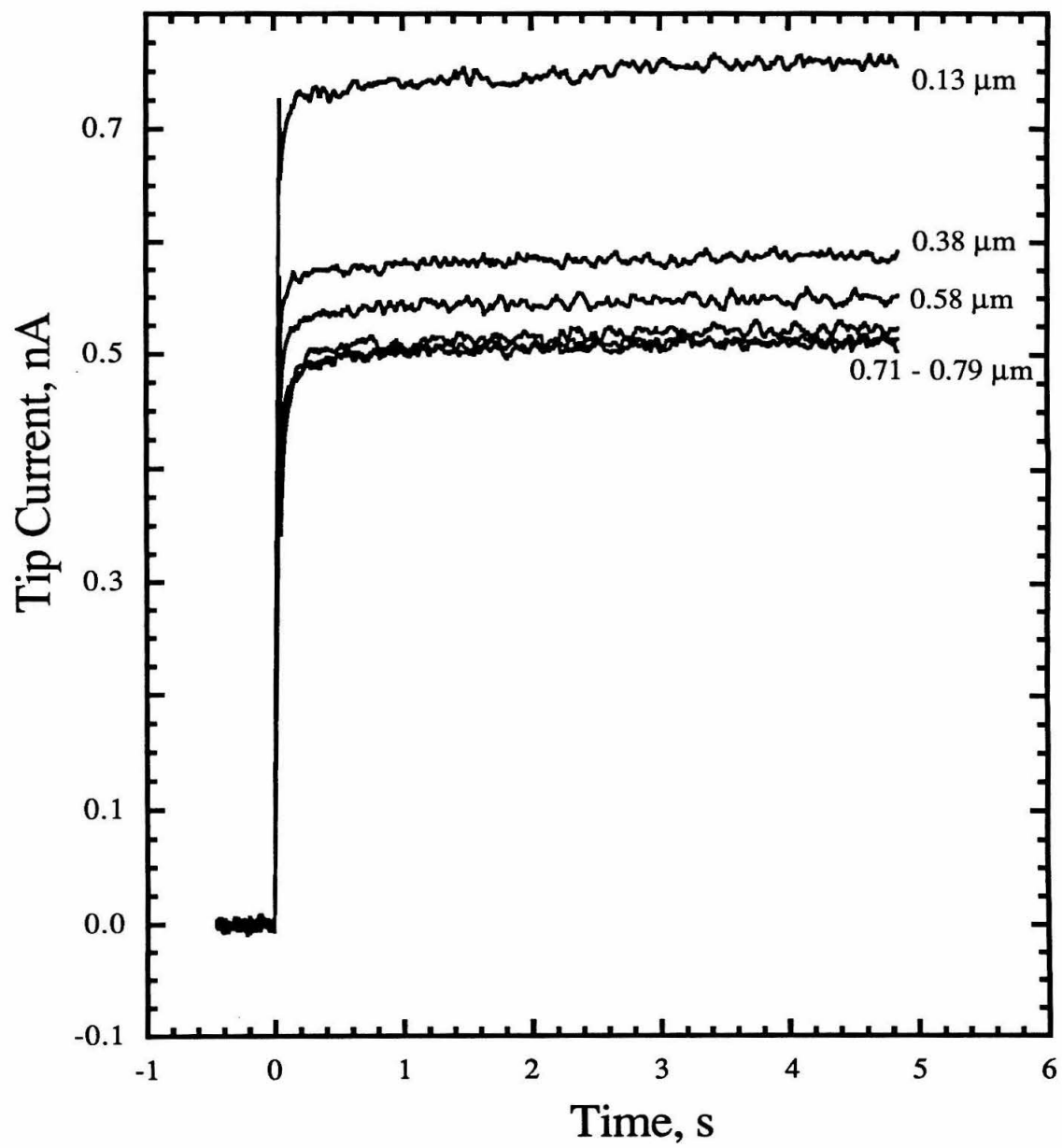


Figure 4.14

Normalized tip current versus time for a substrate undergoing a potential step. Tip is positioned at various distances from the substrate. A 10 pA leakage current is subtracted.

Two curves are plotted for $x = 0.79 \mu\text{m}$. E_{sub} stepped from +100 mV to -400 mV.

$E_{\text{tip}} = 100 \text{ mV}$; tip $r_{\text{app}} = 1.8 \mu\text{m}$; $[\text{Ru}(\text{NH}_3)_6^{3+}] = 0.56 \text{ mM}$.

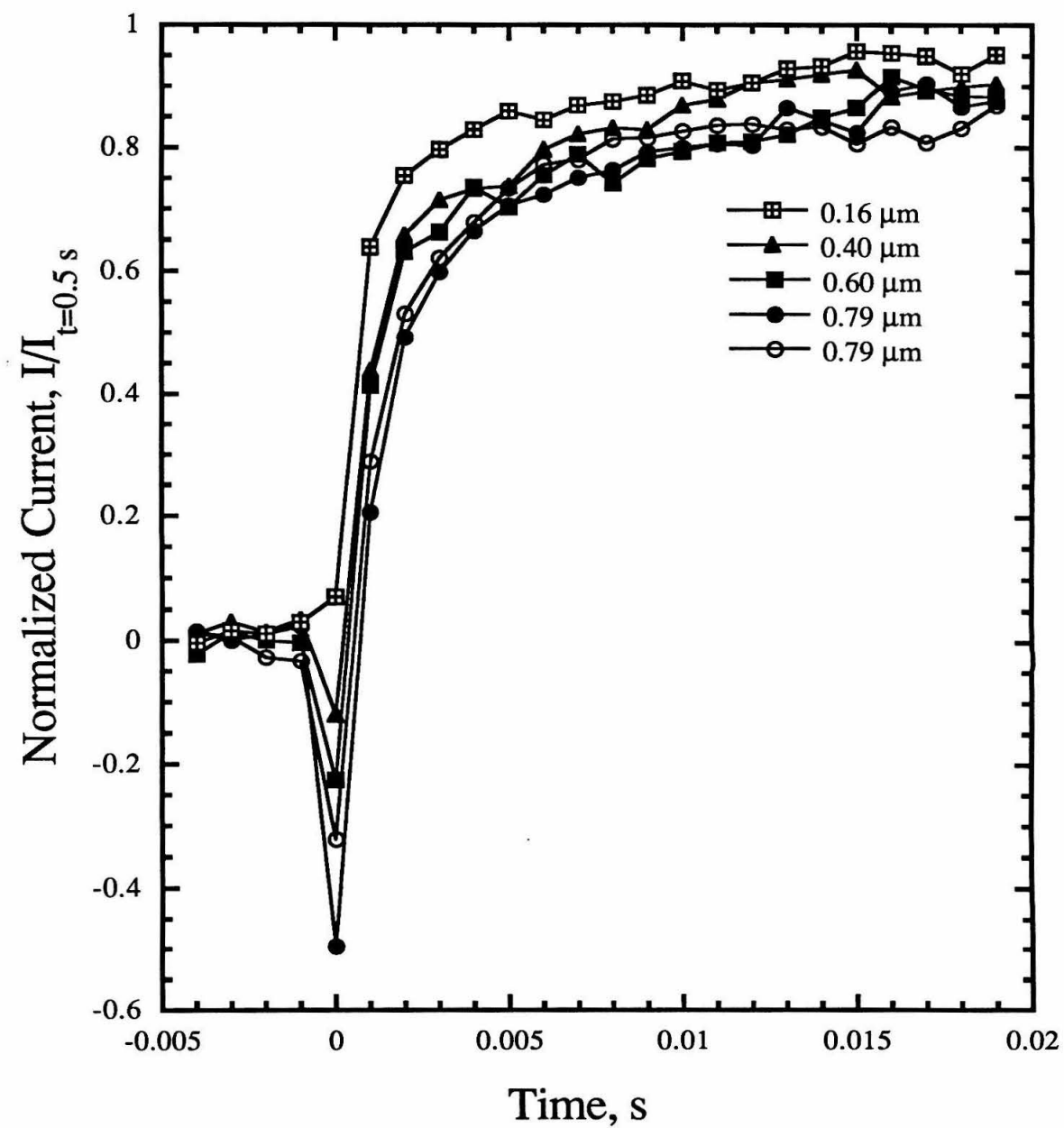


Figure 4.15
Diagram of an insulated tip and its radial diffusion layer.

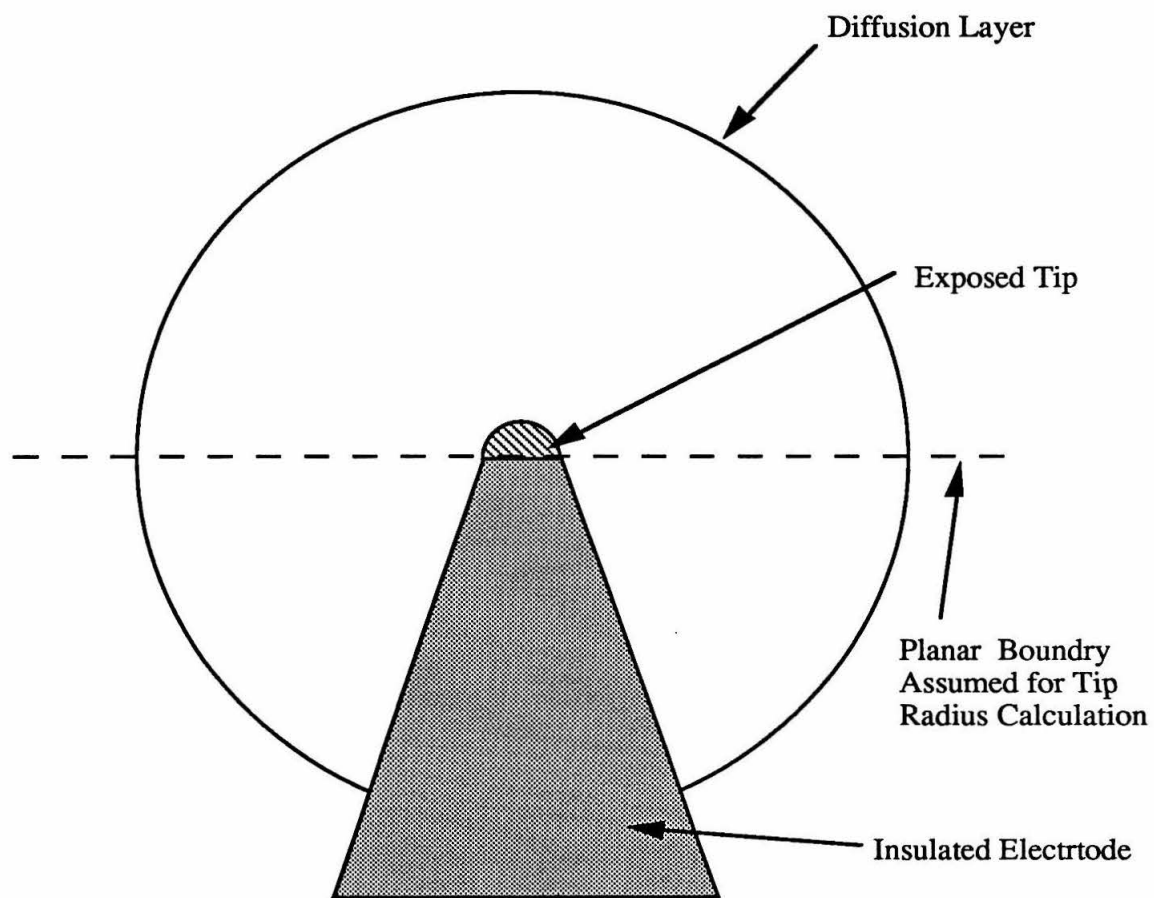


Figure 4.16

Tip current versus time for a substrate undergoing a potential step. Tip is poised at various potentials. A 10 pA leakage current is subtracted. E_{sub} stepped from +100 mV to -400 mV. Tip $r_{\text{app}} = 1.8 \mu\text{m}$; $[\text{Ru}(\text{NH}_3)_6^{3+}] = 0.56 \text{ mM}$.

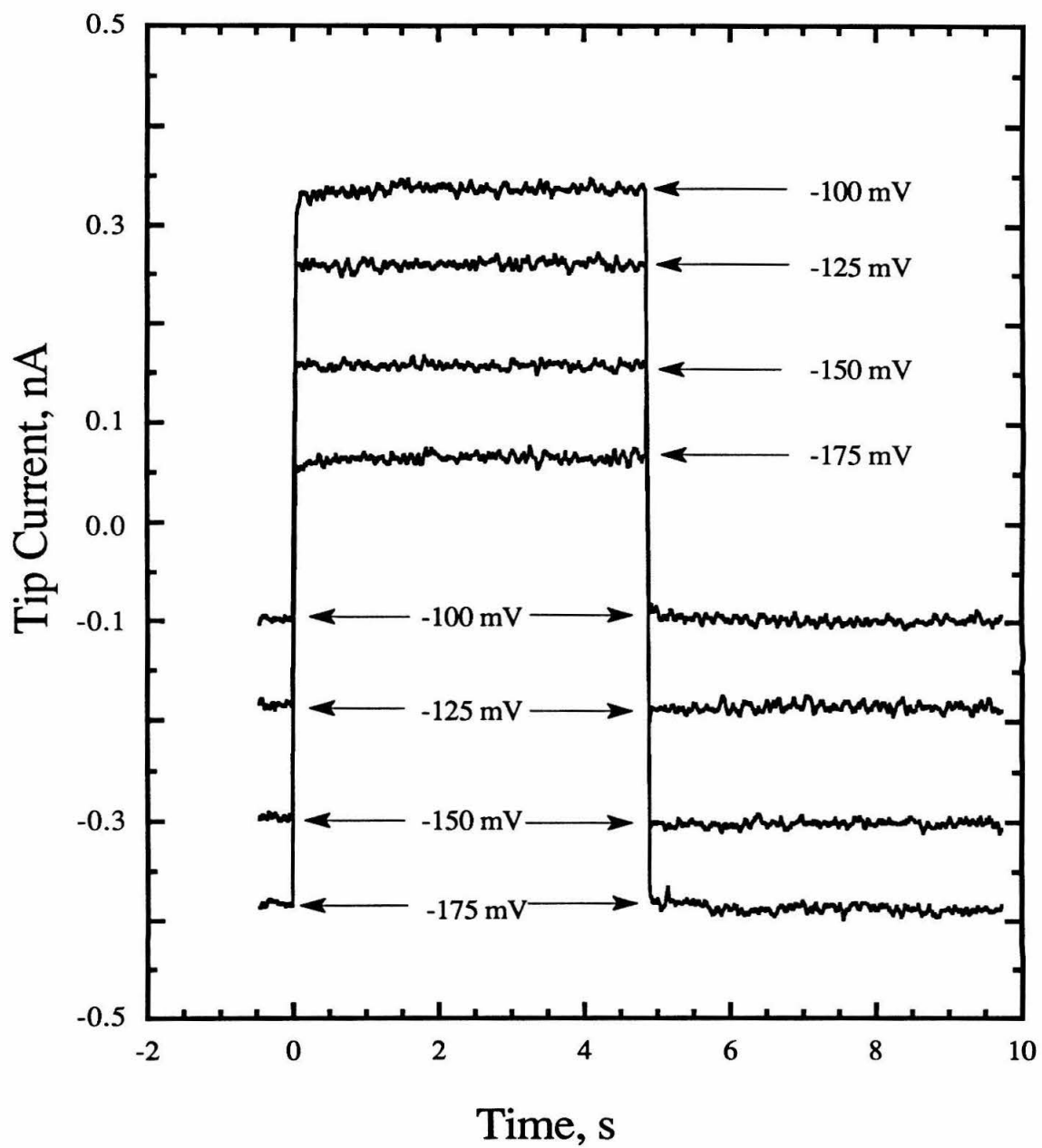


Figure 4.17

Tip current and substrate current versus time for a substrate undergoing a potential step.

E_{sub} stepped from +300 mV to -300 mV. $E_{\text{tip}} = 300$ mV; tip $r_{\text{app}} = 1.8 \mu\text{m}$;

$[\text{Ru}(\text{NH}_3)_5\text{Cl}^{2+}] = 0.61$ mM.

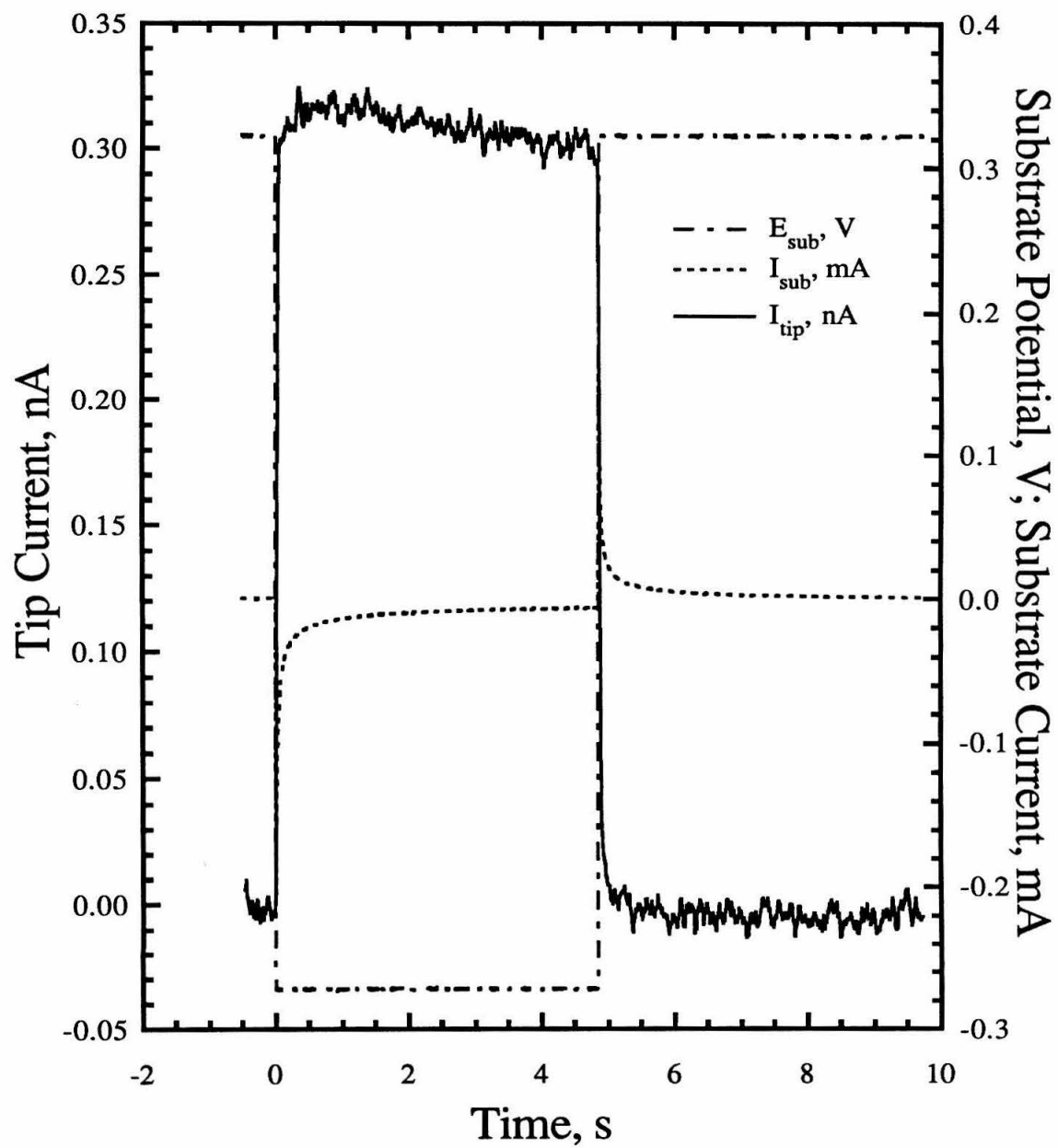


Figure 4.18

Tip current versus time for a substrate undergoing a potential step. E_{sub} stepped from +300 mV to -300 mV. Tip is retracted 0.76 μm from the substrate and adjusted to various potentials. Tip $r_{\text{app}} = 1.8 \mu\text{m}$; $[\text{Ru}(\text{NH}_3)_5\text{Cl}^{2+}] = 0.61 \text{ mM}$.

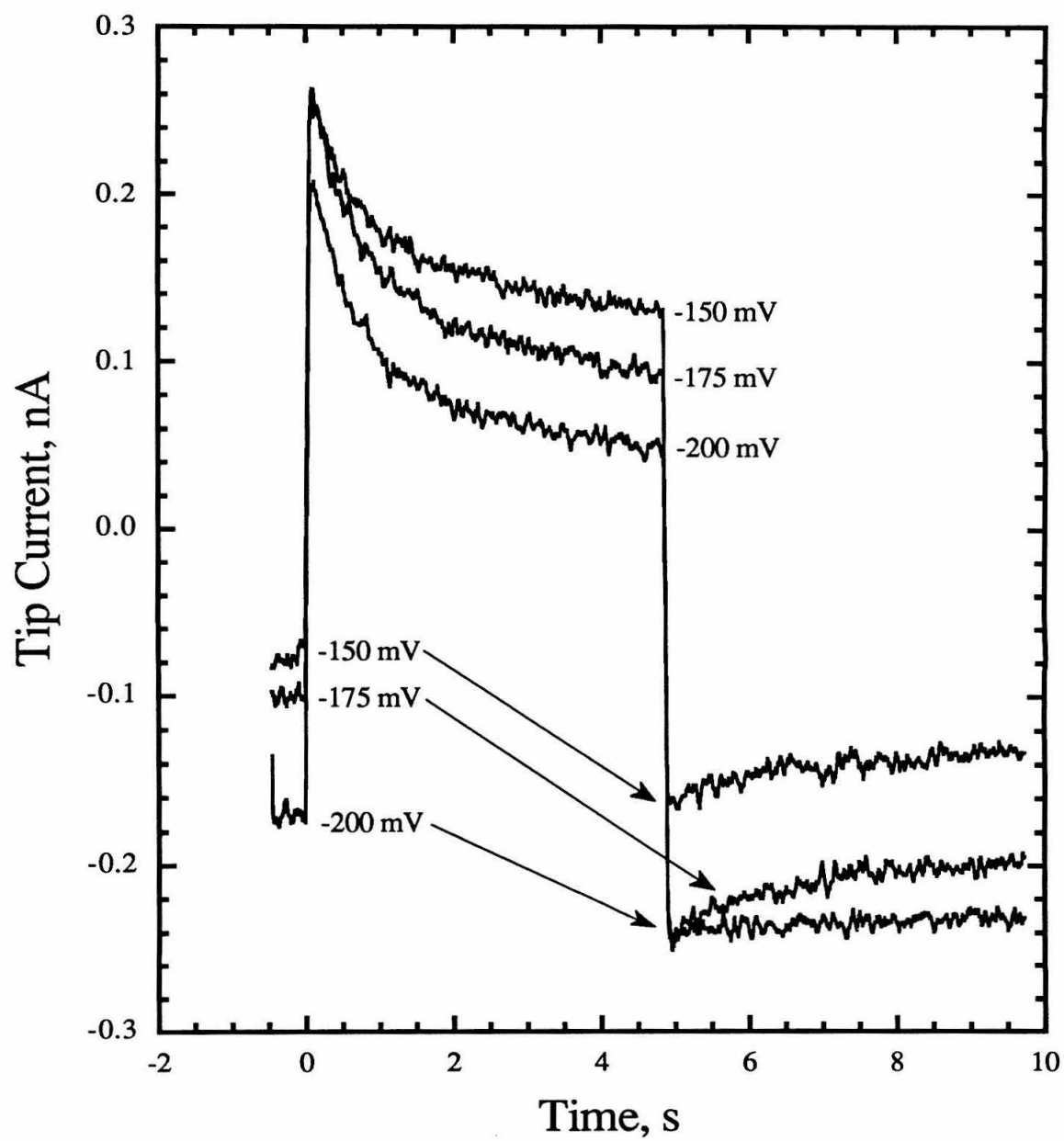


Figure 4.19

Tip current versus time for a substrate undergoing a potential step. E_{sub} stepped from +300 mV to -300 mV. Tip is positioned at various distances from the substrate.

$E_{\text{tip}} = -175$ mV; tip $r_{\text{app}} = 1.8$ μm ; $[\text{Ru}(\text{NH}_3)_5\text{Cl}^{2+}] = 0.61$ mM.

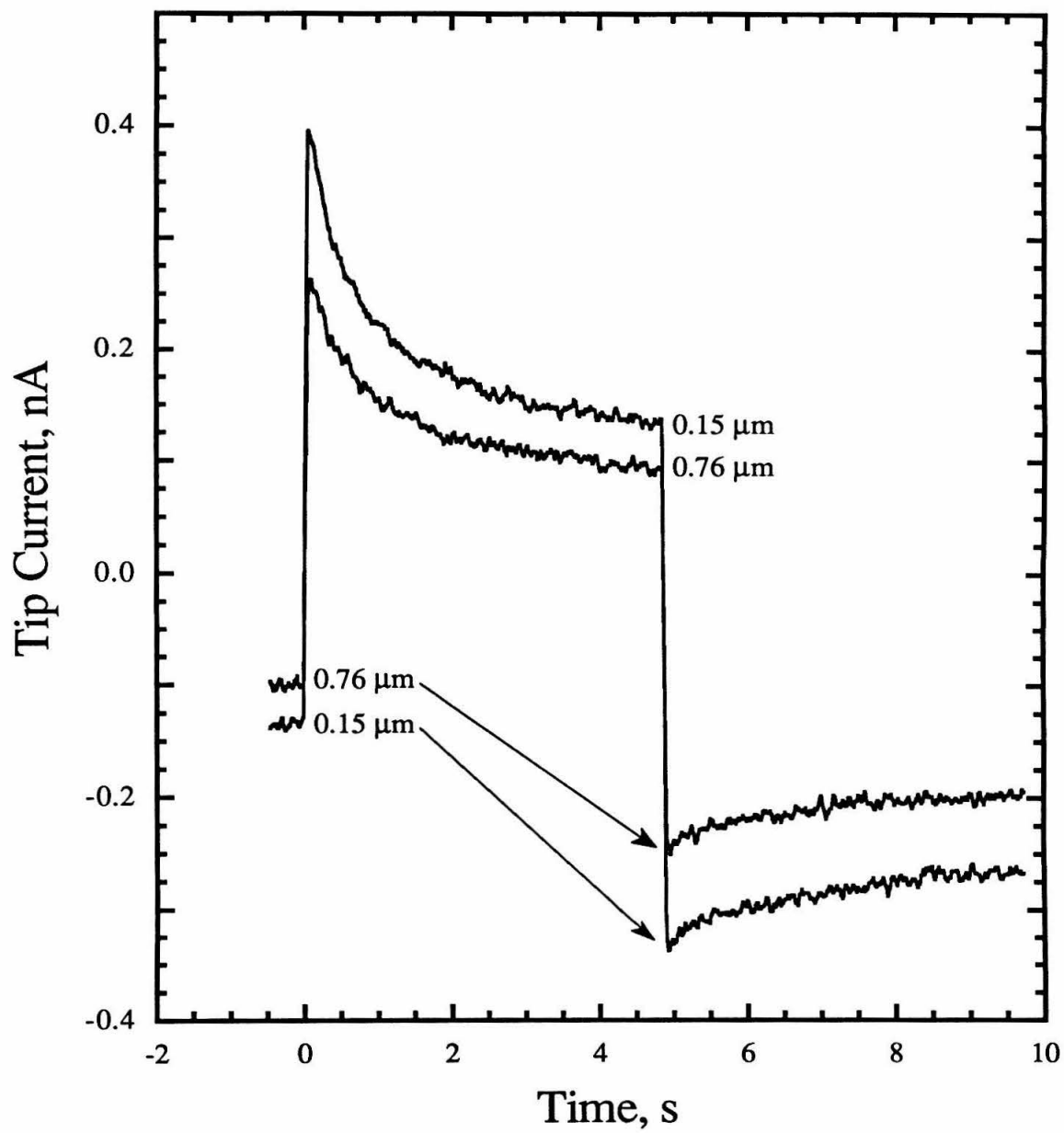


Figure 4.20

Simulated concentration versus time curves of the intermediate product (R) of a E_rC_i reaction, generated at a planar electrode undergoing a potential step, with $k = 4 \text{ s}^{-1}$ and $D_O = 6.6 \times 10^{-6} \text{ cm}^2/\text{s}$.

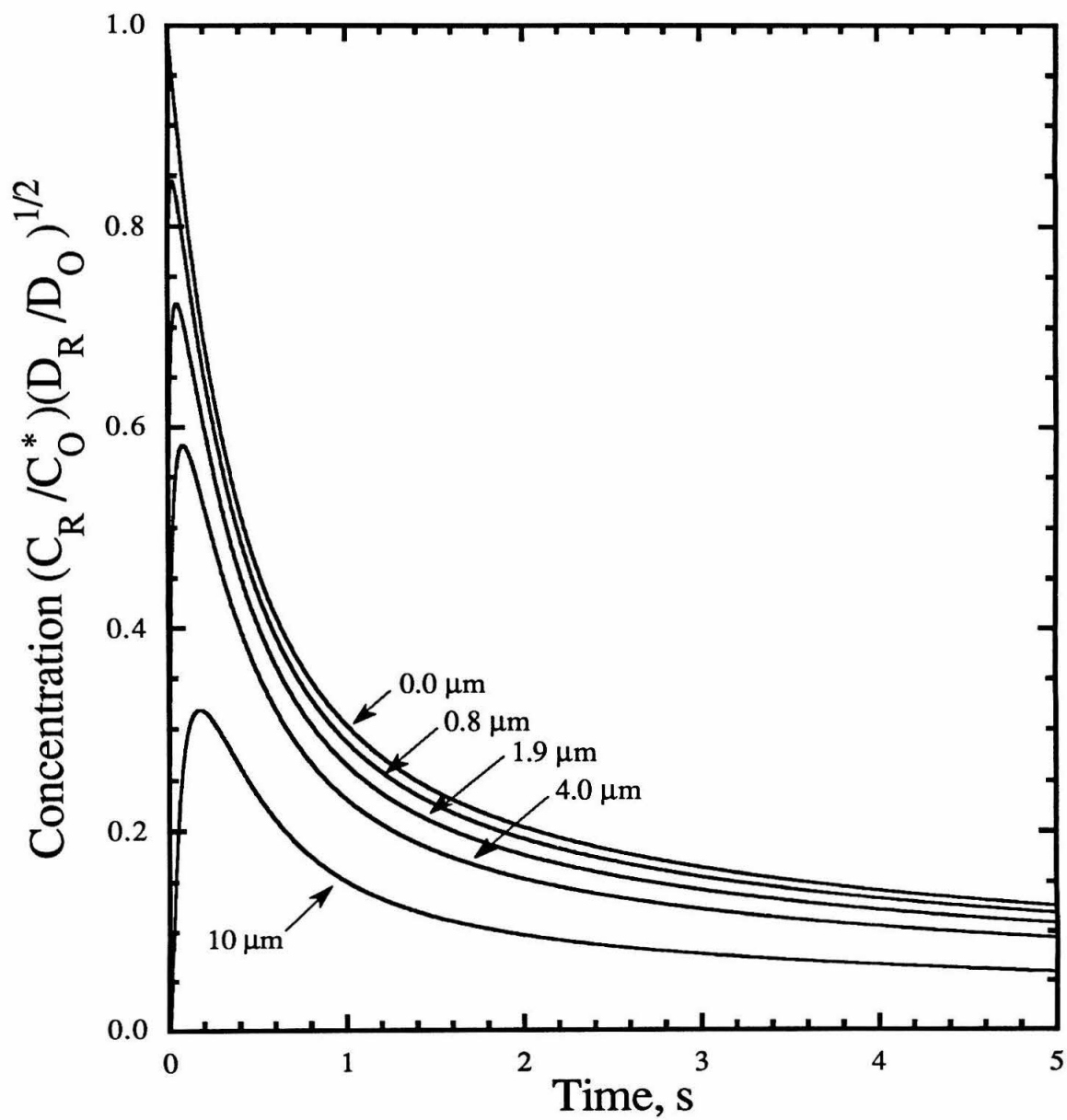


Figure 4.21
Simulated concentration versus time curves of the final product (Z) of a E_rC_1 reaction, generated at a planar electrode undergoing a potential step, with $k = 4 \text{ s}^{-1}$ and $D_O = 6.6 \times 10^{-6} \text{ cm}^2/\text{s}$.

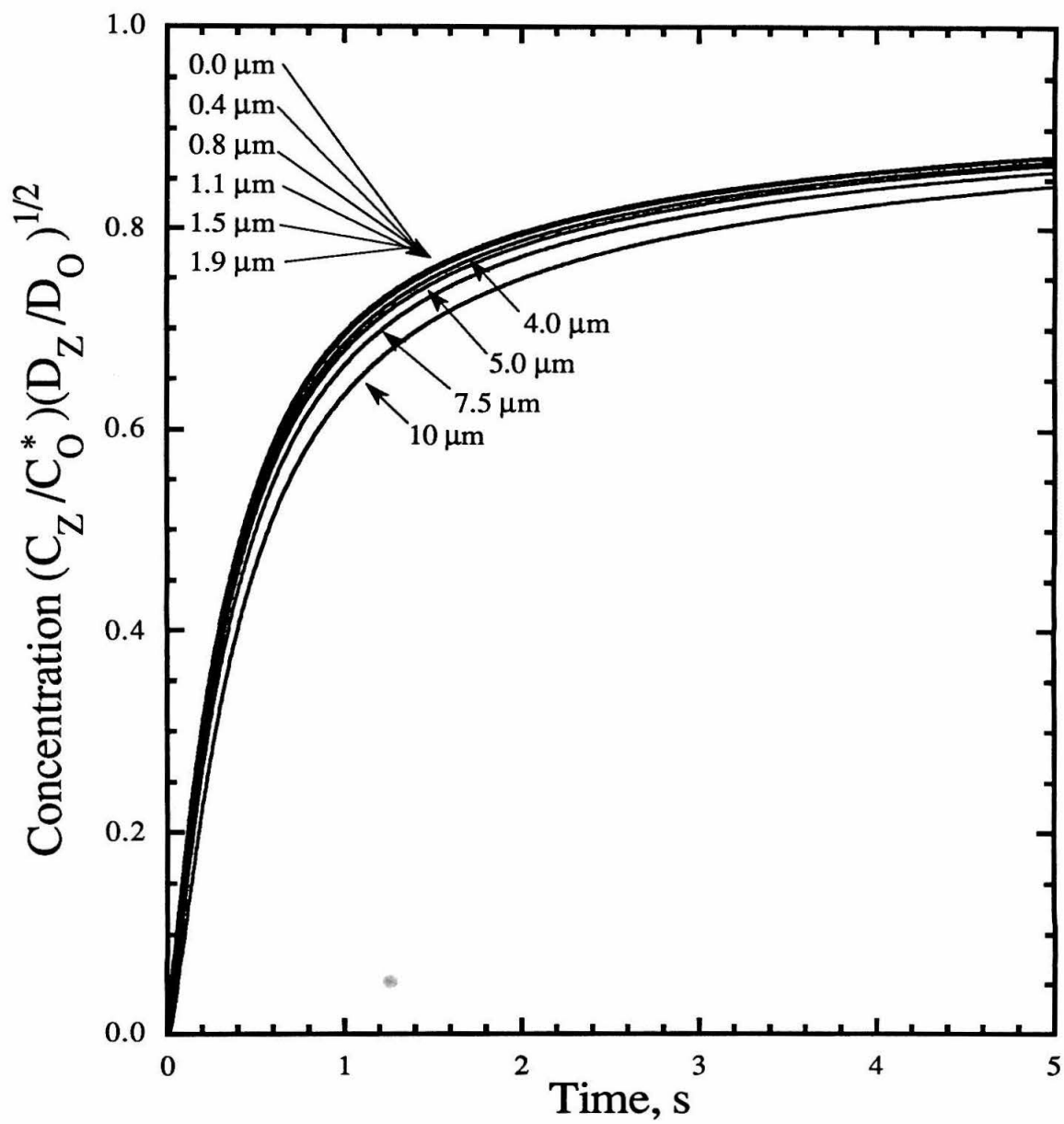


Figure 4.22

Tip current and simulated currents versus time for a substrate undergoing a potential step. Tip is positioned $0.76 \mu\text{m}$ from the substrate. Simulations are for $k = 4 \text{ s}^{-1}$ and $D_{\text{O}} = 6.6 \times 10^{-6} \text{ cm}^2/\text{s}$ for the distances indicated. $E_{\text{tip}} = -175 \text{ mV}$; tip $r_{\text{app}} = 1.8 \mu\text{m}$; $[\text{Ru}(\text{NH}_3)_5\text{Cl}^{2+}] = 0.61 \text{ mM}$.

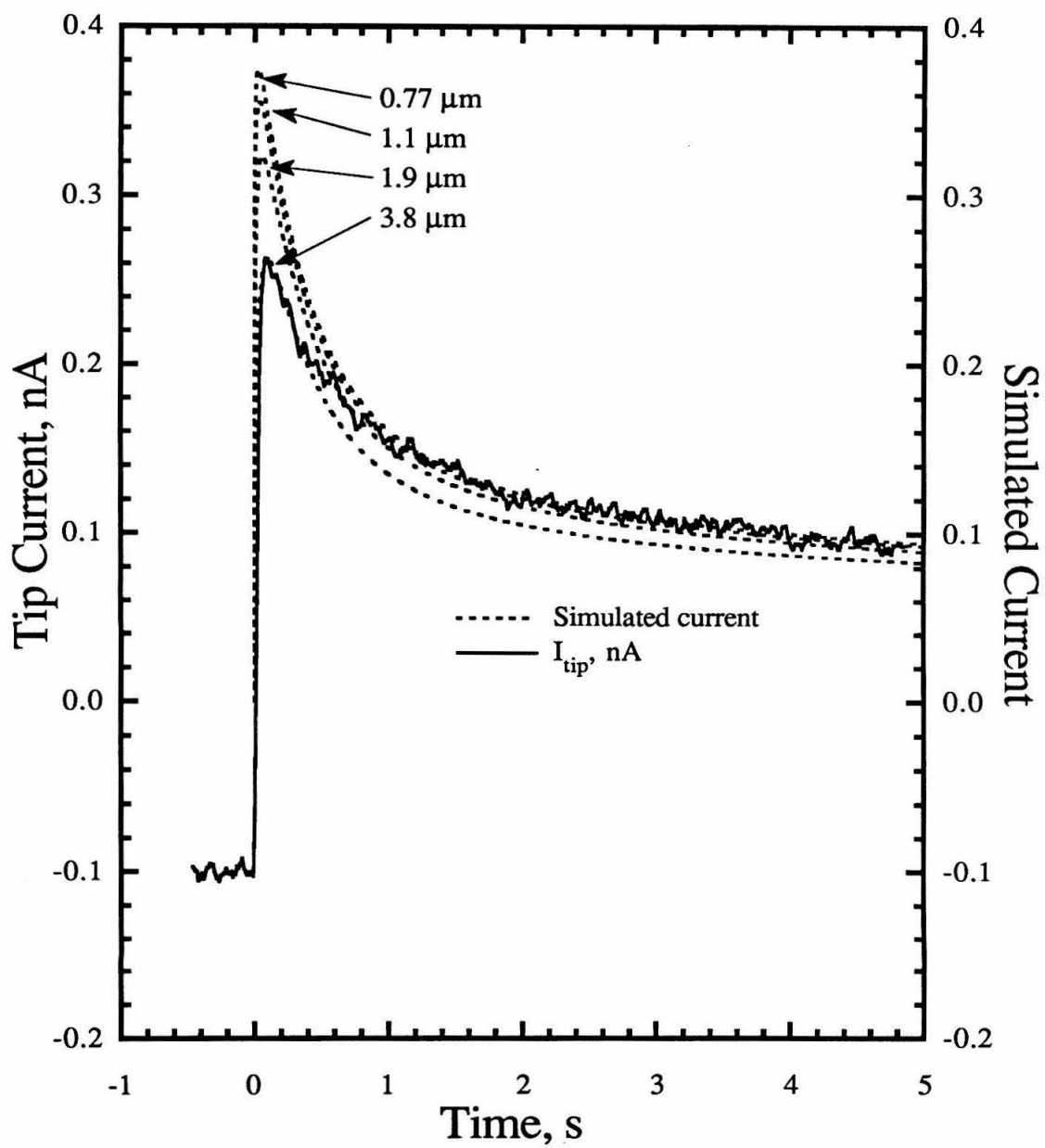


Figure 4.23

Tip current and simulated currents versus time for a substrate undergoing a potential step.

Tip is positioned $0.76 \mu\text{m}$ from the substrate. Simulations are for $k = 2 \text{ s}^{-1}$ and

$D_{\text{O}} = 6.6 \times 10^{-6} \text{ cm}^2/\text{s}$ for the distances indicated. $E_{\text{tip}} = -175 \text{ mV}$; tip $r_{\text{app}} = 1.8 \mu\text{m}$;

$[\text{Ru}(\text{NH}_3)_5\text{Cl}^{2+}] = 0.61 \text{ mM}$.

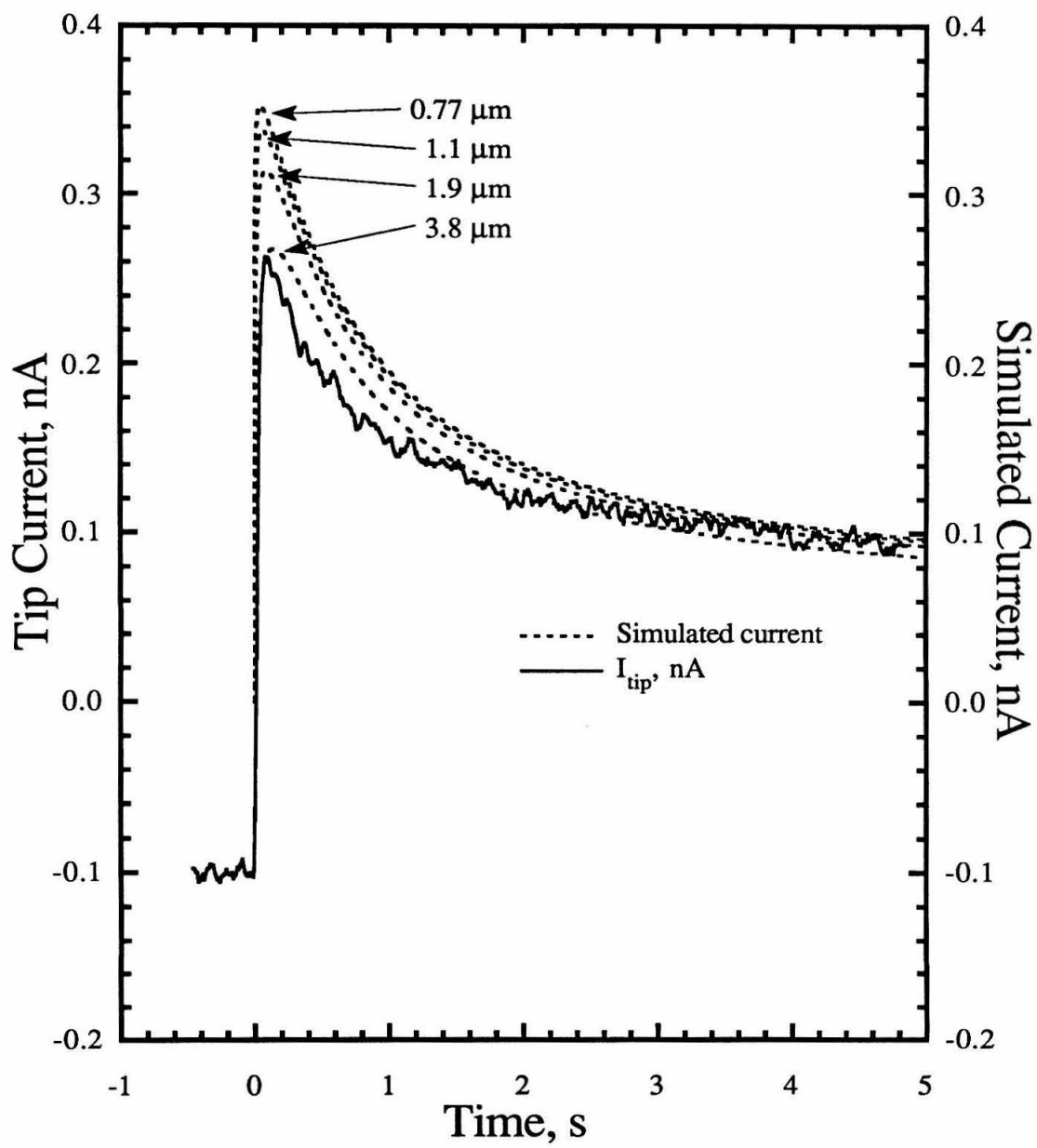


Figure 4.24

Tip current and simulated currents versus time for a substrate undergoing a potential step.

Tip is positioned $0.76 \mu\text{m}$ from the substrate. Simulations are for $k = 10 \text{ s}^{-1}$ and

$D_{\text{O}} = 6.6 \times 10^{-6} \text{ cm}^2/\text{s}$ for the distances indicated. $E_{\text{tip}} = -175 \text{ mV}$; tip $r_{\text{app}} = 1.8 \mu\text{m}$;

$[\text{Ru}(\text{NH}_3)_5\text{Cl}^{2+}] = 0.61 \text{ mM}$.

